

4



AL-TR-88-105

AD:

Final Report  
for the Period  
September 1984  
to July 1989

# Pulsed Plasma Mission Endurance Test

August 1989

Authors:  
R.J. Cassidy

Rocket Research Company  
Olin Defense Systems Group  
11411 Willows Road NE  
Redmond WA 98073-9709

F04611-84-C-0060

AD-A213 462

## Approved for Public Release

Distribution is unlimited. The AL Technical Services Office has reviewed this report, and it is releasable to the National Technical Information Service, where it will be available to the general public, including foreign nationals.

Prepared for the

**Astronautics Laboratory (AFSC)**

Air Force Space Technology Center  
Space Systems Division  
Air Force Systems Command  
Edwards Air Force Base, California 93523-5000

89 10 17 100

## REPORT DOCUMENTATION PAGE

Form Approved  
OMB No. 0704-0188

|   |       |   |  |   |                               |
|---|-------|---|--|---|-------------------------------|
| 1a. REPORT SECURITY CLASSIFICATION<br>UNCLASSIFIED  |       |   | 1b. RESTRICTIVE MARKINGS   |   |                               |
| 2a. SECURITY CLASSIFICATION AUTHORITY   |       |   | 3. DISTRIBUTION/AVAILABILITY OF REPORT<br>Approved for Public Release; Distribution is Unlimited |   |                               |
| 2b. DECLASSIFICATION/DOWNGRADING SCHEDULE   |       |   | 5. MONITORING ORGANIZATION REPORT NUMBER(S)<br>AFAL-TR-88-105                                    |   |                               |
| 4. PERFORMING ORGANIZATION REPORT NUMBER(S)   |       |   | 7a. NAME OF MONITORING ORGANIZATION<br>Astronautics Laboratory (AFSC)                            |   |                               |
| 6a. NAME OF PERFORMING ORGANIZATION<br>Olin Rocket Research Company   |       | 6b. OFFICE SYMBOL<br>(If applicable)        |  | 7b. ADDRESS (City, State, and ZIP Code)<br>AL/LSVE<br>Edwards AFB CA 93523-5000 |                               |
| 6c. ADDRESS (City, State, and ZIP Code)<br>11441 Willows Road N.E.<br>Redmond WA 98073-9709   |       | 8a. NAME OF FUNDING/SPONSORING ORGANIZATION |  | 9. PROCUREMENT INSTRUMENT IDENTIFICATION NUMBER<br>F04611-84-C-0060             |                               |
| 8b. OFFICE SYMBOL<br>(If applicable)  |       | 10. SOURCE OF FUNDING NUMBERS               |  |   |                               |
| 8c. ADDRESS (City, State, and ZIP Code)   |       | PROGRAM ELEMENT NO.<br>62302F               | PROJECT NO.<br>3058  | TASK NO.<br>00  | WORK UNIT ACCESSION NO.<br>EP |
| 11. TITLE (Include Security Classification)<br>Pulsed Plasma Mission Endurance Test (U)   |       |   |  |   |                               |
| 12. PERSONAL AUTHOR(S)<br>Cassidy, R. Joseph  |       |   |  |   |                               |
| 13a. TYPE OF REPORT<br>Final  |       | 13b. TIME COVERED<br>FROM 84,09 TO 89,07    |  | 14. DATE OF REPORT (Year, Month, Day)<br>89,08                                  |                               |
| 15. PAGE COUNT<br>146   |       |   |  |   |                               |
| 16. SUPPLEMENTARY NOTATION  |       |   |  |   |                               |
| 17. COSATI CODES  |       |   | 18. SUBJECT TERMS (Continue on reverse if necessary and identify by block number)                |   |                               |
| FIELD   | GROUP | SUB-GROUP                                   | Electric propulsion, Pulsed plasma, Electromagnetic thruster                                     |   |                               |
| 21  | 03    |   |  |   |                               |
| 19. ABSTRACT (Continue on reverse if necessary and identify by block number)  |       |   |  |   |                               |
| <p>The objectives of this program were to evaluate the performance and to conduct a life investigation of one millipound Teflon Pulsed Plasma Thruster (PPT). The goal of the life demonstration was a total impulse of 70,000 lbf-s (312,000 N-S) or 14 million pulses. The thruster and associated hardware were fabricated under a previous contract and were provided as Government Furnished Property (GFP) to RRC. The PPT thruster was designed for satellite stationkeeping and drag make-up propulsion applications. It is extremely simple in concept, utilizing a solid propellant (Teflon), a simple electrode geometry (rails), and a common form of energy storage (capacitors). In application at the millipound level, this simplicity demonstrated itself ably in test flights aboard the LES-6 spacecraft, the SMS spacecraft, and on the Navy TIP and NOVA satellites. The PPT thrusters performed flawlessly in their role of drag make-up and precision spacecraft positional control. Scaling the PPT thruster to the millipound level for North-South stationkeeping application proved to be somewhat more difficult. The configuration changes required to achieve the higher thrust</p> |       |   |  |   |                               |
| 20. DISTRIBUTION/AVAILABILITY OF ABSTRACT<br><input checked="" type="checkbox"/> UNCLASSIFIED/UNLIMITED <input type="checkbox"/> SAME AS RPT. <input type="checkbox"/> DTIC USERS   |       |   | 21. ABSTRACT SECURITY CLASSIFICATION<br>UNCLASSIFIED   |   |                               |
| 22a. NAME OF RESPONSIBLE INDIVIDUAL<br>TERRY M. SANKS, 1Lt, USAF  |       |   | 22b. TELEPHONE (Include Area Code)<br>(805) 275-5473   |   | 22c. OFFICE SYMBOL<br>AL/LSVE |

AFAL-TR-88-105

Block 19 (concluded)

level complicated the design and made the component requirements more stringent. This report provides the background, program description, and test results from the "PPT Mission Endurance Test" program. It also provides a "lessons learned" overview of the program to benefit future programs. Where appropriate, specific problem areas are addressed with a detailed description of the problems encountered and RRC recommended "fixes" for these problems.

## TABLE OF CONTENTS

| <u>Section</u>                                   | <u>Page</u> |
|--|-------------|
| Executive Summary .....                          | 1           |
| PPT Historical Background.....                   | 3           |
| Program Description .....                        | 8           |
| Results.....                                     | 23          |
| Conclusions .....                                | 38          |
| References.....                                  | 41          |
| APPENDIX A — GFP Damage Assessment               |             |
| APPENDIX B — DI Circuit Final Report             |             |
| APPENDIX C — Acceptance Test Report              |             |
| APPENDIX D — PPT Endurance Test Plan             |             |
| APPENDIX E — Thrust Stand Calibration Procedures |             |

|                    |                                     |  |
|--------------------|-------------------------------------|--|
| Accession For      |                                     |  |
| NTIS GRA&I         | <input checked="" type="checkbox"/> |  |
| DTIC TAB           | <input checked="" type="checkbox"/> |  |
| Unannounced        | <input type="checkbox"/>            |  |
| Justification      |                                     |  |
| By _____           |                                     |  |
| Distribution/      |                                     |  |
| Avail and/or Codes |                                     |  |
| Dist _____         |                                     |  |
| Special            |                                     |  |
| A-1                |                                     |  |

## LIST OF FIGURES

| <b>Figure</b> |  | <b>Page</b> |
|---------------|--|-------------|
| 1             | Pulsed Plasma Thruster.....  | 3           |
| 2             | J X B Interaction.....   | 3           |
| 3             | Side Feed Thruster Configuration.....  | 4           |
| 4             | Igniter Plug Resistance as a Function of Number of Discharges.....                                   | 6           |
| 5             | Stripline Damage from Capacitor Failure .....  | 8           |
| 6             | Experimental Discharge Initiation Circuit Used by JPL.....   | 10          |
| 7             | PPT Thermal Shunt Capacitor Cage.....  | 12          |
| 8             | Rolling Ball Calibrator Schematic.....   | 13          |
| 9             | Arc Damage and Carbon Deposit .....  | 16          |
| 10            | Capacitor Center Electrode Comparison .....  | 16          |
| 11            | Initial Center Post Adapter Design .....   | 17          |
| 12            | Modified Adapter Design with Shoulder .....  | 17          |
| 13            | Stripline Exploded View.....   | 18          |
| 14            | Two-Piece Adapter Redesign.....  | 20          |
| 15            | Capacitor SC 320 PC 014 Condition After Failure.....   | 21          |
| 16            | Storage Capacitor Voltage Drop as a Function of SCR Case Temperature<br>for Operation at 80 Hz ..... | 24          |
| 17            | High Voltage Connector Used at Physics International.....  | 25          |
| 18            | Thrust Stand Data.....   | 27          |
| 19            | Thrust Stand Response to Ball Calibrator.....  | 27          |
| 20            | Capacitor Temperatures .....   | 28          |
| 21            | Thermocouple Measurements for Capacitors 1 and 3.....  | 29          |
| 22            | Thermocouple Measurements for Capacitors 2 and 4.....  | 30          |
| 23            | Converter Cover Temperatures.....  | 32          |
| 24            | PPT Internal Component Temperatures .....  | 32          |
| 25            | Temperature Difference Between Capacitors and Thermal Shunt.....                                     | 33          |
| 26            | Mission Analysis Summary .....   | 34          |
| 27            | Paschen Breakdown Voltage Curve .....  | 36          |
| 28            | Sandia Capacitor Centerpost Adapter.....   | 37          |
| 29            | New PPT Feed Design  |             |

## LIST OF TABLES

| <b>Table</b> |   | <b>Page</b> |
|--------------|---|-------------|
| 1            | Results of Materials Testing.....               | 7           |
| 2            | Results of Capacitor Acceptance Test.....       | 25          |
| 3            | Calculation of Teflon Fuel in PPT Thruster..... | 26          |
| 4            | Lengths as Received at RRC .....                | 26          |
| 5            | Mission Analysis Assumptions.....               | 34          |

## EXECUTIVE SUMMARY

This report documents the work performed by Rocket Research Company (RRC) under AFAL Contract F04611-84-C-0060, "Pulsed Plasma Mission Endurance Test Program". The objectives of this program were to evaluate the performance and to conduct a life investigation of the one millipound Teflon Pulsed Plasma Thruster (PPT). The goal of the life demonstration was a total impulse of 70,000 lbf-s (312,000 N-s) or 14 million pulses. The thruster and associated hardware were fabricated under a previous contract and were provided as Government Furnished Property (GFP) to RRC.

The PPT thruster was designed for satellite stationkeeping and drag make-up propulsion applications. It is extremely simple in concept, utilizing a solid propellant (Teflon), a simple electrode geometry (rails), and a common form of energy storage (capacitors). In application at the micropound level this simplicity demonstrated itself ably in test flights aboard the LES-6 spacecraft, the SMS spacecraft, and on the Navy TIP and NOVA satellites. The PPT thrusters performed flawlessly in their role of drag make-up and precision spacecraft positional control. Scaling the PPT thruster to the millipound level for North-South stationkeeping application proved to be somewhat more difficult. The configuration changes required to achieve the higher thrust level complicated the design and made the component requirements more stringent. This evolution is described in PPT Historical Background.

The PPT life test was awarded to RRC after a similar program at McDonnell Douglas Astronautics Company (MDAC) experienced a capacitor failure and was terminated. In the previous program at MDAC, the thruster was damaged and contaminated from the rupture of the capacitor, which released castor oil into the vacuum chamber containing the thruster. RRC, therefore, anticipated some repair and cleaning of the thruster hardware and vacuum chamber. However, further damage of important components, such as the swinging arm thrust stand, was sustained in transit as a result of improper shipping. The GFP items arrived at RRC in a shambles. A complete description of this episode and the ensuing Engineering Change Proposals (ECPs) is given in the section entitled Program Description.

Capacitor technology was one significant area where technical progress was anticipated between the MDAC life test and this program. The MDAC test had utilized Maxwell castor oil and K-film capacitors which were subject to internal arcing due to imperfections in the K-film windings. Based on these documented problems, the AFAL awarded a technology program to Sandia National Laboratory to develop a new capacitor winding technology. This process was the result of work by the late Dr. G. Howard Mauldin. It employed a perfluorocarbon fluid impregnant and a new winding process to ensure maximum control of winding tension to avoid stretching of the dielectric. The Sandia capacitor program produced capacitors for use in the PPT life test. Details of the capacitor acceptance testing and of the general integration issues encountered are given in the Program Description section.

It is hoped that future efforts can benefit from the experience of this program. While certain aspects of the design must be reworked, the millipound PPT concept is still technically viable. But even if the design were simplified and a unit were to pass a life test, questions arise regarding the mission utility of the millipound PPT. Other thruster concepts such as

the arcjet and the ion thruster are now competing for the North-South stationkeeping market. This report will include an examination of the mission trades in an attempt to answer these questions. In addition, a review of the design of the millipound engine will be made, with comments on the problems specific to each component. RRC suggested design improvements will be noted where applicable, with an emphasis on improved function and modularity for ease of testing. The results and lessons learned will be presented in later sections of this report.

In summary, this report will provide the background, program description, and test results from the "PPT Mission Endurance Test" program. It will also provide a "lessons learned" overview of the program to benefit future programs. Where appropriate, specific problem areas will be addressed with a detailed description of the problems encountered and RRC recommended "fixes" for these problems.

## PPT HISTORICAL BACKGROUND

The thruster tested in this program was a millipound Pulsed Plasma Thruster (PPT). The PPT design is a simple one, as shown schematically in Figure 1. The only moving part in the device is the fuel bar, which is fed with negator springs into the discharge region between the two electrodes. An energy storage capacitor provides the electrical energy for the main discharge, while a separate spark plug circuit is used to initiate the discharge. Once the Teflon fuel is ablated and ionized by the arc, it is accelerated between the rail electrodes under the action of a  $j \times B$ , or Lorentz body force. Figure 2 describes the  $j \times B$  interaction and the resultant force. The PPT was first developed as a micropound-class thruster and then scaled to the millipound level. A brief history of the development of the PPT is given in this section.

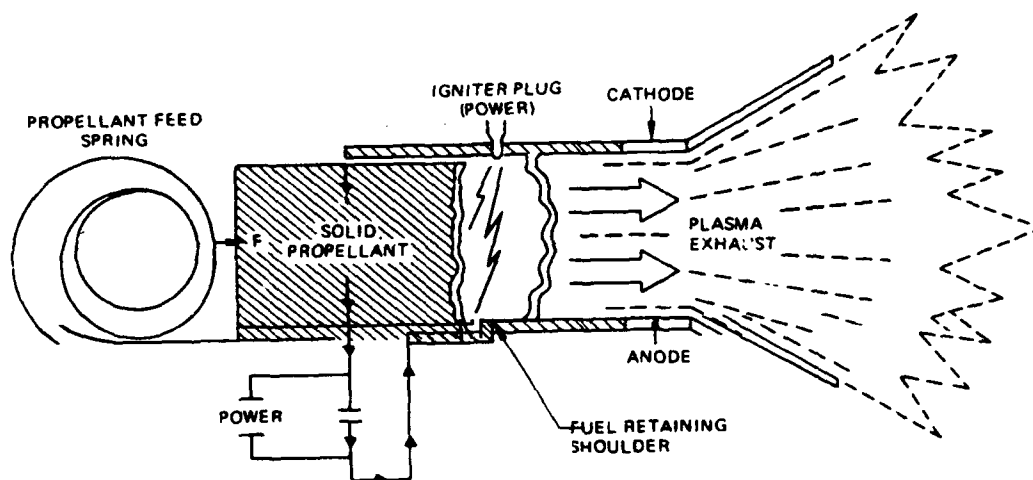


Fig. 1. Pulsed Plasma Thruster

The Pulsed Plasma Thruster was first conceived in the 1950s by groups in the United States, Europe, and the Soviet Union. It was the Soviets who first flew a PPT in 1964 aboard the Zond-2 spacecraft.<sup>(1)</sup> The Zond-2 mission was an interplanetary transfer to Mars and the PPT thruster was used to provide spacecraft attitude control to keep the solar arrays pointed toward the sun. The Soviets have since routinely used thrusters of the pulsed plasma type for attitude control on various missions. In the United

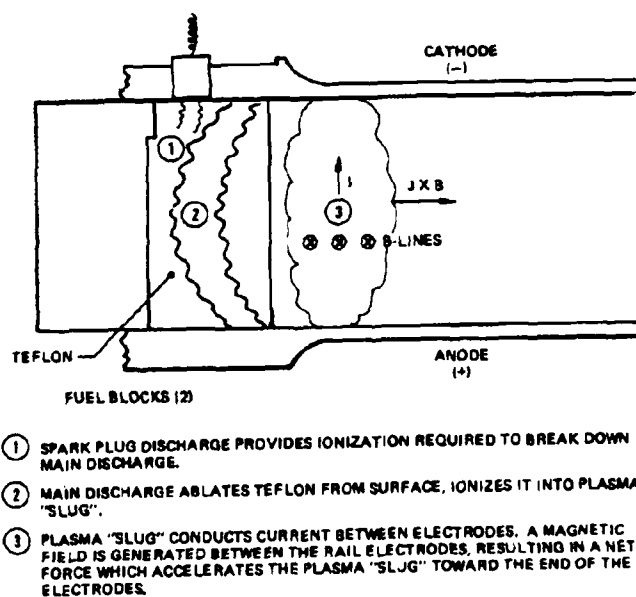
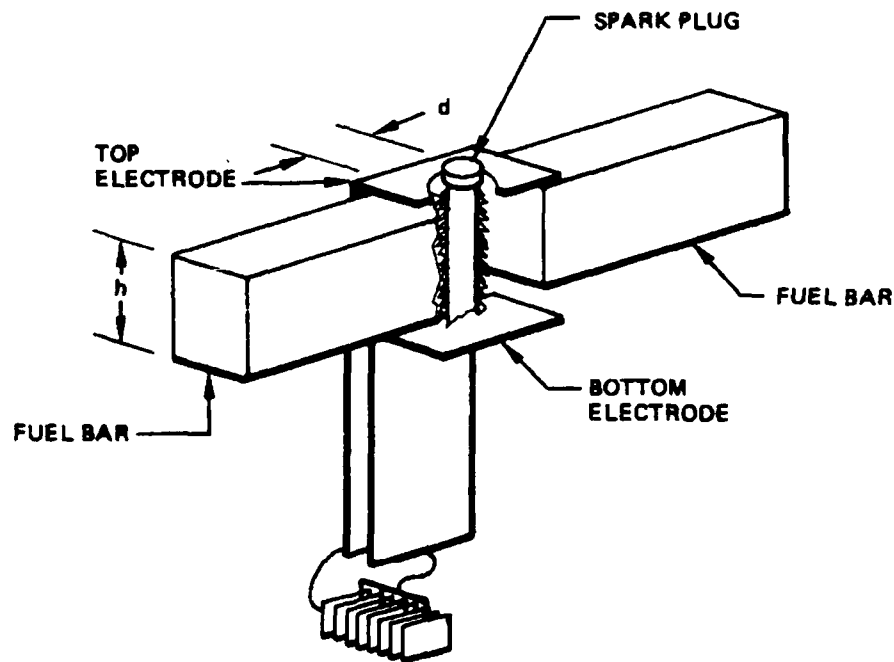


Fig. 2.  $J \times B$  Interaction



States, the PPT development work for the present solid Teflon device began in the early 1960's. Initially, General Electric, Cornell Aeronautical Labs, and Fairchild-Hiller were involved in this development. In 1966, MIT Lincoln Laboratories began technology development of a Teflon PPT microthruster.<sup>(2)</sup> This led to the first U.S. flight of the PPT in 1970 aboard the Lincoln Experimental Satellite 6 (LES-6).<sup>(3)</sup> This flight unit was a breech-fed design, which achieved 20 micropounds of thrust at an Isp of 1200 s. The flight unit performed flawlessly. This successful space demonstration, coupled with mission analyses showing the benefits of this type of device for attitude control and North-South stationkeeping, led researchers to attempt means of scaling the device up to the millipound level. The millipound thruster development effort also began at Lincoln Laboratories. As a means of increasing the mass ablated per discharge, a side feed thruster was investigated.<sup>(4)</sup> The Teflon was fed in from both sides in this device, as shown in Figure 3. In 1972, the Air Force Astronautics Laboratory (AFAL) embarked on development of a millipound PPT with a contract to Fairchild Corporation.<sup>(5)</sup>



**Fig. 3. Side Feed Thruster Configuration**

This device evolved into the flight design PPT which finally was to be life tested under the present contract. The interim period was not without its problems. Early problems with the millipound thruster included electrode erosion, uneven wear of the Teflon fuel bars, and build-up of carbon deposits on the discharge initiation spark plug. Contracts were funded by the AFAL to deal with each of these problem areas.<sup>(6,7)</sup> For the most part, these were successful. The major problem which emerged in the millipound thruster was the lack of a suitable, long-life, high-energy-density capacitor. This problem would prove to be the most difficult to overcome. The capacitor problem came about as a result of two differences between the micropound PPT and the millipound PPT. The first difference is the requirement for more energy per pulse in the millipound thruster. The second is the requirement for more

total pulses. Finding a capacitor to meet the combination of these two requirements was difficult. Capacitors soon became the most critical technology to the success of the millipound PPT. To meet the thruster system goal of 310,000 N-s total impulse, the capacitors had to be capable of 14 million discharges. Early tests showed that the capacitors would fail far short of this goal. As a result, AFAL contracted with Maxwell laboratories to develop and evaluate a special high-energy-density capacitor for the PPT.<sup>(8)</sup> This evaluation was completed in 1980 and the results were very discouraging. The capacitor design in these tests consisted of Kureha polyvinylidene (K-film), aluminum foil, and silicon oil. Overvoltage tests were conducted as a means of accelerated testing and extrapolation from these results indicated that 14 million pulses were possible. However, when tested at the PPT operational voltage of 2300 V, all units failed in less than 100,000 pulses. A possible explanation for the early capacitor failure in thruster testing was the voltage reversal of the thruster discharge. This ringing discharge resulted from the RLC characteristics of the discharge circuit (i.e. the PFN, stripline, electrodes, and plasma discharge). The AFAL, in 1981, established an in-house effort to develop a capacitor evaluation system which included the voltage reversal effect.<sup>(9)</sup> This system was used to evaluate several Maxwell capacitors, but was never used with Sandia capacitors due to delays in the production of the Sandia units and a decision to terminate the internal test effort. All of the Maxwell capacitors tested failed well short of one million pulses.

At the same time other efforts continued to solve problems encountered in early tests of the millipound PPT system. At JPL, a program was initiated by the AFAL to redesign the discharge initiation circuit with the goal of reduced spark plug carbon build-up. The carbon build-up and insulator embrittlement of the plug led to a lower plug resistance as time of operation increased. JPL investigated this process and determined that the deposits and embrittlement were the result of high currents from the main discharge flowing through the plug and back to the cathode through the one Ohm coupling resistor.<sup>(10)</sup> JPL's solution to this problem was to decouple the spark plug from the main discharge by replacing the one Ohm resistor with an inductor. This inductor reduced coupling currents from several thousand Amperes to a few tens of Amperes. Another important aspect of the redesigned initiation circuit was the increase in operational voltage from 600 Volts to 2000 Volts, which reduced the pulse length of the plug discharge. This technique proved effective in lowering the build-up of exhaust products on the plug insulators. In tests at JPL, the plug resistance was measured as a function of the number of discharges and found to decrease from several hundred Ohms to approximately 100 Ohms in 100,000 discharges, then to remain constant for the remainder of one million pulses. Previous testing with the Fairchild discharge initiation circuit had found plug resistance dropped to approximately 3 ohms in one million pulses, resulting in erratic thruster operation.

At Fairchild, work was funded by AFAL to modify the existing DI circuit to include the coupling inductor. It was determined to be beyond the scope of the contract to incorporate the JPL DI circuit design, however. Several million discharges were run with the coupling inductor replacing the original coupling resistor. The results indicated an initial drop from 90 ohms to approximately 10 ohms in less than 200,000 pulses. The plug resistance then stabilized for the remainder of the 4 million discharges at between 5 and 20 ohms, as shown in Figure 4.

Additional work at Fairchild funded by AFAL included anode electrode erosion studies.<sup>(11)</sup> Previous testing at Fairchild had revealed an unacceptably high erosion rate of the anode

electrode (12 micrograms/discharge). Fairchild investigated three avenues to reduce the erosion rate. First, alternate materials were investigated. Second, changes were made to

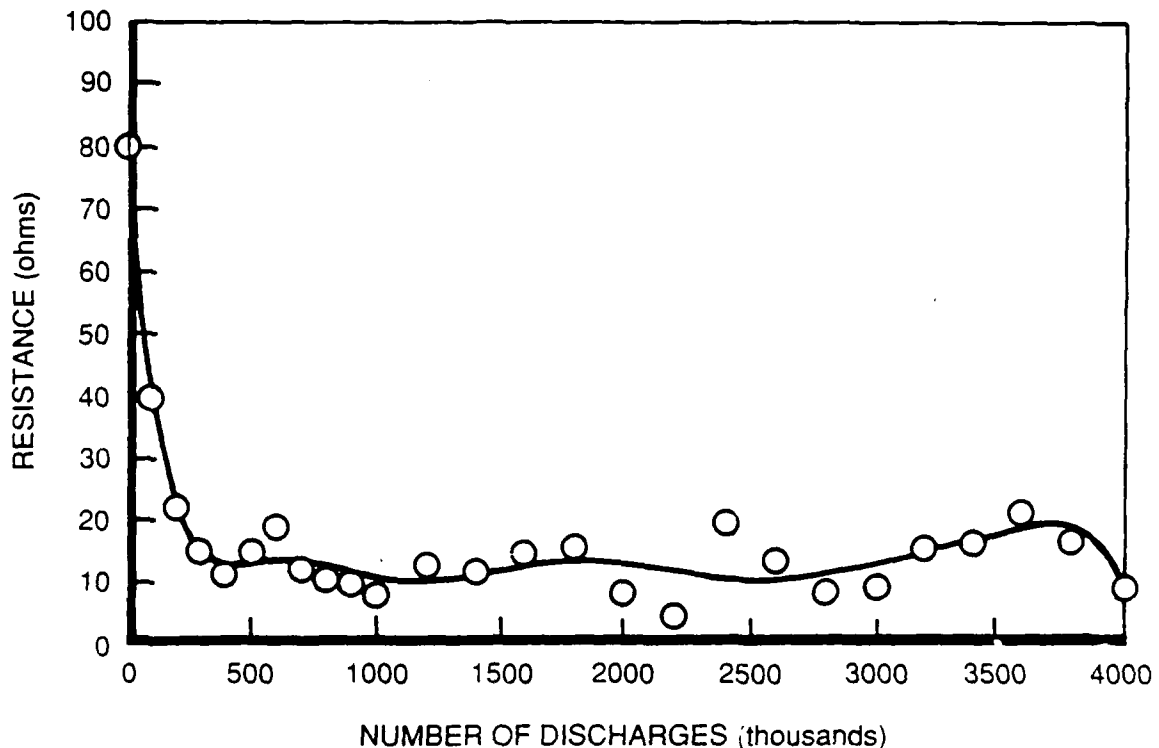


**Fig. 4. Igniter Plug Resistance as a Function of Number of Discharges**

the anode geometry. And finally, the discharge energy was reduced to determine its effect on the erosion rate. The results proved very interesting. In the materials testing, copper was found to have the lowest erosion rate per discharge for any material tested, except graphite. The results are summarized in Table 1. The appearance of the metals tested in the Fairchild results indicated that the erosion mechanism was melting due to a high heat flux to the anode surface. The next tests were then performed with modified anode geometries in an attempt to reduce the heat flux to the anode. By combining a thermal analysis with the motion of the arc along the electrodes, a conclusion was reached that longer electrodes should be used to reduce erosion. Basically, this was a means of reducing the residence time of the arc on the upstream surfaces of the anode electrode. When electrode length was increased from 2.75 in. (7 cm) to 5.8 in. (14.7 cm), the erosion rate dropped from 12 micrograms/discharge to 1.9 micrograms/discharge. A further increase in length to 6.8 in. (17.3 cm) lowered the erosion rate to 0.76 micrograms/discharge. A 200,000 pulse test of the 6.8 in. electrodes revealed no apparent melting on the anode surface. The success of this method in reducing anode erosion prompted Fairchild to implement this design change and forego the plans to lower the discharge energy, although a modification of the discharge initiation circuitry was made to reduce deposits on the spark plug, as described above.

At the completion of these technology programs, AFAL planned to integrate all the design improvements into a single flight-prototype thruster. A 14 million pulse life test was planned for an in-house facility at AFAL. Fairchild was contracted to build the flight-

**Table 1. Results of Materials Testing**

| <b>Anode Material</b>           | <b>Number of Discharges</b> | <b>I<sub>AVE</sub> (MLB-S)</b> | <b>I<sub>sp</sub>(s)</b> | <b>Anode Erosion Per Dischg. (μg)</b> | <b>Cathode Erosion Per Dischg. (μg)</b> | <b>Anode Erosion per Total Impulse (mg/lb-s)</b> |
|---------------------------------|-----------------------------|--------------------------------|--------------------------|---------------------------------------|---|--|
| Copper                          | 103,508                     | 5.42                           | 1,660                    | 11.99                                 | 4.36                                    | 2.214  |
| Graphite                        | 101,452                     | 4.53                           | 2,180                    | 4.59                                  | 3.17                                    | 1.012  |
| Thoriated Tungsten              | 98,148                      | 5.23                           | 1,820                    | 40.25                                 | 4.10                                    | 7.694  |
| Tantalum                        | 101,800                     | 5.36                           | 1,800                    | 27.72                                 | 1.76                                    | 5.171  |
| Tungsten Coated Copper (10 MIL) | 101,489                     | 5.39                           | 1,810                    | 15.16                                 | 1.55                                    | 2.812  |
| Arc Cast Molybdenum             | 100,207                     | 5.37                           | 1,780                    | 16.93                                 | 3.48                                    | 3.158  |
| 25% Copper 75% Tungsten         | 100,953                     | 5.40                           | 1,750                    | 27.81                                 | 3.86                                    | 5.155  |
| Platinum                        | 95,222                      | 5.36                           | 1,500                    | 22.79                                 | 1.18                                    | 4.252  |

prototype thruster. One unit was built and delivered to AFAL for the in-house life test. During the AFAL in-house test, a second unit was built by Fairchild. The AFAL test encountered difficulties with the capacitors and the feeding of the fuel bars. The Maxwell capacitors were failing after several hundred thousand pulses and the fuel bars in the helical feed system were jamming and failing to feed, which resulted in increased electrode erosion. A catastrophic capacitor failure ended the AFAL life test by damaging the facility with less than one million pulses on the thruster. The difficulties encountered in the thruster test program led AFAL to suggest design changes in the second flight prototype unit under construction at Fairchild. Specifically, the feed system design was identified as a potential problem area. The capacitors were also an area of ongoing concern. AFAL funded Sandia National Laboratories to provide capacitors based on the perfluorocarbon liquid/plastic film capacitor technology developed by Dr. Mauldin. It was determined that waiting for these capacitors would create too long a delay in the program, since a life test was deemed extremely important to the planned Advanced Technology Development (ATD) program for the PPT. Therefore, the decision was made to begin a life test with Maxwell capacitors of the old castor oil, K-film, and paper design.

The life test of the second flight prototype thruster was a competitive procurement won by the McDonnell Douglas Astronautics Company (MDAC). MDAC did not possess the background knowledge of the PPT which Fairchild did, but MDAC automated test facilities promised to expedite the performance of the life test. Unfortunately, the MDAC test met with an early capacitor failure as well. The capacitor failure resulted in damage to the thruster and the facility. MDAC was not prepared to repair the PPT damage under their contract, so the life test came to an abrupt halt. The AFAL decided to contract with industry for a second try at the 14 million pulse life test. This time, the Sandia capacitors would be ready and made available for use in the life test. This competitive procurement was awarded to RRC and will be described in detail in the following section of this report.

## PROGRAM DESCRIPTION

The "Pulsed Plasma Mission Endurance Test" program was awarded to RRC in 1985 by the AFAL (then AFRPL). The prototype flight thruster was at that time almost eight years old. It had been under life test at McDonnell Douglas Astronautics Company (MDAC) in 1983, when a Maxwell capacitor of the castor oil type failed, ruptured its case, and released oil into the vacuum chamber. In addition to the oil contamination of all of the thruster components and the cryo pump, the capacitor explosion had damaged the stripline which carried the current to the electrodes. Figure 5 illustrates the condition of the stripline following the capacitor explosion. The intent of the RRC program was to clean up the oil, repair the thruster, and start a new life test. Under a separate program, AFAL had obtained the first of the new Sandia capacitors and expectations were high that these capacitors would provide the missing element to a successful 14 million pulse life test.

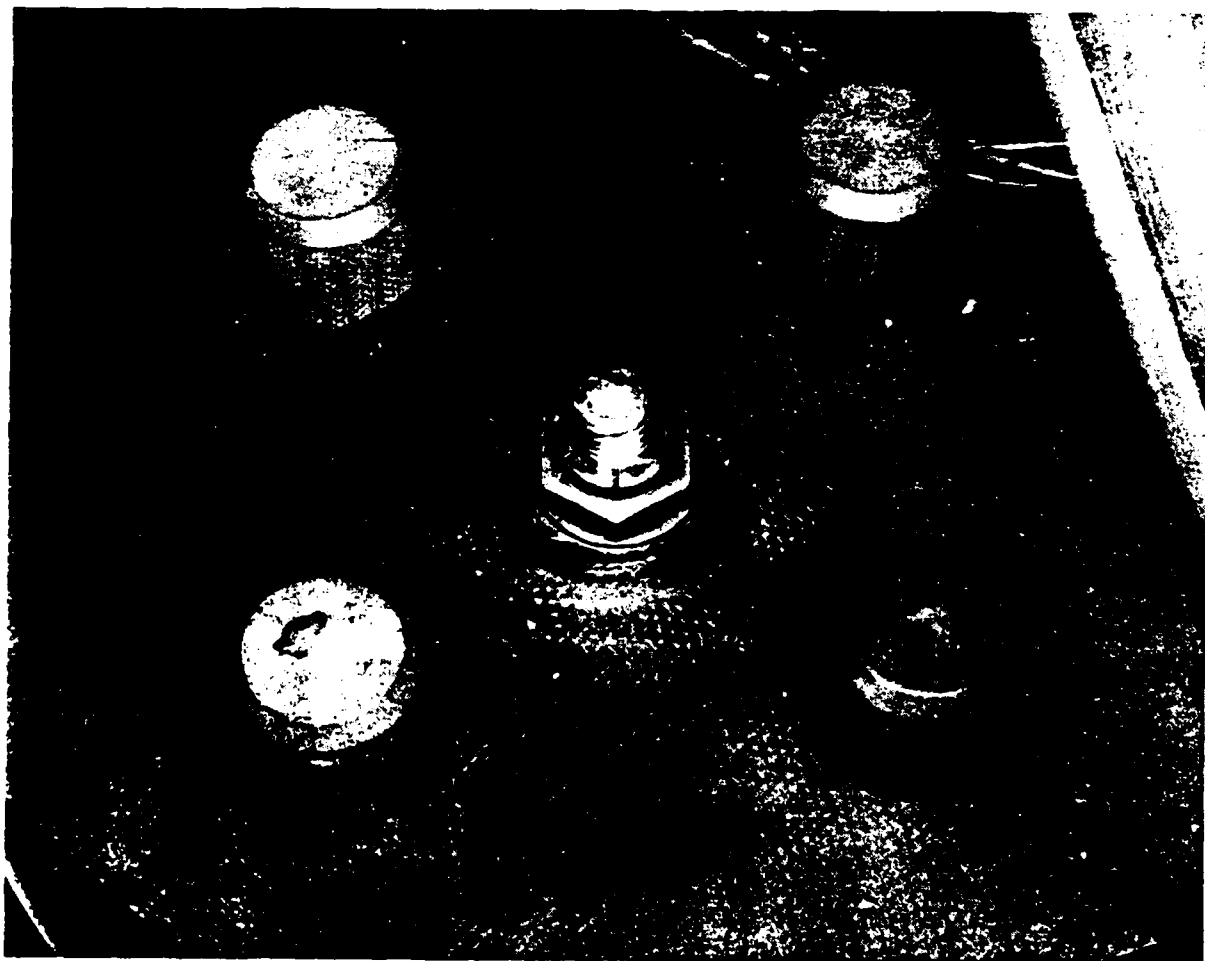


**Fig. 5. Stripline Damage from Capacitor Failure**

However, the program began on a sour note. During shipment of the test hardware from California, damage to the equipment was sustained due to improper packing and securing of the components. Upon arrival at RRC, the items which had been damaged included the thrust stand, the thruster nozzle and electrodes, and the thruster control console and cryo

pump compressor housing. Most severely damaged was the thrust stand, which had been improperly secured inside the vacuum chamber and had pivoted approximately plus or minus 30 degrees repeatedly during the transfer. The movement sheared off both Bendix flexures, knocked loose the LVDT core assembly, and damaged the micrometer set point indicator. A survey of the damage was made as soon as it was discovered upon arrival at RRC and the AFAL project manager and AFFTC contracts were notified immediately. A copy of the damage assessment is included as Appendix A of this report. As a result of this incident, RRC requested and was granted two Engineering Change Proposals (ECPs) - one to perform a thorough damage assessment of the thrust stand and a second to perform repairs to the items damaged in shipment.

A major delay in the program schedule was incurred due to the damaged Government Furnished Property (GFP), but enthusiasm at RRC was still high for the start of the life test. However, more difficulties were encountered that were not previously anticipated, such as the lack of documentation for the MDAC-modified test console, which meant that a complete rework of the ground test console wiring had to be performed.

At the same time, Physics International (PI) was proceeding under subcontract to RRC to develop a new Discharge Initiation (DI) circuit. This effort was progressing quite well, with a benchtop version of the DI circuit tested to 14 million pulses with no failures. The DI circuit was completed and delivered to RRC in October of 1985. A final report on the DI circuit development subcontract is included as Appendix B of this report. Details of the development and testing of the DI circuit can be found in this appendix. The design of this new DI circuit was based on the work performed at JPL under the earlier AFAL contract examining spark plug degradation.<sup>(12)</sup> Figure 6 shows the JPL design compared with the RRC/PI design. The basic change from the JPL DI circuit design was the replacement of the Krytron switch with an SCR switch, which both improved the lifetime and made the design compatible with a flight-prototype thruster.

The Sandia capacitors were gradually being fabricated and shipped to RRC. As they began to arrive, the problem of acceptance testing of the capacitors was addressed. Originally, the capacitors were to be fully acceptance tested when shipped to RRC. However, delays in fabricating the capacitors and changes in AFAL plans, including the close-out of the AFAL in-house capacitor test facility, transferred this responsibility to RRC. An ECP was submitted for the capacitor acceptance testing. The first problem encountered was the lack of adequate voltage hold-off capability in the GFP vacuum chamber electrical passthroughs. The passthroughs were not rated to the full 3000 V required to perform a capacitor hi-pot test. During thruster operation, the passthroughs were required to handle only 28 V input from the ground test console power supply to the thruster power converter, which supplied the full 2300 V capacitor charging voltage. This presented a problem for the capacitor acceptance testing, since there were no other access ports available for electrical passthroughs. This fact, coupled with the lack of an adequate high voltage power supply, led RRC to subcontract with Physics International (PI) to perform the capacitor acceptance testing. PI had the proper facilities and trained personnel in the pulsed power area, which made them an ideal candidate for the capacitor acceptance tests. The ECP was approved by AFAL and the capacitor acceptance testing was performed by PI under sub-contract to RRC. RRC, PI, and AFAL coordinated plans for the test procedures which were used by PI in the acceptance tests. These procedures were also coordinated with Dr. Mauldin at Sandia.



The capacitor acceptance testing consisted of the following steps:

1. Each capacitor was logged by serial number when it arrived. A separate log book was kept for each capacitor. A photo was also made of each capacitor's condition upon arrival.
2. Capacitance and Equivalent Series Resistance (ESR) of each capacitor was measured and logged.
3. Capacitors were hi-potted to their rated voltage +20 percent for 5 minutes. Afterward, capacitance and ESR were again measured and logged. Capacitors were visually inspected for defects.
4. Capacitors were vacuum soaked at  $10^{-4}$  torr for 4 hours. Afterward, they were removed and visually inspected for defects.
5. Capacitors were hi-potted in vacuum at 3kV for 10 minutes and then at 2 kV for an additional 10 minutes. Afterward, capacitance and ESR were measured and recorded and a visual inspection was made. If visual defects were found a photo was taken and placed in the log book.
6. Capacitors were then replaced in the vacuum chamber and pulsed at 0.2 Hz into a resistance which created a 20 percent voltage reversal. This test was continued for 2 hours. Capacitor temperature was recorded as a function of time at fifteen minute intervals. Capacitor voltage and current were also recorded.
7. Following the duty cycle test, the capacitors were removed and inspected for visually apparent defects. Capacitor ESR and capacitance was also measured. A photo of each capacitor was also made and placed in the log book.

The basis for rejection of a capacitor from these tests was determined from one of the following criteria:

1. A change in capacitance (plus or minus 5%)
2. A change in ESR (plus or minus 5%)
3. Evidence of physical change (can bulging, etc.)
4. Excessive rise in temperature during 0.2 Hz testing ( $>5^{\circ}\text{C}$ ).

The results of the capacitor acceptance testing are described in the following section. A complete report documenting the tests is included as Appendix C.

In parallel with the capacitor acceptance testing at PI, work was continuing at RRC on the repair and cleanup of the GFP test hardware. The thrust stand was remounted on new Bendix flexures and the LVDT was replaced. The test console was rewired and tested for correct signal output. The thruster was completely disassembled and thoroughly cleaned to remove the oil from all components. The stripline was removed and repaired with Kapton tape where the insulation had cracked. Some elements were completely replaced. These included the Discharge Initiation (DI) circuit and the capacitor housing assembly. A new capacitor housing assembly was required to provide an improved thermal path for heat



removal from the Sandia capacitors. To maximize the conducted heat path, RRC selected copper as the material, in spite of the fact that this added some 25 pounds of weight to the thruster. The removal of heat from the capacitors was judged to be more important for the life test, than maintaining a reduced weight configuration. The RRC capacitor housing design is shown in Figure 7. The bottom plate was dished out to conform with the bottom of the capacitor cans to provide a good conduction path across the interface. In addition, silicon heat transfer grease was used to ensure good heat transfer. Discussions with Dr. Mauldin at Sandia indicated that the capacitors were designed to reject heat at the ends with most of the heat rejected through the bottom or the end opposite the electrodes. Therefore, the RRC designed housing utilized 1/2 inch thick copper plate for the lower thermal shunt. The thermal shunt was linked directly to the water-cooled baseplate of the thruster. The top plate was fabricated from 1/4 inch copper sheet and provided the mounting surface for the capacitors. The two plates of copper were held together with a series of 16 tie rods, as shown in Figure 7.

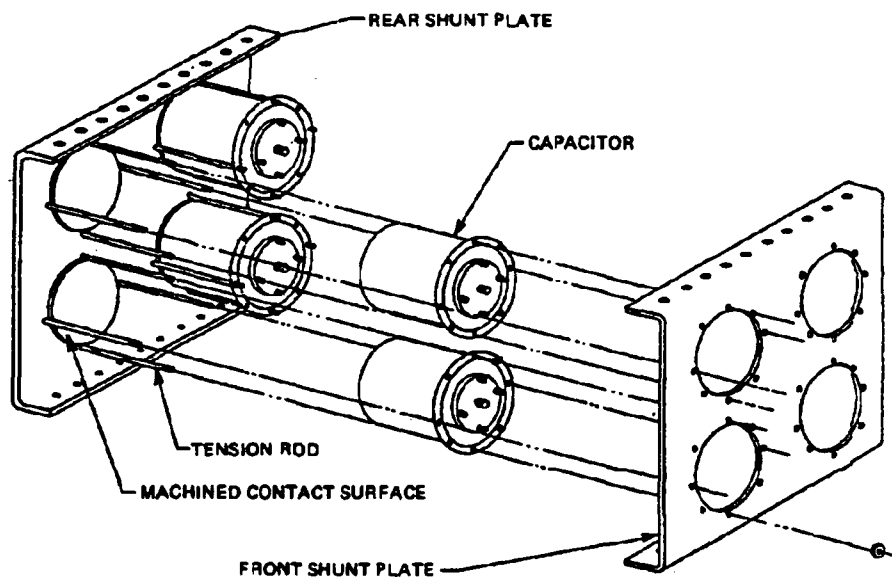


**Fig. 7. PPT Thermal Shunt Capacitor Cage**

After the completion of the thrust stand repairs and the ground test console rewiring, a calibration of the thrust stand was performed using the rolling ball calibrator. The rolling ball calibrator was designed by Fairchild to provide an impulsive calibration of the swinging arm thrust stand. It was necessary to provide an impulsive calibration since the PPT pulses were of only about 30 microseconds duration. The rolling ball calibrator operation is described schematically in Figure 8. The balls are of known mass and are released down a ramp to achieve a known velocity. The balls strike a target plate attached to the thruster and impart energy into the thruster via an elastic collision. The thruster recoils and the thrust stand measures the deflection. A stripchart recorder was used to record the signal output of the LVDT. The pulse shape and amplitude were used to calculate the impulse measured by the thrust stand, which was then compared to the actual impulse calculated from the known mass and velocity of the ball, and the empirically measured rebound distance.<sup>(13)</sup> Adjustments to the LVDT sensing element were made as required to bring the thrust stand measurement into line with the theoretical value.

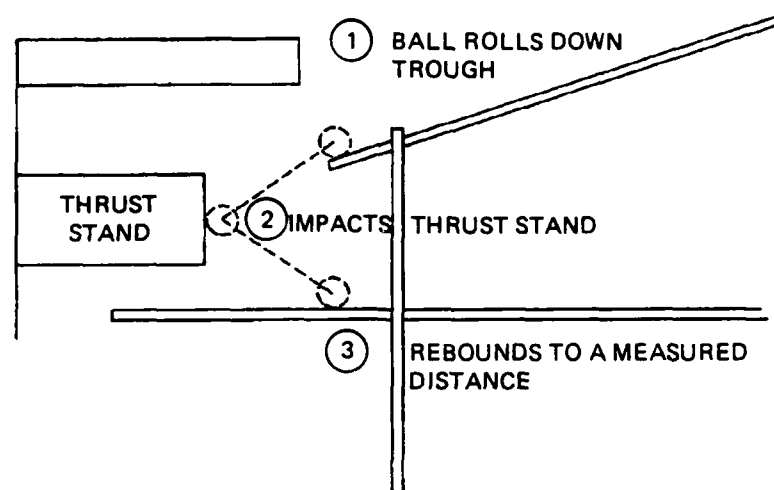


**Fig. 8. Rolling Ball Calibrator Schematic**

Once the calibration of the thrust stand was completed, only the integration of the thruster, thrust stand, and wiring into the test vacuum chamber remained to prepare for the start of the life test. A test plan was prepared and submitted to AFAL for review. The test plan documented the procedures to be followed in the life test, the data to be taken, and contingencies in case of failure. A copy of the test plan is included with this report as Appendix D. At this time, another setback to the program occurred. During the mounting of the thruster onto the thrust stand, one of the new Bendix flexures was broken and the other was potentially damaged. The cause of this mishap was traced to a Fairchild document showing the installation of the Bendix flexures. The drawing was poorly labeled, leading to confusion over which end of the flexure was to be oriented up. Because of this, the flexures had been installed upside-down and had failed when the weight of the thruster was placed on the stand. Fortunately, extra flexures had been ordered as spares, so the impact to the program was relatively minor. The incident, however, pointed out once again the difficulties of working with an unfamiliar system that is not well documented. Following replacement of the flexures, a calibration of the thrust stand was made inside the vacuum chamber with the thruster in place on the stand. Preparations were underway for the start of the life test.

The first attempt to start monitored testing of the thruster came on April 18, 1986. The entire test system had been checked out under atmospheric conditions and appeared ready for test. Every operation short of actually firing the thruster had been performed without an indication of a problem. The next step was to pump down the vacuum chamber and begin checkout firings of the thruster. These firings were to be monitored by RRC test personnel for the first several thousand shots before placing the test in a completely automated mode. The vacuum system for the test chamber consisted of a small roughing pump to evacuate the chamber into the  $10^{-3}$  torr pressure range, where the large cryo pump could take over and bring the chamber pressure down to its ultimate  $10^{-6}$  torr for the thruster testing. Such a low background pressure was required not only to properly simulate the operating conditions of space, but also to ensure that spurious arcing did not occur inside the thruster in the high voltage sections of the capacitor charging circuit. The first time the pumping system was operated, the roughing pump was unable to achieve the required pressure for hand off to the cryo pump. After several attempts to solve the problem by searching for

leaks, tightening the door seal, and reworking the roughing pump, a decision was made to attempt the hand off to the cryo pump at a slightly higher than desired pressure. The only problem that this potentially posed was that the cold surfaces within the cryo pump might be saturated with gas molecules after a short time and the chamber would have to be opened to allow the frozen gases to be "boiled off". Since this was to be a short test to verify the operation of the thruster, the decision was made to proceed. The cryo pump operated satisfactorily despite the higher pressure hand off. A pressure of  $10^{-5}$  torr was achieved and a thruster firing was attempted. The firing circuit indicated a malfunction and after several tries to recycle, the test was aborted. The problem was later traced to the spark plug. Plug resistance was low, resulting in the same type of erratic thruster firing that had been seen earlier at Fairchild. The plug was removed and replaced with a spare plug obtained from AFAL. Another checkout test was attempted with the new plug on May 9, 1986, but this time the vacuum system was not able to even approach the hand off pressure range. RRC test personnel spent several days tearing down and rebuilding the GFP pump to ensure that its internal seals were good and that it was operating correctly. Finally after several tries and failures to pump down the chamber, a decision was made to substitute an RRC roughing pump for the GFP pump to prevent further program delays. This solution resolved the vacuum problem and a test was successfully run on May 30, 1986. Five single shot pulses were fired. All indications were that the thruster was operating normally. After each pulse the vacuum indicator rose suspiciously high and did not recover completely to the original level. After the fifth shot, it did not recover below  $10^{-4}$  torr, thus necessitating that the test be halted and the chamber opened.

The problem this time turned out to be the cryo pump. Apparently, the inner array had been contaminated by the castor oil from the MDAC test failure. This did not pose a problem when pumping the heavier molecules, such as those comprising the air in the chamber. However, when the thruster exhaust products were pumped, light elements such as hydrogen were released, and the cryo pump could not properly evacuate them from the chamber. The cryo pump inner elements had to be replaced before testing could continue, resulting in yet another unanticipated delay. The cryo pump repair was completed on June 27, 1986.

Another checkout test was run as soon as the repairs were complete. This time twelve single shot firings were made, all without incident. The vacuum recovery was now almost instantaneous after each pulse. The thruster fire control was set to automatic after the 12th shot to begin the monitored automated test, but a malfunction occurred and the capacitors would not charge. The problem was traced to an arc in the capacitor dump relay box external to the thruster. This box was not a part of the thruster, but rather a safety feature to provide a means of discharging the capacitors should a failure result in the capacitors being left in a charged state. This problem was repaired and the test was scheduled for restart on July 3, 1986. Upon restarting the test, only one single shot was successfully fired. On the second attempt, the bank would not charge. This symptom was indicative of internal arcing, leading to a suspicion of the dump relay box again. However, on examination, no signs of arcing could be found in this location. Continuity checks were made that confirmed the insulation was sound in the relay box. The thruster was therefore removed from the chamber to facilitate more complete inspection of the unit.

The thruster disassembly and inspection revealed what appeared to be evidence of arcing across the surface of the insulators separating the electrodes. A black deposit had built up

on these surfaces. The black deposit was suspected to be providing a carbon trail on the surface for the arc to discharge across. The insulators were removed and cleaned by sandblasting and then chemically cleaning the surface. The thruster was reassembled and an attempt was again made to get the life test underway. On the first single pulse firing attempt, the same thruster malfunction was observed. Arcing was again visible from within the thruster. The test was halted and the thruster was removed from the chamber. Each time the chamber had to be opened after a wait of several hours to allow the cryo pump to warm up. This resulted in the loss of an entire day even if the failure was detected early in the morning. A complete D&I of the thruster was now felt to be warranted, even though it would be time consuming and difficult.

When the capacitor housing was removed from the thruster, signs of arcing were apparent near the stripline/capacitor interface. Removal of the stripline revealed a heavy coating of black carbonaceous deposit on the surface of the capacitor insulator. Figure 9 shows the extent of the arcing and the deposit which was formed. This deposit was the source of the high resistance short which was preventing full charging of the capacitor bank. Further examination of the capacitor was made to determine what caused the arcing to occur. The most likely scenario involved the center mounting post adapter. The mounting post adapters were fabricated by RRC after the Sandia capacitors arrived with no center posts. The Sandia capacitor design varied from the Maxwell capacitor design in this regard, which meant that the Sandia capacitors would not interface with the stripline. Figure 10 illustrates the difference between the Maxwell and the Sandia capacitor electrode configurations. Apparently, no specification was included in the Sandia contract with AFAL documenting how the center post should be configured. RRC was faced with the problem of making the capacitors work with the existing stripline and decided upon the simple adapter design shown in Figure 11. This seemed to be an adequate solution, provided two nuts were used to clamp the stripline securely to the center post adapter. In the case of the arcing which occurred at the center post, what had apparently happened was that the lower nut, underneath the stripline, had dropped off the bottom of the 1/4-20 threaded portion of center post adapter, thus breaking the surface contact with the stripline and resulting in an arc.

This assessment of the incident led RRC to redesign the center post adapter with a mounting shoulder to make contact with the stripline, and with improved contact to the Sandia capacitor center electrode. The revised mounting adapter design is shown in Figure 12. These adapters were fabricated and installed on four of the Sandia capacitors, including the one which had a coating deposited by the arc from the earlier testing. This capacitor had been thoroughly cleaned to remove all visible traces of the deposit. The thruster was reassembled and prepared for another attempt at the start of the test. The next try occurred on August 22, 1986. The chamber was evacuated to  $10^{-5}$  torr backpressure. Upon giving the single shot command to the thruster, internal arcing was observed and the thruster did not fire. No further shots were attempted. The chamber was vented and the thruster was removed for inspection. Inspection revealed arcing had occurred on the same capacitor as the previous incident. As before, a thick black coating covered the top of the capacitor. Close examination revealed that the stripline was deformed into a slight upward bow. Two probable causes were identified for the arcing problems. The first was that stripline deformation dating back to the MDAC capacitor explosion was resulting in poor surface contact with the capacitor. The second was that the capacitor insulator was not capable of holding off the voltage, possibly due to damage incurred during the earlier arcing.

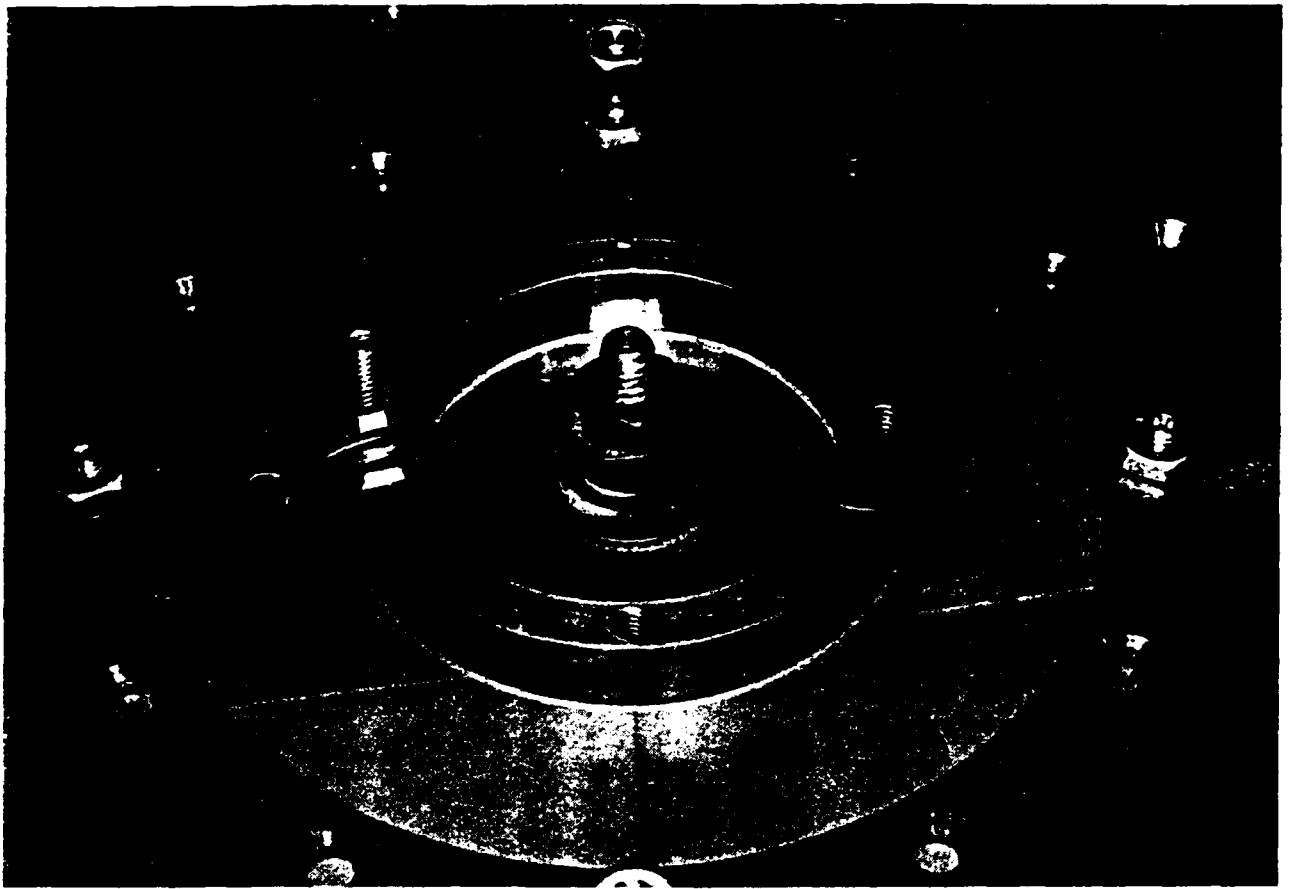


Fig. 9. Arc Damage and Carbon Deposit

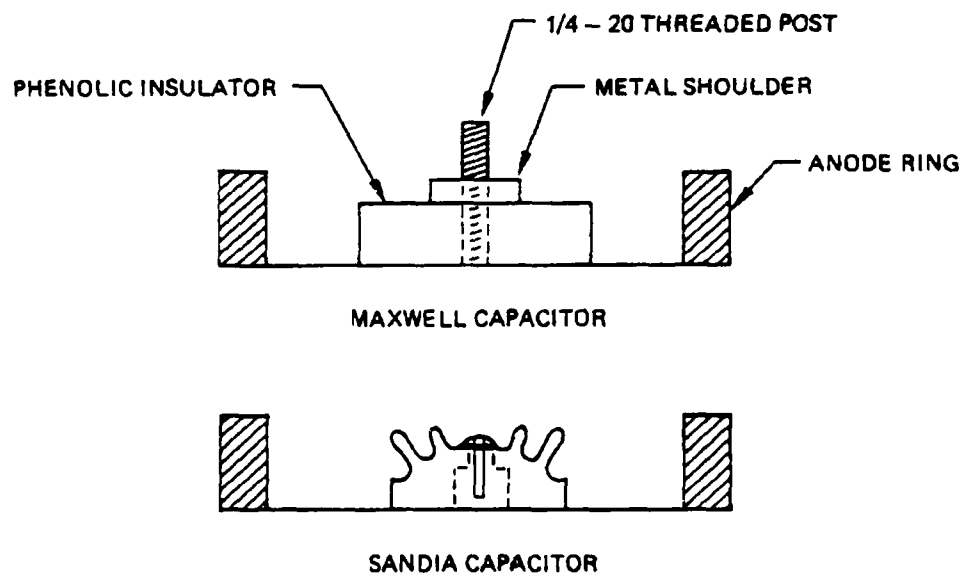
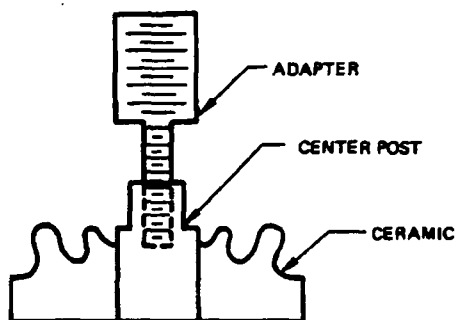


Fig. 10. Capacitor Center Electrode Comparison



**Fig. 11. Initial Center Post Adapter Design**

To resolve the stripline problem, an ECP was submitted to AFAL requesting authorization and funding to fabricate a new stripline. Details of the stripline design were obtained from the literature and by studying the existing stripline. Contact was also made with Dr. William Guman at Fairchild to determine some specifics of the construction, such as the type of adhesive used. A delay of several months was experienced while awaiting approval of the ECP. Finally, the ECP was negotiated in November 1986, and the stripline fabrication began in January 1987. A slow, careful process was followed to fabricate the stripline, since its integrity was crucial to the testing. First, samples of the NEMA board material were bonded with the Hysol adhesive recommended by Dr. Guman. Various adhesive application techniques and clamping pressures were experimented with to achieve a uniform adhesive layer, free of voids and with good bond integrity. After a number of these samples had been made, the parts were fabricated for the new stripline and preparations were made to join them together. The individual pieces of the stripline assembly are shown in the exploded view of Figure 13. The conductor element was fabricated from a sheet of 0.032 inch thick oxygen-free copper. This was sandwiched between two sheets of NEMA board (epoxy-impregnated Fiberglass). A third sheet of NEMA board was cut to the contour of the copper sheet and was also sandwiched between the outer two insulators. This effectively surrounded the copper on all sides with the NEMA board. Holes were cut in the insulator at the positions where it would attach to the capacitors. A tab of the copper extended out in the center for connection to the electrode assembly. The fabrication and bonding process proceeded smoothly and the new stripline turned out very well.

Once the new stripline assembly was completed, a hi-pot test was conducted in the vacuum chamber to check for insulator soundness. The stripline held off 3000 V at  $10^{-4}$  torr backpressure. The thruster was again reassembled and preparations were made to start the life test. On May 6, 1987, the thruster was given a single shot command to fire, but once again an internal arc was the result. Subsequent firing attempts demonstrated the same type of behavior seen in the earlier tests where the capacitors were shorting. The thruster was torn down again to find the source of the arcing. This time the traces of arcing were seen at two capacitor center posts. The conclusion determined from this result was that the insulator rings on the Sandia capacitors were not effective at holding off the 2300 V maximum charging voltage between the center post and the anode ring.

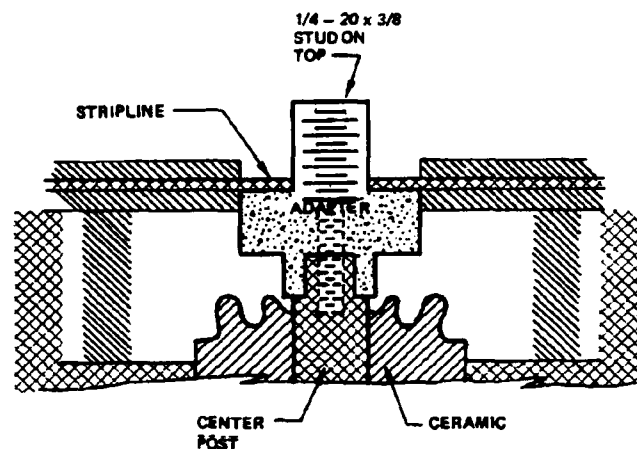


**Fig. 12. Modified Adapter Design with Shoulder**

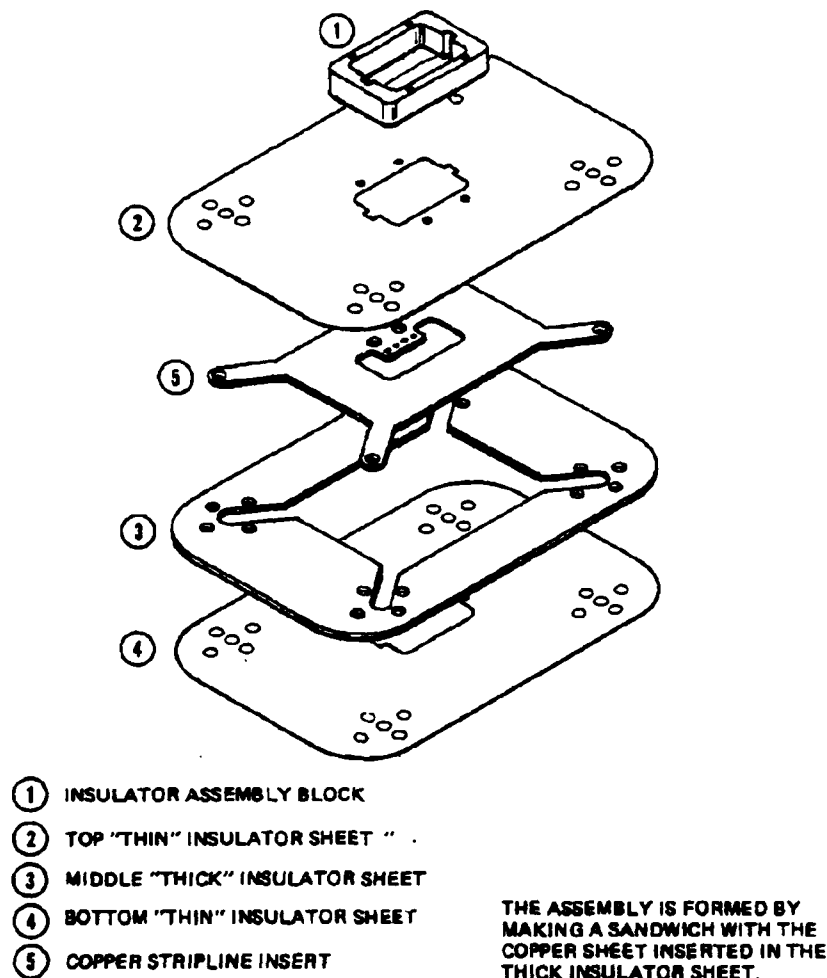


**Fig. 13. Stripline Exploded View**

The insulator problem should have been found in the vacuum hi-pot tests or in the vacuum cycling tests at PI, but was not, possibly because the center post adapters were not used in that test series. The insulator deficiency required a modification to the entire capacitor electrode area. The insulator modification involved filling the entire area inside the metal anode ring with a high dielectric strength epoxy to prevent a breakdown between the anode and the cathode. To expedite the restart of the life test, the epoxy was allowed to dry until tacky and then the capacitors were replaced in the thruster and the entire assembly was placed in the vacuum chamber and evacuated to a rough vacuum. This was done both to speed up the turnaround time to get the test underway and to ensure that any air pockets in the epoxy were drawn out under vacuum.

Following the insulation of the capacitor electrodes, the test was restarted with more single shot checkout firings. The insulation proved effective in preventing the internal arcing. Fourteen individual pulses were fired in single shot mode. The monitored portion of the automated test was not started, however, because the AC power breaker in the ground test console was tripping each time the thruster was fired. The problem was traced to the 28 V

power supply in the ground test console. The output of the supply was extremely noisy. Voltage spikes from this supply were causing the circuit breaker to trip when the thruster was fired. To expedite the start of the life test, the power supply was removed for repairs and replaced by an RRC-owned Sorenson 28 V power supply. Two shots were fired after the power supply substitution. Neither shot caused the circuit breaker to trip, but on the second shot, a thruster component failure occurred. This was evident because the telemetry indicated that the capacitors were instantaneously charged when the third firing attempt was made. Usually a slow charging profile was observed.

Subsequent investigation, including removal of the thruster once again from the test chamber, discovered that a charging lead was broken. This was repaired and the thruster was reassembled, replaced on the thrust stand, and the test was restarted. This time, after 30 successful single shot firings, the console was placed in automated firing mode and began firing the thruster once every ten seconds. The test proceeded nominally for 61 shots in automated mode, with thrust signals recorded on the strip chart recorder. Then the telemetry system recorded a thruster misfire. The console firing selector was switched back to single shot mode and another firing was attempted with an observer at the chamber port to look for arcing. Internal arcing was observed on this firing. The charging telemetry indicated that the capacitors would not fully charge. This was consistent with the previously observed behavior when internal arcing had occurred. However, because the capacitors were now completely insulated, the stripline/capacitor interface was not the first suspect. The thruster was disassembled and arc traces were found on the insulator surfaces around and between the electrodes. As a first step, these surfaces were removed and cleaned. Further checkout tests indicated that either the short was still present or the console control functions were not operating correctly. Several techniques were attempted to determine if the arcing was actually occurring, including placing mirrors inside the chamber to look inside the thruster and placing a current probe on the charging lead. These techniques were not successful at pinpointing the location, but did confirm that an internal discharge was taking place.

The next step taken was to completely disassemble the thruster and individually troubleshoot the electronic components. Through this process, an arc was discovered inside the DI circuit. This explained the thruster misfiring, but not the breakdown in the charging circuit prior to the maximum of 2500 V. The DI circuit problem was repaired and the thruster was returned to the vacuum chamber for further checkout tests. The firing sequence telemetry again indicated a breakdown prior to the maximum charging voltage, this time at approximately 800 V.

The only remaining possibility for a short was a breakdown in the stripline or internal shorting of the capacitors. The capacitor housing was therefore removed from the thruster and disassembled. Upon disassembly the problem was apparent. The epoxy insulator had not fully cured before the capacitors were placed in the thruster. As a result, the epoxy had sagged and left only a thin layer covering the upper side of the capacitor. After many discharges, this layer was not sufficient to withstand the voltage gradient and the arc punched through the insulator. Repeated firings to troubleshoot the problem created a thick layer of black deposit on the exposed surface. A second capacitor was found to have small arcing traces around the base of the center post. When the stripline was removed, the center post adapter dropped free. The small 4-40 threaded portion of the adapter had melted through. Apparently, the adapter did not have any surface contact with the center post



except through the threaded rod. This 4-40 screw did not have a sufficient cross section to carry the tens of thousands of amperes during the thruster discharge. These findings resulted in a second revision to the adapter design modification and a revised procedure for curing the epoxy insulator material.

The new adapter design consisted of two pieces, one of which was to be shrink-fitted over the exterior of the capacitor center post. The second piece attached to the first with a 4-40 screw which threaded down into the capacitor. The advantage of this design was that it maximized surface area contact between the capacitor, the adapter, and the stripline. Therefore, the current was no longer carried solely by the 4-40 screw. Figure 14 illustrates this new adapter design. Two new capacitors were insulated with the epoxy material and all of the capacitors were fitted with the new center post adapters. The thruster was carefully reassembled. Each individual component was checked out on the bench before being integrated into the thruster. This thorough pretest checkout was completed and the thruster was certified ready to begin the life test on October 21, 1987.

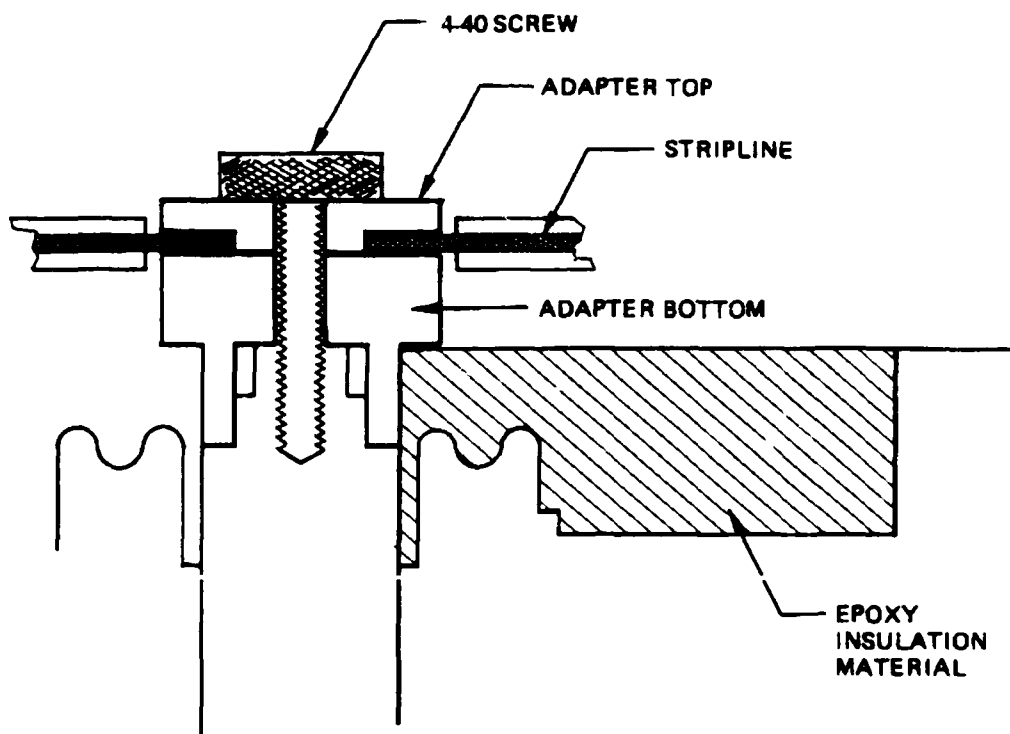
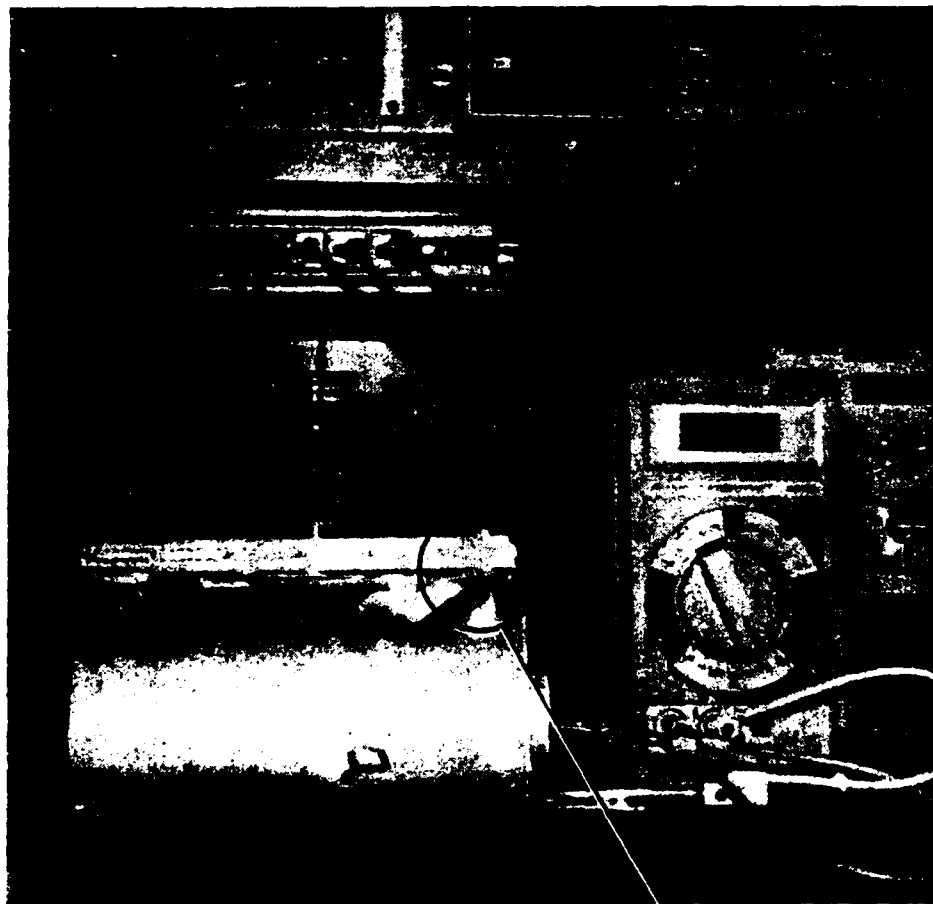


**Fig. 14. Two-Piece Adapter Redesign**

The first several single shot pulses were fired without incident. All telemetry, including thrust stand response and thermocouple readings looked normal. No indications of internal arcking were seen. The console fire control was switched to automatic after approximately 10 single shot firings. The transition was accomplished without incident and the firing rate was gradually increased from one shot every ten seconds to the final value of one shot every five seconds. The thruster continued to operate normally. Thermocouple readings were monitored at 250 pulse intervals for the first 1000 pulses. The only problem was a slow drift in the baseline of the thrust signal on the stripchart. An amplifier in the LVDT output channel was responsible for the drift. This did not affect the test and was corrected

by a periodic rezeroing of the signal, while attempts were made to adjust the amplifier gain. The test continued in automated mode for approximately four hours. At approximately 2:40 p.m., a failure of the number 2 capacitor occurred. The ground test console sensed the capacitor failure as a short in the load and switched to thruster malfunction mode. RRC personnel discovered the test was stopped and determined the cause to be inside the vacuum chamber. The chamber was vented and subsequent investigation revealed that the capacitor bank was reading a dead short on an ohmmeter. The thruster was then removed from the chamber and disassembled to allow inspection of the capacitor bank. This inspection found the number 2 capacitor had failed by shorting internally. The capacitor case was intact, but bulged out near the top flange, very close to the fill tube. Figure 15 shows the post-test condition of the capacitor.



NOTE: BULGE IN CASE

**Fig. 15. Capacitor SC 320 PC 014 Condition After Failure**

After the capacitor failure, the thruster was repaired by replacing the failed capacitor, and the thruster was prepared again to restart the life test. Confidence was now high that the problems which had prevented the conduct of the test were solved. The test was restarted on November 10, 1987. Although the thruster was firing correctly in automated mode most

of the time, a "double-pulse" anomaly was noted after the first few pulses. This "double-pulse" occurred when the charging current from the 28 V power supply did not cut off after the capacitors were fully charged, resulting in a rapid recharge of the capacitors and a secondary discharge. After approximately 30 pulses, the anomalous firings ceased. The test continued without incident for approximately 100 pulses, at which time the 28 V power supply failed. The test personnel shut down the system, replaced the 28 V power supply with the RRC Sorenson power supply, and restarted the test. The thruster fired normally for the first five pulses after restart, but then went into a continuous or very rapid discharge mode. The spark plug circuit wiring which runs outside of the chamber into the ground test console became very hot and began to melt away its insulation. The system was shut down manually by test personnel. After checking to ensure that no electrical fires had ensued from the overheated wiring, test personnel vented the chamber to look for an explanation. This was a very unusual failure, unlike any experienced previously on the program.

The strange continuous discharge, the large current drawn through the spark plug wiring, and the anomalous double pulsing were all viewed as clues to the cause of this failure. The capacitor bank did not show any indication of a failure, nor did the DI circuit. Electrical circuit troubleshooting revealed that the source of the failure was in the DC-DC power converter or the "black box." The converter had been manufactured in 1979 by Wilmore Electronics, a subcontractor to Fairchild. RRC technicians began troubleshooting the converter. A point of contact was located at Wilmore, because certain drawings were missing from the converter design package. These drawings were determined to be of the section of the converter which contained the defect. When reached, the contact at Wilmore informed RRC that the drawings were purposely omitted because they were considered proprietary to Wilmore. Without the drawings, the converter could not be easily repaired. Due to criticality of funds, Lt. Sanks was contacted at AFAL to inform him of this latest problem and asked for a determination of how to proceed. The AFAL decision was to terminate the contract at this point, rather than fund another ECP to repair the converter.

The cumulative record of failures under this program does not suggest optimism for the attainment of 14 million pulses with the current design. In accumulating just over 3400 pulses, seven separate failures were encountered due to internal arcing, one occurred due to a DI circuit flaw, another due to a capacitor failure, and a final failure was the result of a failure in the flight electronics package. The internal arcing failures were the direct result of a design mismatch between the Sandia capacitors and the thruster stripline. These problems could have been prevented with a design change to the capacitor electrode configuration, as demonstrated in the later tests at RRC. However, the premature failure of the Sandia capacitor, after fewer than 4000 pulses is not encouraging. The same is true of the flight electronics failure which ultimately ended the test. These two components; the capacitors and the flight electronics, appear to be the Achilles heel of the millipound PPT thruster.

## RESULTS

Although the objective of the PPT Mission Endurance Test was not met, many useful results were obtained in the course of the program. These results will be described in this section. Some of the results presented will be in the form of data which was gathered in the course of the program, while others are either troubleshooting methods which were found useful during the course of the program or cautionary remarks regarding pitfalls to avoid. The organization of this section will follow along the division between data and lessons learned. The first will be of interest for the current program, while the second section is included for the potential benefit of a future program.

### Test Program Data

The data gathered in the program include test results from the Discharge Initiation (DI) circuit development, the capacitor acceptance testing, and the start of the thruster life test. The first to be discussed will be that from the DI circuit testing. The DI circuit was bench-tested at Physics International (PI) for a total of over 15 million shots. One failure occurred after the required 14 million shots lifetime had been demonstrated. An SCR in the circuit failed in the vacuum testing. This failure was attributed to overheating during prior testing at 80 Hz. An interesting correlation between capacitor voltage droop and SCR temperature was found. Figure 16 illustrates these findings. The SCR heating was found not to affect operation in air, but may have caused a hermetic seal to fail, placing the junction under a vacuum and allowing internal arcing to occur. In the vacuum testing, 15 minutes of operation at 8 Hz was accomplished prior to the SCR failure. Following the SCR failure the circuit continued to operate at half voltage with the other good SCR. The bench test results demonstrated the capability of the DI circuit to perform the 14 million required pulses at a much more difficult duty cycle than the 1/5 Hz of the actual test. Details of the DI circuit design and testing are given in Appendix B.

The capacitor acceptance testing yielded many interesting results also. Even before the actual acceptance tests began at PI, results affecting the final capacitor design were discovered at Sandia. The first set of capacitors shipped to RRC from Sandia were not used after it was found that the EB-welding used to seal the cans had damaged the capacitor windings. A second set was manufactured using a modified welding method which lessened the probability of welding damage to the windings. Capacitor acceptance testing was performed at PI on a set of five Sandia capacitors. The results were: four passed, one failed. The failure occurred during the vacuum duty cycle pulsing test at approximately 52 minutes into the 2 hour test. A loud bang was heard by the technician conducting the test. The power supply meters indicated constant current flow and a constant voltage. The technician removed the charging cables and vented the chamber. An ohmmeter reading showed the capacitor to be shorted. Calculation of Equivalent Series Resistance (ESR) for the capacitor confirmed that an internal short had occurred. The pretest ESR was 0.104 ohm. The post-test value was 0.006 ohm. The capacitor temperature was not recorded as a function of time so no data was obtained on temperature rise prior to the failure. However, an examination of the test apparatus revealed that the coaxial cable supplying the power to the capacitor had failed, causing the capacitor to discharge through a low inductance short. The capacitor then failed by shorting internally. This capacitor was sent back to Sandia for a postmortem analysis.

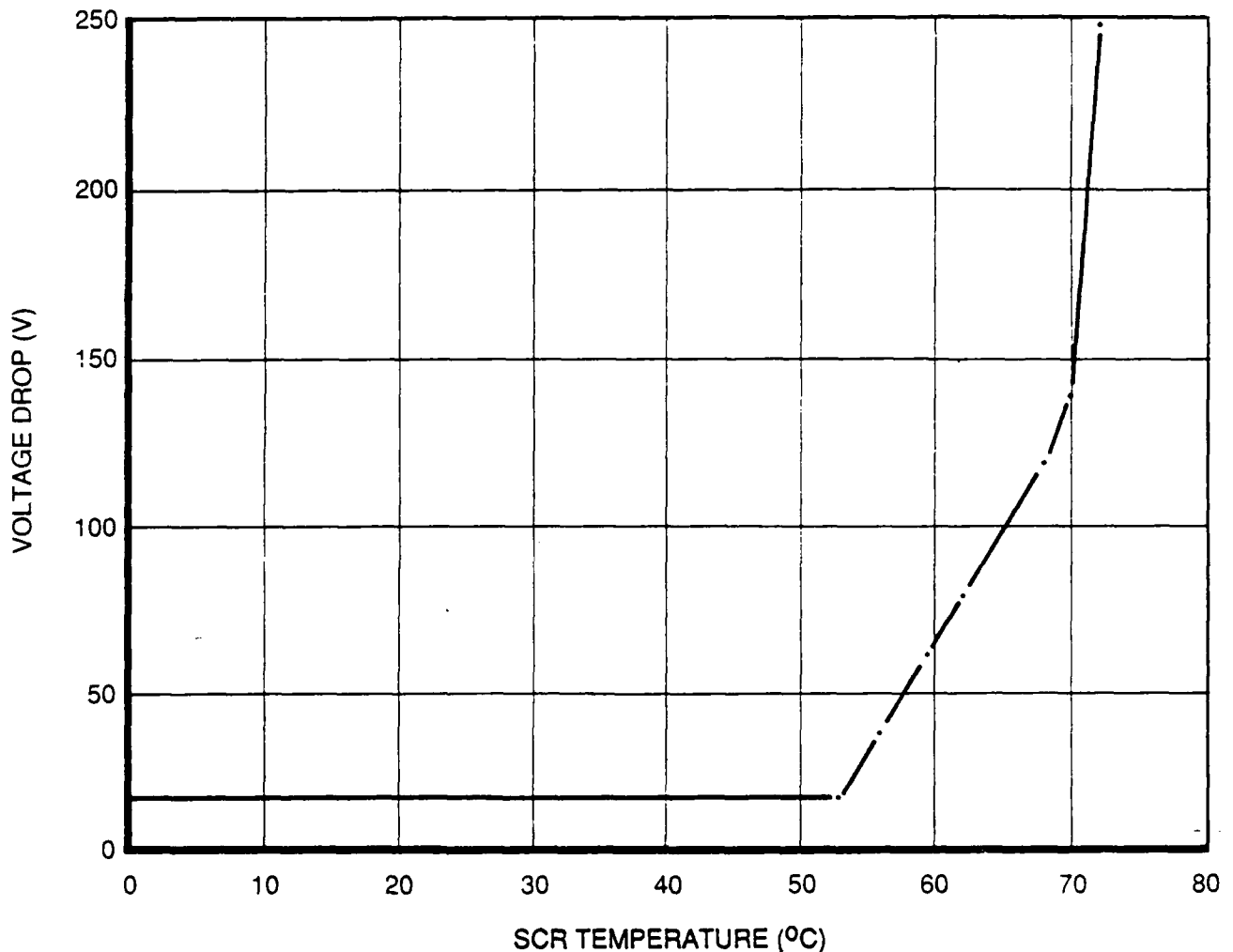


**Fig. 16. Storage Capacitor Voltage Drop as a Function of SCR Case Temperature for Operation at 80 Hz**

The results of the acceptance testing for the four remaining capacitors were used as a predictive tool to determine potential failure points. Table 2 gives the measured pretest and post-test values for the five capacitors tested at PI. Based on these results, PI personnel predicted that capacitor SC 320 PC 014 would probably fail in the life test. The variation in ESR was the chief basis for this prediction. In fact, this capacitor did fail only slightly more than 3000 pulses into the life test. This result increases confidence that such acceptance testing can be used as a screening process to eliminate capacitors which might fail in application. If placed into practice, such a procedure could be implemented as the capacitors are manufactured, thus preventing delivery of faulty units. The procedures used can easily be accomplished in less than one day and can also be automated, if desired. A side result of the capacitor testing at PI was the creation of a false impression of security regarding the voltage stand-off capabilities of the capacitor insulators. In tests at  $10^{-6}$  torr, the capacitors held off 3000 V in the hi-pot test and 2300 V in the duty cycle test. Since these conditions simulated the expected thruster operating conditions, no problems were anticipated. The

difference in the PI acceptance testing and the actual installation in the thruster was the center post connection. Figure 17 shows the connection used at PI for the acceptance tests. The high voltage cable is connected directly to the center-tapped post with a 4-40 threaded screw. This configuration probably prevented the type of arc-over encountered at RRC when the center post adapters were added to interface with the stripline. Pressure in the electrode region may have also played a role. In two separate instances recorded in the logbooks, PI technicians left voltage on the capacitors when venting the chamber, resulting in arc-overs. These arc-overs were the result of the rising pressure in the tank passing through the Paschen breakdown minimum. The values of ESR and capacitance for the capacitors involved did not change as a result of these incidents. However, one of the capacitors involved, SC 320 PC 014, was the capacitor which failed in the life test. The fact that the ESR had been fluctuating prior to this incident and that another capacitor, SC 320 AF 010, was involved in arc-overs at PI and previously at RRC, lowers the probability that the arcing caused any capacitor damage.

**Table 2. Results of Capacitor Acceptance Test**

|                                  | CAP #004        |                     | CAP #010        |                     | CAP #014        |                     | CAP # 015       |                     | CAP #016        |                     |
|----------------------------------|-----------------|---------------------|-----------------|---------------------|-----------------|---------------------|-----------------|---------------------|-----------------|---------------------|
|                                  | C<br>( $\mu$ f) | ESR<br>( $\Omega$ ) | C<br>( $\mu$ f) | ESR<br>( $\Omega$ ) | C<br>( $\mu$ f) | ESR<br>( $\Omega$ ) | C<br>( $\mu$ f) | ESR<br>( $\Omega$ ) | C<br>( $\mu$ f) | ESR<br>( $\Omega$ ) |
| As Received 2/11/86              | 57.3            | 0.15                | 58.0            | 0.11                | 58.7            | 0.302               | 57.8            | 0.11                | 57.5            | 0.11                |
| After Vacuum and High Pot in Air | 57.5            | 0.15                | 58.1            | 0.10                | 58.4            | 0.18                | 57.4            | 0.10                | 57.1            | 0.10                |
| After High Pot in Vacuum         | 57.6            | 0.15                | 58.1            | 0.10                | 58.1            | 0.23                | 58.1            | 0.10                | 57.7            | 0.11                |
| After Rep-Rate                   | 57.6            | 0.11                | 58.2            | 0.10                | 58.7            | 0.10                | —               | —                   | 57.8            | 0.11                |



**Fig. 17. High Voltage Connector Used at Physics International**

The preparations for life test at RRC produced a result of some significance. The amount of Teflon fuel in the thruster was determined to be sufficient for only approximately 9 million pulses, instead of the required 14 million. The determination was made via the following procedure. The weight of the Teflon remaining in the thruster was determined from measurements of the bars and the known density and mass properties of Teflon. The calculation is detailed in Table 3. The mass ablated per pulse was taken from measurements made at JPL to be 1.56 mg/pulse.<sup>(14)</sup> For a total mass of 13.87 kg of propellant, only 8.89 million pulses would exhaust the propellant supply. This assumes no feed system difficulties as the propellant bars grow shorter and it assumes a uniform ablation of the individual bars. Both of these assumptions are suspect. Therefore, the conclusion of this investigation was that the thruster was capable of achieving fewer than 8 million pulses with the fuel bars it currently held.

**Table 3. Calculation of Teflon Fuel in PPT Thruster**

|   |  |                                |
|---|--|--------------------------------|
| Teflon Density  | 0.077 lb/in <sup>3</sup>   | Ref. Weight Engineers Handbook |
| Inner Bar Volume:   | 2 x (26.8") x (3") x (0.5") = 80.6 in <sup>3</sup>   |                                |
| Middle Bar Volume:  | 2 x (44.51") x (3") x (0.5") = 133.5 in <sup>3</sup>   |                                |
| Outer Bar Volume:   | 2 x (61.05") x (3") x (0.5") = 183.15 in <sup>3</sup>  |                                |
| Mass = (ρ) x (Vol.)   |  |                                |
| ∴ Mass = M <sub>INNER</sub> + M <sub>MID</sub> + M <sub>OUTER</sub> |  |                                |
|   | = 2.82 kg + 4.67 kg + 6.41 kg  | = 13.89 kg                     |
|   | = (6.21 lbm) + (10.28 lbm) + (14.1 lbm)  | = (30.6 lbm)                   |
| Total Pulse @ 1.56 x 10 <sup>-3</sup> g/pulse                       |  |                                |
|   | $\frac{13.89 \text{ kg}}{1.56 \times 10^{-6} \text{ kg/pulse}} = 8.909 \times 10^6 \text{ Pulses}$ |                                |

A secondary conclusion was reached based on the above results that the fuel bar ablation was highly nonuniform. The measurements made on the fuel bars indicated that the inner bars had ablated much more than the outer bars or that the bars were intentionally made in different lengths to account for nonuniform ablation. The bar lengths as received at RRC are given in Table 4. the inner bars are obviously much shorter, and contain less mass in roughly the ratio of the bar lengths, because the other two dimensions of the bars are the same. Therefore, if the bars were not purposely made to account for a 2 to 3 times greater ablation of the outer bars over the inner bars, the inner bars would exhaust their fuel first and the thruster would operate in a degraded manner with the two remaining sets of bars. The consequences of this might be reduced impulse bit, higher electrode erosion, or even failure of the thruster to fire properly.

**Table 4. Lengths as Received at RRC**

|        |   |           |            |
|--------|---|-----------|------------|
| Inner  | : | 68.0 cm   | (26.8 in)  |
| Middle | : | 113.0 cm  | (44.51 in) |
| Outer  | : | 155.07 cm | (61.05 in) |

The initial set of firings of the thruster at RRC was troubled by stray arcing, but when firings were completed, the data taken indicated the thruster was operating as expected. Thrust stand data from the first automated firing are shown in Figure 18. The data have been analyzed to derive the impulse delivered per pulse. An individual pulse was digitized from the stripchart and expanded to show the detail of the pulse shape. Duration of the pulse is determined by the thrust stand response time. As such, the thrust stand signal is only an analog of the actual thruster impulse, but can be calibrated from the thrust stand response to the impact of the steel ball from the rolling ball calibrator. The calibration procedure developed by Fairchild was carefully adhered to by RRC personnel. This procedure is included as Appendix E. The thrust stand response to the steel ball impact is shown in Figure 19. The impulse delivered to the thrust stand can be calculated from the equation:

$$I = m_{\text{ball}}(V_{\text{ox}} + V'_{\text{ox}})$$

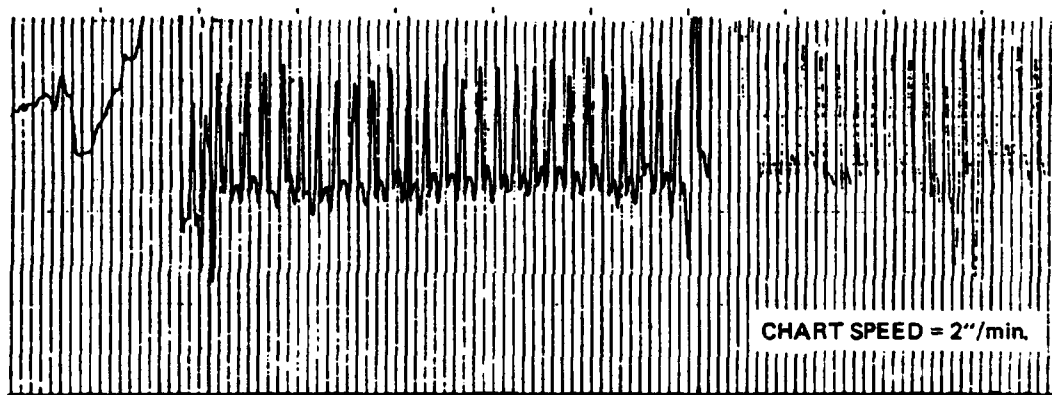


Fig. 18. Thrust Stand Data

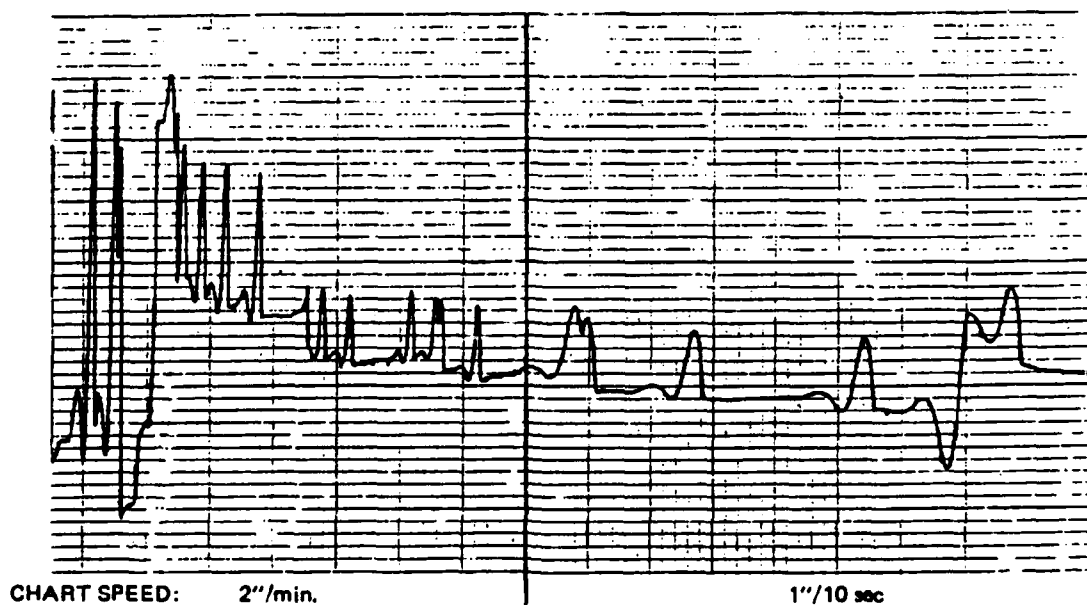


Fig. 19. Thrust Stand Response to Ball Calibrator



The area under the curve of the thrust stand response can therefore be assumed to be equal to the impulse derived by the above equation. The impulse delivered by the thruster firing can then be calculated by determining the area under the curve of the thrust stand response to the thruster firing, and then ratioing it to the area under the calibration response. The nominal impulse bit of the PPT discharge is 22 mN-s (5 mlbf-s). The results from the initial test series show a very repeatable impulse of 29 mN-s (6.5 mlbf-s). Later results in the two subsequent tests confirmed this thrust value, which is roughly 30 percent higher than the nominal.

The long duration (four hours) test accomplished one major goal of the program by obtaining temperature data on the capacitors. The data trends for all four capacitors begin to level off after approximately 2000 pulses, indicating that the capacitors are reaching thermal equilibrium. Figures 20-22 show the temperature as a function of pulse count for each of the four capacitors. Thermocouples were located on the top and bottom of each capacitor case.

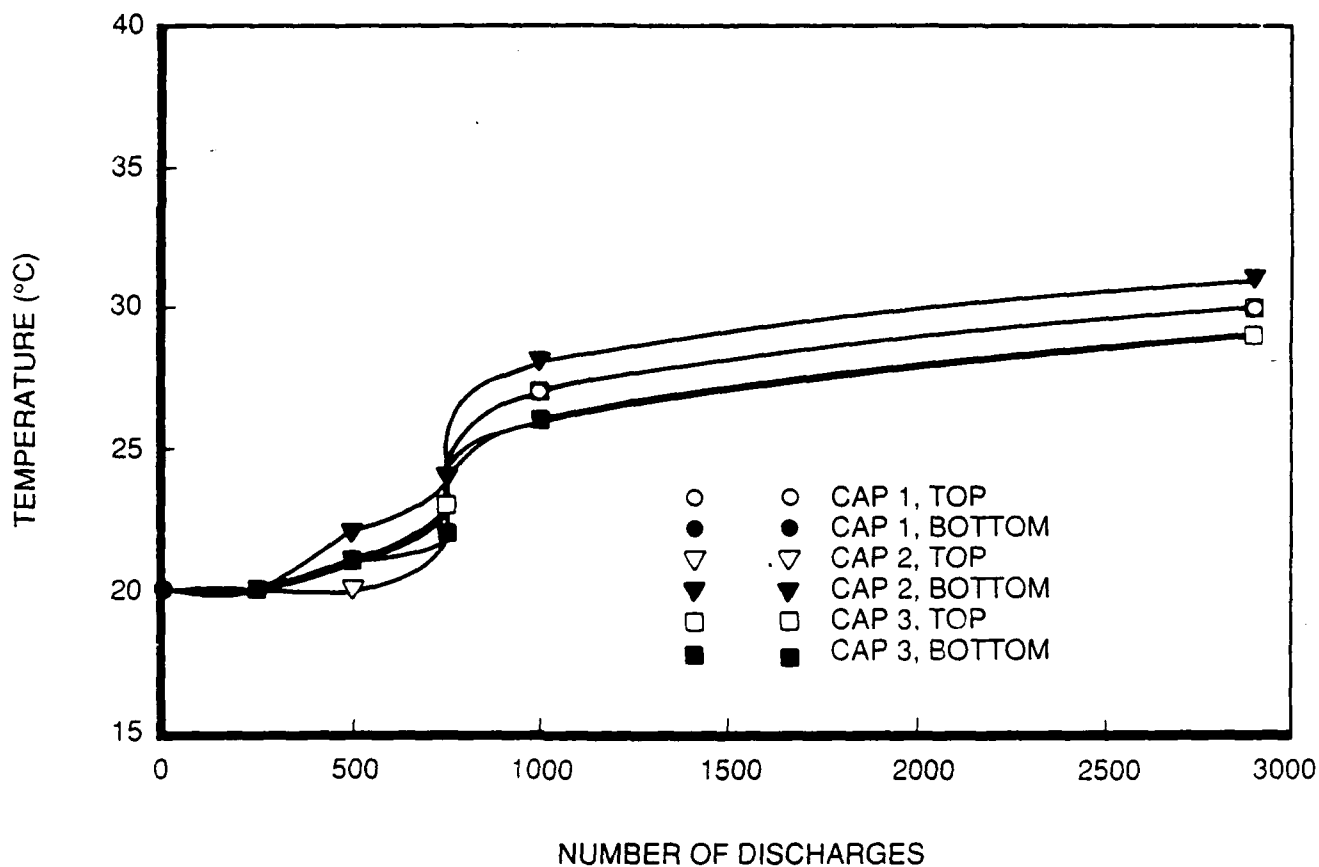
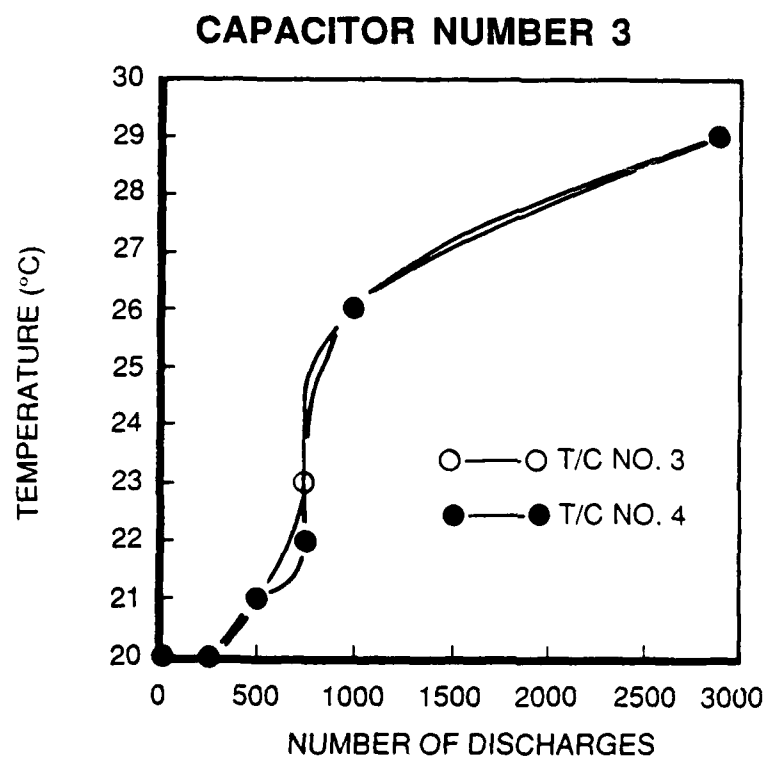
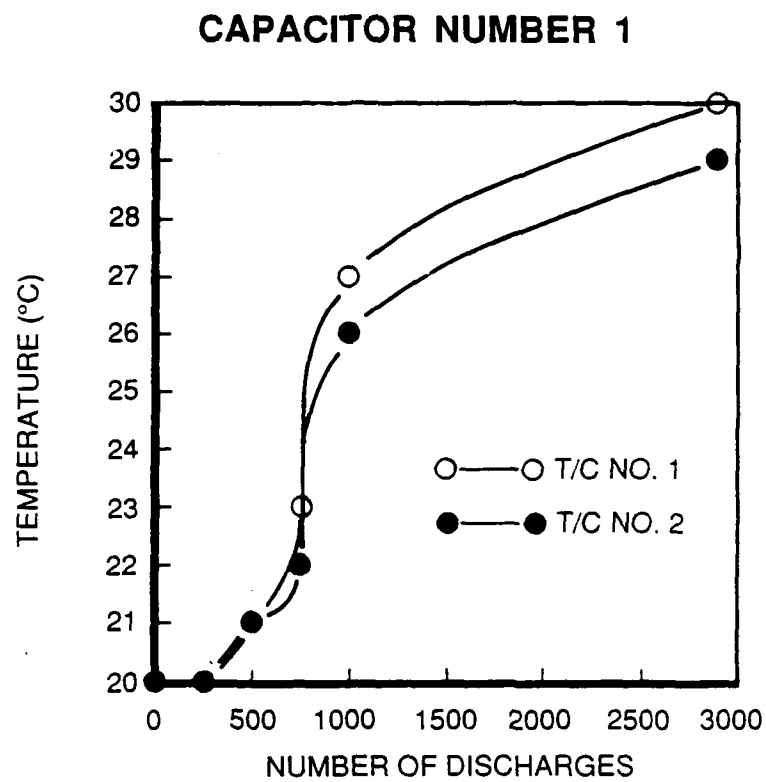
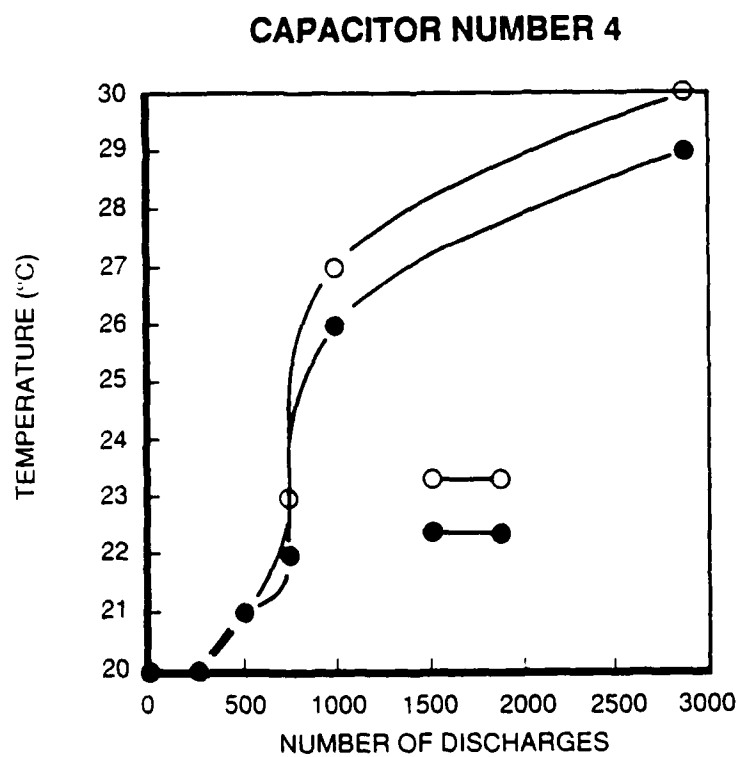
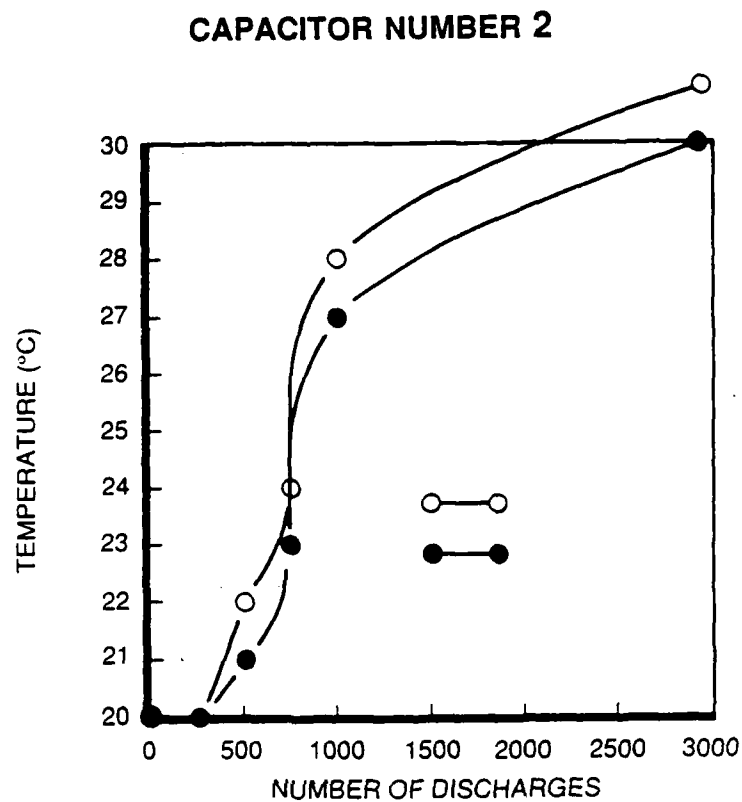


Fig. 20. Capacitor Temperatures



**Fig. 21. Thermocouple Measurements for Capacitors 1 and 3**



**Fig. 22. Thermocouple Measurements for Capacitors 2 and 4**

According to Dr. Mauldin at Sandia, the capacitors were expected to reject the bulk of the heat through the bottom end of the case. A difference in temperature was seen between the top and bottom of the capacitor for capacitors 1, 2, and 4. This difference was approximately 2°C after the initial thermal transient. The capacitor which failed (number 2) was recording the highest temperature of the four. Capacitor number 2 showed the largest delta between the top and the bottom case temperatures as well. The highest temperature recorded was the bottom of capacitor number 2. The expected sharp rise in temperature immediately prior to failure did not occur. In fact, the sharpest rise in temperature occurred at between 500 and 1000 pulses, and it occurred for all the capacitors. It is possible that this sharp rise of approximately 8°C in only 400 - 500 pulses was indicative of impending failure of all the capacitors. However, the indication from the capacitor acceptance testing that capacitor number 2 would fail due to its large swings in ESR, coupled with its larger than average temperature increase, suggest that the problem was specific to this capacitor. Capacitor number 3 showed no difference between the top and the bottom temperature at any of the recording intervals. Capacitors 1 and 4 exhibited the inverse trend of capacitor number 2, by recording higher temperatures at the top thermocouple. The significance of this observation is unknown, but it may be attributable to better thermal contact between the capacitor mounting housing and the base of these capacitors. The results of this test confirmed the prediction made by PI, based on the acceptance test criteria, that the fluctuating ESR of capacitor number 2 made it a candidate for early failure. If the ESR of capacitor number 2 increased significantly, then its internally generated heat would increase correspondingly. Therefore, the temperature data are consistent with the ESR results.

Other temperatures were measured during the test also. These included the thermal shunt, the converter power transistor, the power converter cover, and the stripline heatsinks. The data from these measurements are shown in Figure 23 and 24. Figure 23 shows the temperatures measured on the power converter cover near the base and on its top surface. These follow the same general pattern observed in the capacitor temperature measurements, including the unusual temperature rise between 500 and 1000 pulses. Of more interest for electronics reliability, the temperature of one of the power transistors inside the power converter was also measured. These data and those for the thermal shunt are given in Figure 24. The power transistor heated up more rapidly than any of the other components, which is to be expected due to its smaller size and lower thermal mass. However, in spite of the different trend between 0 and 500 pulses, the data still show a jump upward between 500 and 1000 pulses. The power transistor temperature begins to level off at approximately 40°C and appears likely to reach thermal equilibrium well below 50°C. Reliability of these parts is expected to be high if their temperature is maintained at or below 50°C. The thermal shunt temperature data is of interest to determine how large a delta T existed across the boundary between the shunt and the capacitors. As is evident from Figure 24, the shunt temperature climbed to a peak of 29°C. The delta T between each of the capacitors and the shunt is shown in Figure 25. As this figure shows, the delta T is never more than 2°C. This raises a concern over how effectively the shunt is transferring heat away from the capacitors to the cooling plate. For effective heat transfer, the shunt should remain several degrees cooler than the capacitor cases. Instead, its temperature is rising along with the capacitors. Note that the thermal shunt also exhibited the sudden jump in temperature between 500 and 1000 pulses.

The temperatures of the stripline supports were also measured during this test. The stripline supports are the vertical support members which extend from the stripline

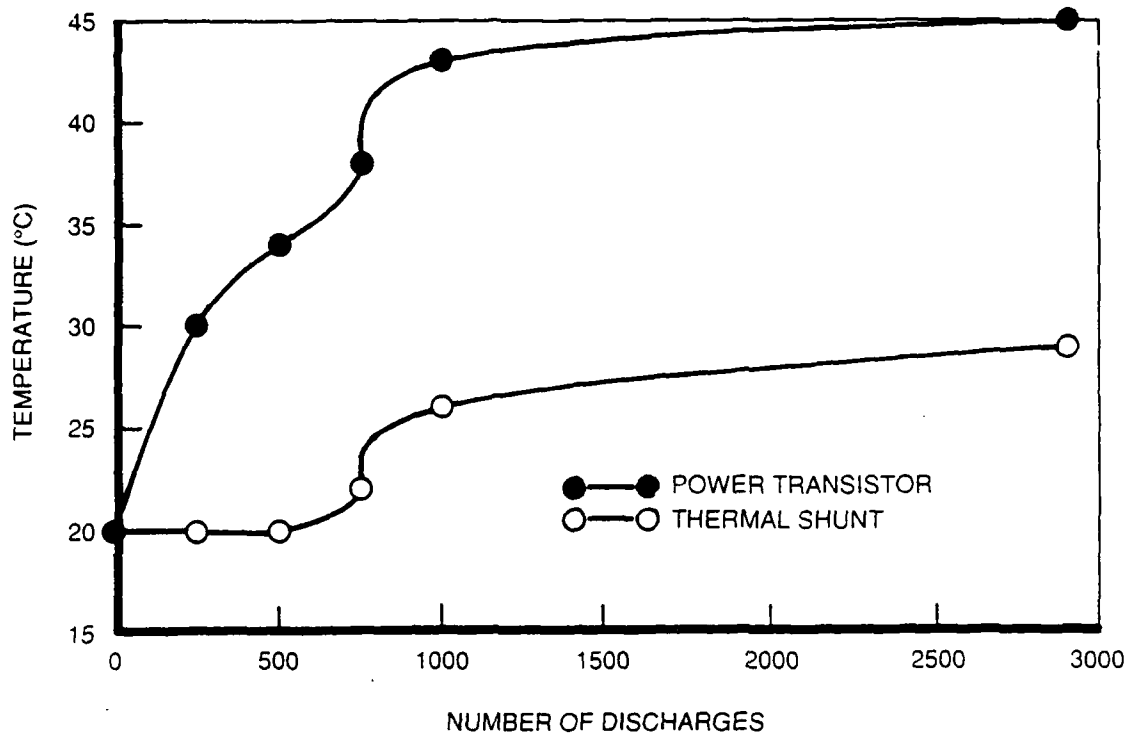


**Fig. 23. Converter Cover Temperatures**

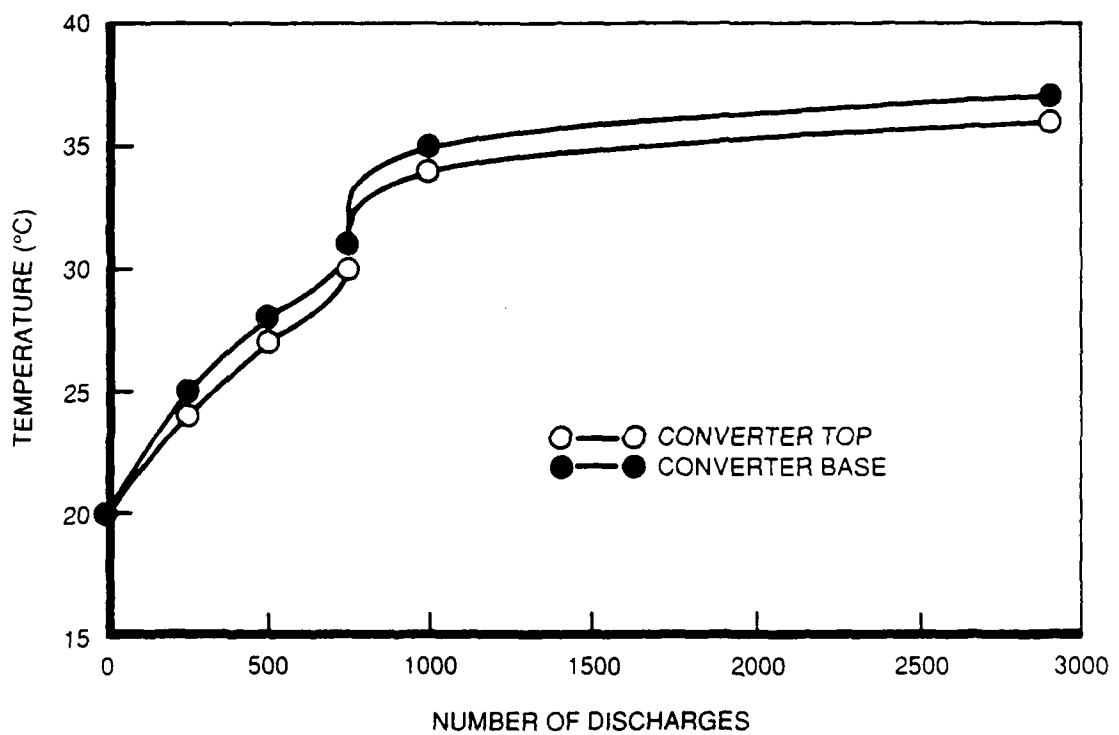


**Fig. 24. PPT Internal Component Temperatures**

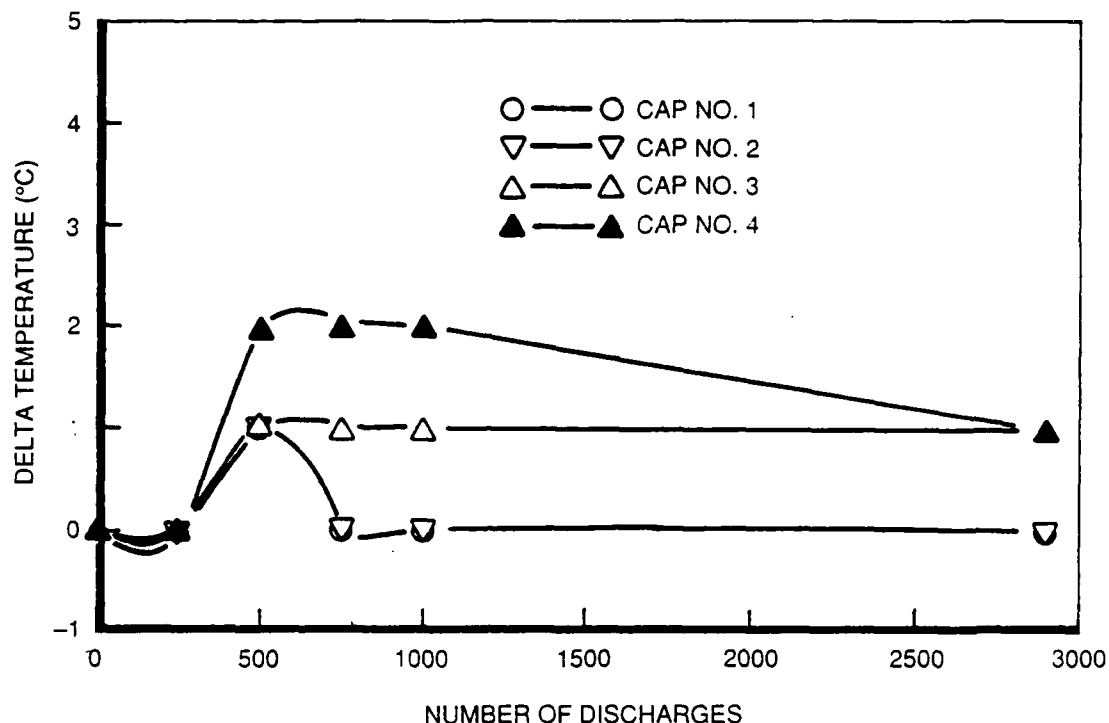


**Fig. 25. Temperature Difference Between Capacitors and Thermal Shunt**

between the capacitors and the electrodes. Because of their location, they are indicative of the heat conducted back toward the capacitors from the electrodes. The trend is virtually identical for the anode (top) and the cathode (bottom). The cathode support is marginally cooler, raising questions about the effectiveness of the bottom cooling plate. The cathode support attaches directly to this plate, while the anode plate does not. It is clear that these components receive a higher thermal input than the capacitor thermal shunt, as evidenced by their more rapid temperature rise. The striplines both experience the rapid rise in temperature between 500 and 1000 pulses. Maximum temperatures appear to be between 55 and 60°C for both supports.

The repeated failure of the PPT to achieve the required lifetime for N-S stationkeeping raised questions regarding its mission applicability, especially in light of recent developments in arcjet and ion thruster technologies. A brief mission study was conducted to illustrate the tradeoffs between the three systems. A summary of the results is shown in Figure 26. The assumptions made in the study are listed in Table 5, as is a mass breakdown for the PPT thruster. The study shows that the PPT is competitive on a total propulsion mass basis with the arcjet or the ion engine. However, the inert mass and the system complexity of the PPT system do not compare favorably with the ion engine or the arcjet.

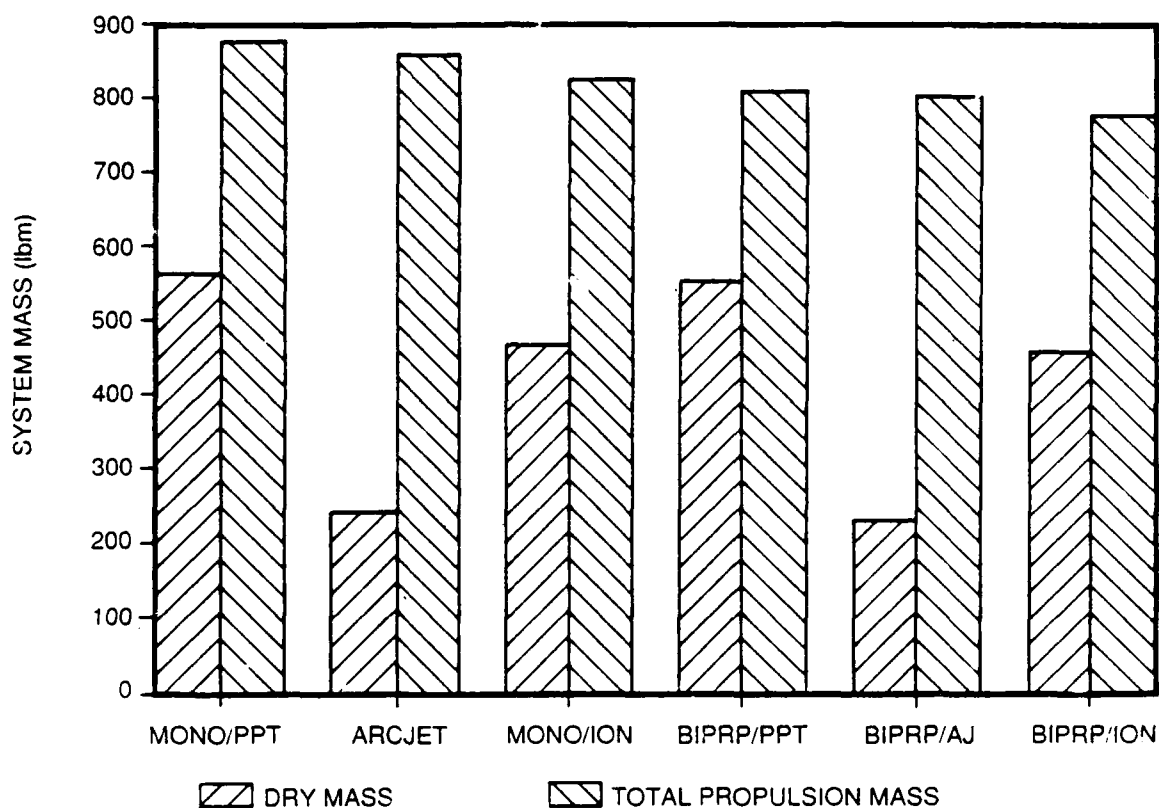


**Fig. 26. Mission Analysis Summary**

**Table 5. Mission Analysis Assumptions**

**TOTAL IMPULSE REQUIREMENT:** 836,224 N-s (188,000 lbf-s)

**SATELLITE MASS:** 1,818 kg (4,000 lbm)

**STATIONKEEPING THRUSTER SPECIFIC IMPULSE:**

PPT: 11,743 N-s/kg (1,200 lbf-s/lbm)

Arcjet: 5,880 N-s/kg (600 lbf-s/lbm)

Ion: 29,400 N-s/kg (3,000 lbf-s/lbm)

**MASS BREAKDOWN OF PPT THRUSTER:**

Teflon Propellant: 20.45 kg (45 lbm)

Capacitors: 15.9 kg (35 lbm)

Electronics: 4.54 kg (10 lbm)

Structure: 4.54 kg (10 lbm)

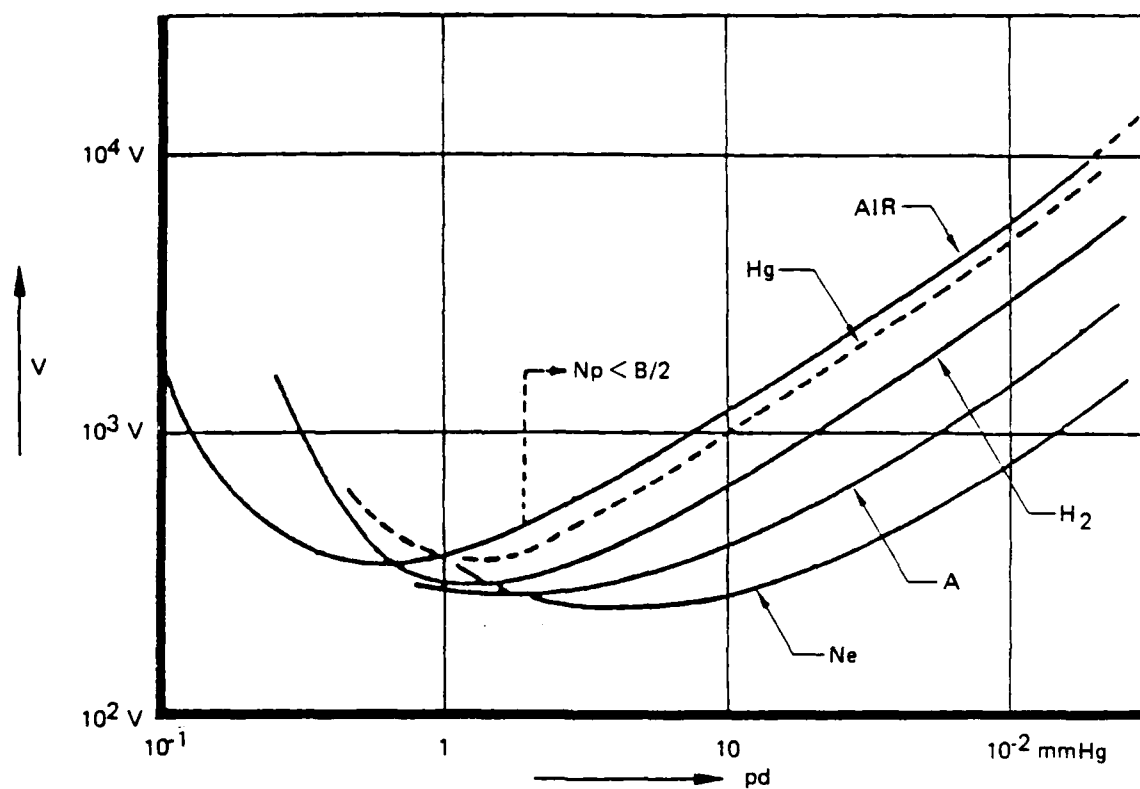
**TOTAL:** 45.43 KG (100 lbm)

## Lessons Learned

The most important lesson learned from the PPT program was the importance of configuration control when systems are modified. Many of the setbacks and delays encountered in this program could have been averted if better configuration control had been exercised. For instance, the capacitor/stripline arcing problems which plagued the early attempts to start the life test were really the result of a poorly documented design change from the Maxwell center post design to the Sandia design. If the capacitors had been built to the specifications of the Maxwell capacitor electrodes, they would have interfaced with the stripline and no modifications would have been required to the center post or the insulation. Another example encountered in this program was the ground test console, which was modified by MDAC, but did not include documentation of the modifications. Another lesson from the program involved the thruster design. Originally intended as a flight prototype unit, the thruster was not designed for ease of assembly and disassembly. With the addition of the new capacitor technology and the subsequent problems encountered, the requirement for disassembly and reassembly of the thruster increased substantially. Unfortunately, removal of the capacitor housing required removal of the entire capacitor/stripline/electrode assembly. This could only be accomplished by first removing the DI circuit and the power converter. In short, to remove the capacitors it was necessary to completely gut the thruster, leaving only the propellant bars in place. This was a time consuming and tedious process, since the electrode insulator pieces had to be carefully fitted together and shimmed to ensure proper alignment. The lesson from this experience is to first test new technology in a simplified, modular unit designed for ease of assembly and dis-assembly, such as the straight-feed PPT design used in tests at Fairchild and JPL. The intent of this program was a "hands-off" life test. The flight prototype PPT unit would have been appropriate for that type of test. Unfortunately, the component technology (i.e. the Sandia capacitors) was not proven enough to allow such a test.

Voltage hold-off in vacuum was an interesting lesson learned by experience in this program. Due to the design change of the Sandia capacitor electrode, a series of center post adapters were designed by RRC to enable mating of the center electrode with the stripline. In this process, arcing was found to occur from the center post to the uninsulated portions of the case. This arcing occurred in spite of a 1 cm (0.25 inch) annular insulator ring about the center electrode. Prior testing at PI had charged these same capacitors to a greater voltage (3000 V) both at atmospheric and vacuum conditions ( $10^{-6}$  torr) without any arcing. Arcing was seen to occur in the tests at PI, but only when the voltage was accidentally left on the capacitors as the chamber was vented to atmospheric pressure. This arcing occurred due to the increasing ambient pressure in the chamber, which reached a point where the Paschen minimum sparking potential was less than the voltage on the capacitor, resulting in a breakdown. The Paschen curve for several gases is shown in Figure 27. The minimum sparking potential is a function of the product of pressure and the separation distance of the electrodes. Returning to the arcing observed in the PPT, pressure should not have played a role, since the thruster firing sequence was never initiated until the vacuum chamber pressure reached at least  $10^{-5}$  torr. Therefore, another difference between the PI tests and the tests installed in the thruster must have been responsible. The only difference was the addition of the center post adapters.





MINIMUM SPARKING POTENTIALS

| GAS                 | CATHODE | VOLTS<br>$V_{mm}$ | mm. hg cm<br>(pd)mm |
|---------------------|---------|-------------------|---------------------|
| He - -              | Fe      | 150               | 2-5                 |
| Ne - -              | "       | 244               | 3                   |
| A - -               | "       | 265               | 1-5                 |
| N <sub>2</sub> - -  | "       | 275               | 0-75                |
| O <sub>2</sub> - -  | "       | 450               | 0-7                 |
| Air - -             | "       | 330               | 0-57                |
| H <sub>2</sub> - -  | Pt      | 295               | 1-25                |
| CO <sub>2</sub> - - | ?       | 420               | 0-5                 |
| Hg - -              | W       | 425               | 1-8                 |
| Hg - -              | Fe      | 520               | ~2                  |
| Hg - -              | Hf      | 330               | ?                   |
| Na - -              | Fe ?    | 335               | 0-04                |

REFERENCE: COBINE, GASEOUS CONDUCTORS

Fig. 27. Paschen Breakdown Voltage Curve

The center post adapters changed the geometry of the electrode, as shown in Figure 28. This geometry change, among other things, allowed a direct line-of-sight view across the insulator to the anode. The adapter designs also presented a sharp right angle corner to the anode surface, which could have served to intensify the voltage gradient between the electrodes. It is suspected that this change caused the arcing. Only a complete insulation of the capacitor tops inside the anode ring was sufficient to stop the arcing. The final design incorporated a modified center post adapter which made better face contact with the stripline than the previous ones, and a completely insulated anode face to remove any possibility of arcing.

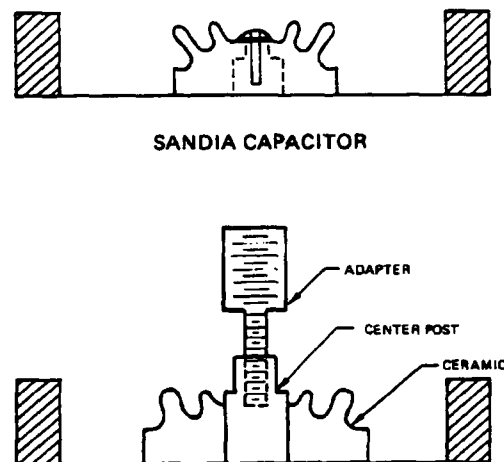


Fig. 28. Sandia Capacitor Centerpost Adapter

The bulk of the effort expended on this program was spent on the capacitors. The Sandia capacitors, for all their innovative design, were not the panacea to the PPT program that they were hoped to be. The electrode design was the major source of difficulty and this could be easily rectified with a redesign. However, the fact remains that one capacitor in five did not pass an acceptance test, and one of the remaining four failed in thruster operation after only slightly over 3000 discharges. These facts, coupled with the death of Dr. Mauldin, make the outlook grim where the Sandia capacitors are concerned. If future millipound PPT efforts were to begin, perhaps a redesign of the thruster should be considered which would allow use of a more proven capacitor technology, such as the General Electric phenol-xylyl-ethane (PXE) impregnated polypropylene capacitors now used in Pulsed Electrothermal (PET) thruster research. These capacitors have been in use for years in applications at the Stanford Linear Accelerator (SLAC). They have a design life of  $10^9$  discharges and are capable of operation at up to 400 Hz. A redesign of the PPT would be required because these capacitors are not as compact as the Maxwell or Sandia capacitors, but the improvement in lifetime almost certainly outweighs that factor. Recommendations for possible redesigns of the PPT are given in the following section.

Troubleshooting techniques were an important lesson learned on the program. One in particular which saved much time was the use of a bench-top simulator of the capacitor charging circuit. This was used to check out all the components of the charging and the discharge initiation (DI) circuits. The bench-top simulator consisted of the electronics boxes, charging leads, a 28 V power supply, a high speed digital scope and a single Sandia capacitor. This set up allowed testing for component failures without going through the long arduous process of cycling through the vacuum system to attempt to fire the thruster after each modification. An additional benefit of this method was that it allowed additional diagnostics to be employed which were not available when the electronics were installed in the thruster.

## CONCLUSIONS

The Pulsed Plasma Thruster Mission Endurance Test resulted in a failure to meet the specified lifetime goal. Yet many informative results were obtained in the course of the program. From the results, several conclusions can be made about the program and the PPT thruster in general. The Pulsed Plasma Thruster Mission Endurance Test program results show that the capacitor problems which have plagued the millipound PPT are still a problem. Also, the thruster design makes testing difficult and leads to jamming of the fuel bars. The thruster electronics design is dated and should be reworked as the Discharge Initiation circuit was. In summary, the PPT design should be revisited for updates and simplification. Mission analysis results should be inherent to any redesign effort. Improvements to the thruster design must be made if the PPT is to be mission competitive with arcjet and ion thruster systems.

The first and most general conclusion regarding the program is that it suffered from a lack of documentation and traceability. This is not surprising considering that it began at Fairchild, moved to MDAC, and ended up almost ten years later at RRC. The lack of traceability extended to both sides of the contractual fence. On the Air Force side, the project manager who started the program was not the one who finished it. In fact, the baton was passed at least six times over the course of the effort to life test the millipound PPT. The rough equivalent is true of procurement personnel in the contracts area at AFFTC.

On the contractor side, the Fairchild personnel who worked the program were disbanded after the life test was moved to MDAC. Only one of them remained at Fairchild (Dr. Bill Guman) and he was a valuable contact during the present effort. The MDAC personnel also disbanded after the failure of the life test at MDAC. None of the MDAC personnel was available for consultations on this program. In the components area, contacts were made at Sandia Laboratories with Dr. Mauldin for the capacitors and with Jerry Harris at Wilmore Electronics for the power converter. The untimely death of Dr. Mauldin prevented his evaluation of the failed capacitors. Unfortunately, no other personnel at Sandia retained the expertise on the high energy density capacitors used in this program. The Wilmore contact was of no assistance because the information required to fix the converter was held proprietary by the company. Once again, the program, through time and misfortune, generally suffered from a lack of traceability and continuity.

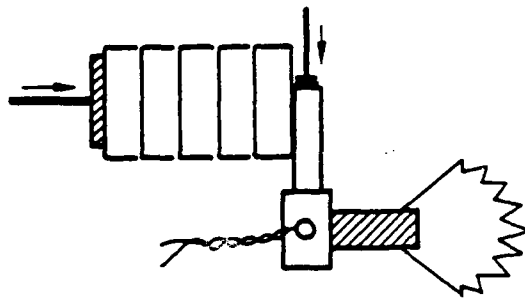
With the above conclusion stated, it is clear that the present program started with several handicaps. One by one these handicaps were overcome. Examples included the Ground Test Console rework and the thrust stand repair and calibration. The thruster was brought to the point of beginning the life test in the face of all these obstacles. The capacitor failure, internal arcing in the DI circuit, and the converter failure were all legitimate failures, not incidents caused by a lack of documentation. Taken by themselves, they would not have resulted in the termination of the program. Indeed, several failures of this type were planned into the program originally by RRC. The problem was that the contingency allowance budgeted by RRC was eaten away by the persistent failures which did result from a lack of documentation, such as the multiple instances of internal arcing at the capacitor electrodes. This was what ultimately spelled the end of the program.

One of the reasons that so much of the contingency funds were used in these repairs was the difficult nature of disassembling the thruster. This leads to the recommendation that a simpler, more modular thruster design be used to prove the lifetime of the components, especially new technology such as the capacitors. If a more modular thruster design had been used, the turnaround time to repair or replace components would have been significantly shortened, thus resulting in lessened schedule impacts and cost savings. If a future technology program were to be attempted, a suggested redesign of the thruster would include the following provisions:

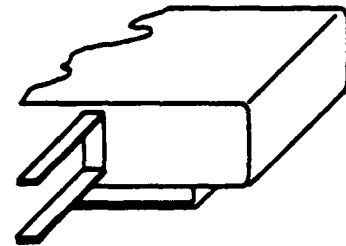
1. Ready access to the capacitors
2. A quick decouple connector between the stripline and the electrodes.
3. Modular electronics with easy access to connectors.
4. Fewer fasteners required to secure components.

In addition to design changes which would improve the maintainability of the PPT thruster, some suggestions regarding the reliability can also be made. The first and foremost of these is to redesign the thruster to enable the use of some larger, lower energy density capacitors. A proven lifetime of greater than  $10^9$  pulses should be a requirement for any capacitor considered for the PPT. A redesign of the thruster electronics should also be performed to reduce the parts count of the power converter. New, state-of-the-art components are undoubtedly more capable than the electronics inside the converter now. The size and complexity of the power converter could be reduced substantially, with a corresponding increase in reliability.

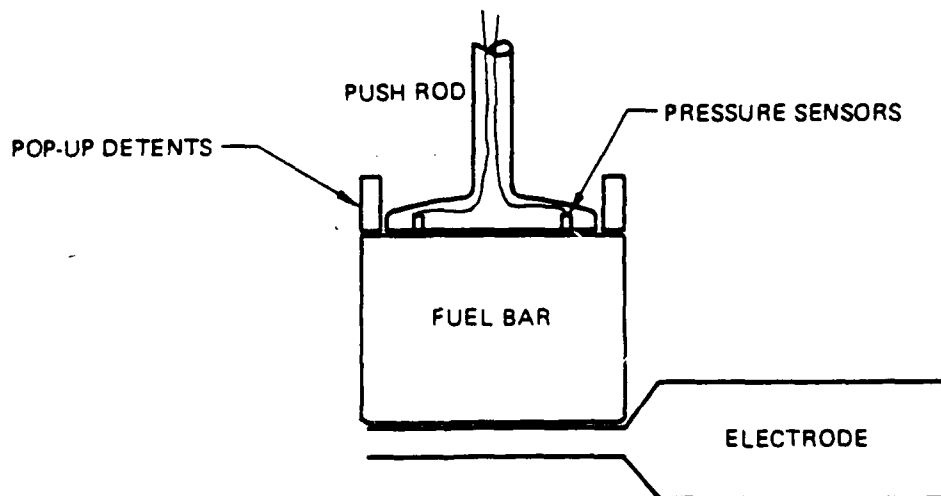
With a redesign of the electronics, a simpler propellant feed system remains as the only additional recommended modification. The helical feed system was designed as a way to package 10 years worth of N-S stationkeeping propellant into a reasonably small space. It created problems, however, such as propellant binding and did not work as well as planned. In a total redesign of the PPT, the constraint of the enclosure defined by the fuel bars should be removed. A possible option instead is to employ straight fuel bar segments divided into equal lengths and feed from a magazine into the fuel feed tracks. This method would require more moving parts, but would eliminate fuel bar binding and misfeeds. A possible design for this type of feed system is shown in Figure 29. A second option is to operate the PPT on a liquid fuel stored in a central tank. This eliminates the requirement to carry all of the fuel along in each unit. The fuel could be metered and injected through a plenum and a series of orifices in the backplate of the discharge chamber. For higher thrust applications, the pulsing rate could be increased to several hundred Hz, thus eliminating the need for a high speed propellant valve.



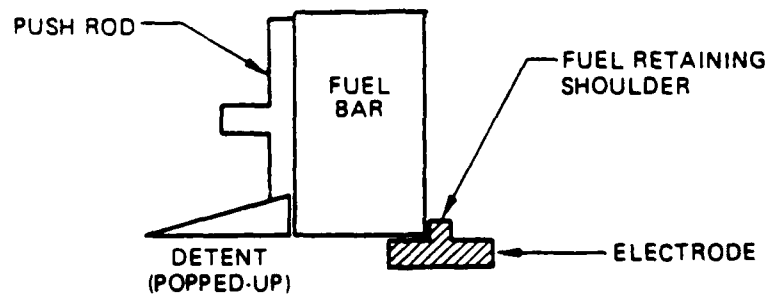
TOP VIEW



OBLIQUE VIEW OF  
FEED HOUSING



TOP VIEW - DETAIL



WHEN DETENT POPS UP - PUSH ROD RETRACTS  
TO ALLOW NEXT FUEL BAR TO FEED

SIDE VIEW - DETAIL

Fig. 29. New PPT Feed Design

## REFERENCES

1. Zhurin, V. V., "Electric Propulsion in the USSR," AIAA Paper 76-1073, November 1976.
2. Vondra, R. J., et.al., "Analysis of Solid Teflon Pulsed Plasma Thruster," J. Spacecraft and Rockets, Vol. 7, No. 12, December 1970.
3. Vondra, R. J., et. al., "Pulsed Electric Thruster for Satellite Control," Proc. IEEE, Vol. 59, No. 2, February 1971, pp. 271-77.
4. Vondra, R. J. and Thomassen, K. I., "Performance Improvements in Solid Fuel Microthrusters," J. Spacecraft and Rockets, Vol. 9, No. 10, October 1972.
5. Palumbo, D. J. and Guman, W. J., "Pulsed Plasma Propulsion Technology," AFRPL-TR-73-79, September 1973.
6. Palumbo, D. J. and Guman, W. J., "Effects of Propellant and Electrode Geometry on Pulsed Ablative Plasma Thruster Performance," J. Spacecraft and Rockets, Vol. 13, No. 3, March 1976.
7. Aston, G., Pless, L. C., and Brady, M. E., "Pulsed Plasma Thruster Ignition Study," AFRPL-TR-81-105, May 1982.
8. Vondra, R. J., "One Millipound Pulsed Plasma Thruster Development," AIAA-82-1877, November 1982.
9. Becker, T. and Freeman, J. R., "An Advanced High Energy Density Capacitor Evaluation System," 1981 JANNAP Propulsion Meeting Proceedings, CPIA Publication 340, Vol. II, pp. 309-26, May 1981.
10. Ibid., reference 7.
11. Palumbo, D. J., Begun, M., and Guman, W. J., "Electrode Erosion Processes in Pulsed Plasma Thrusters," AFRPL-TR-79-14, March 1979.
12. Ibid., reference 7.
13. Fairchild Republic Company, "Thrust Stand Operations Manual," November 1976.
14. Rudolph, L. K., et. al., "Plume Characterization of a One-Millipound Solid Teflon Pulsed Plasma Thruster," AFRPL-TR-79-60, September 1979.

## **APPENDIX A - GFP DAMAGE ASSESSMENT**

**INITIAL GOVERNMENT FURNISHED PROPERTY**

**DAMAGE ASSESSMENT**

**AFRPL CONTRACT NO. F04611-84-C-0060**

**"PULSED PLASMA MISSION ENDURANCE TEST"**

**Prepared by:**

**Rocket Research Company  
11441 Willows Road  
Redmond, Washington 98052-1012**

**Submitted to:**

**Air Force Flight Test Center  
Directorate of Contracting/PKRA  
M/S 130  
Edwards AFB, California 93523-5320**

**February 20, 1985**



## INITIAL DAMAGE ASSESSMENT SUMMARY

This report is written to document the condition of the Government Furnished Property (GFP) as received by the Rocket Research Company (RRC). The report supplants the PPT shipment condition letter (RRC Msg. No. 3460-85-013) dated January 30, 1985 previously released through RRC contracts to AFFTC. Provided herein is a more detailed description complete with referenced photographs of the condition of the GFP and the receipt process.

All of the PPT GFP shipped from McDonnell Douglas Astronautics Company by B&G Trucking arrived at RRC by motor truck on January 28, 1985. RRC technicians assisted the freight company's employees in unloading and uncrating the equipment. All the equipment had been packaged in several sturdy plywood crates. No damage was evident on the exterior of the crates. The crates were carefully removed and the GFP moved into the RRC Test Lab, cell 108. All the smaller crates were placed inside the largest one and are stored behind the Lab building.

Visual examination of the equipment revealed significant damage to the thrust stand and thruster and minor damage to the thruster control console and cryopump compressor housing. As soon as the damage was discovered, the RRC PPT project office was notified. The project office in turn notified AFRPL and has had subsequent discussions with DCASMA in Seattle.

On January 29, 1985, a series of color photographs were taken to document the condition of the equipment. The following is a detailed description of those photographs and the equipment damage they document. A principal flaw in the packing procedure was that the thrust stand had not been removed from the altitude chamber and packaged separately. The stand normally sits on a three point mounting inside the tank to provide for leveling and sensitivity adjustments and was left in this position for shipment. Hence, the stand was free to jump out of the baseplate sockets and move around due to the vibrations from the truck.

Photos 2885-11 and 2855-12 are general views of the thrust stand in the altitude chamber. This is the position the stand was in when the chamber door was first opened. Note that

the stand is sitting askew on the support box and that the LVDT core slug assembly is not in place on the end of the moving arm. Photo 2885-10 is a view from below the stand at the corner nearest the chamber door. The screw projecting through the stand baseplate in front of the pink card should be sitting in the socket above the two screws in the block above the gearmotor. Photo 2885-5 is a closer view of this area. All of the semicircular gouges in the bottom of the baseplate have been caused by bouncing on the top of the leveling screw socket above the motor. Note also the narrow end of the plate by the pink card. Both lower corners of this end have been worn off from chafing against the chamber door. The corresponding wear marks on the door are shown in photo 2885-7. The rust evident in this photo at the bottom of the pass-through area may be a result of vibration induced draining the cooling water lines running to the thruster cooling plate. Photo 2885-4 is a close-up of the corner of the support box which is nearest the viewer in photo 2885-11. Note the gouges in the top of the support box caused by the thrust stand baseplate moving back and forth over it. Photo 2885-8 is a view below the baseplate just behind the yellow block on the front of the stand seen in photo 2885-11. Note the numerous gouges in the top edge of the support box and the damaged threads on the leveling screw caused by the screw being bounced against the support box.

Photo 2885-6 is a view of the support plate in front of the support box. The material scattered over the plate and on the angle on the support box is aluminum shavings from the bottom of the thrust stand baseplate and the top of the support box. Photo 2885-15 is a close up view of the leveling screw in the corner of the thrust stand furthest from the viewer in photo 2885-11. The large bolt at left center is the leveling screw which should be resting in the socket mounted in the rectangular block at right center. Note the holes gouged into the top of the support box by the tip of the leveling screw. Photo 2885-3 is a close up of the bottom of the thrust stand stop support posts. The one to the left is for the fixed stops and the one to the right is for the adjustable stops. The rectangular dark area on the baseplate is where the post should be. Note the fine aluminum filings on the baseplate. These are from the bottom of the post and the thrust stand moving beam in the area of the adjustable stops. The left post has been loosened and moved around as a result of the thrust stand beam swinging around. Note that the fixed stops were not intended to be shipping restraints, but rather are to support the thrust stand moving beam while the thruster is being installed or removed. Photo 2885-14 is a close up of the near side adjustable stop. Note the damage to the thrust stand beam caused by bouncing against the end of the stop screw. The opposite side of the beam does not have

corresponding damage because the stop screw has vibrated out and is missing entirely (it was found on the bottom of the chamber).

The damage discussed thus far is clearly the result of not removing the thrust stand from the chamber and packaging it separately with proper disassembly and restraints. This damage may be only cosmetic. A more detailed evaluation can be made following removal of the thrust stand. The remainder of the damage to the thrust stand may be much more significant. Photo 2885-9 is a view of the bottom of the altitude chamber below the thrust stand support box support plate. The C-clamps in the foreground are used to attach the thruster to the thrust stand moving beam. Note that the plastic insulator disks are missing from the nearer clamp. The aluminum object with the long screw in the middle distance is the mount and adjuster for the LVDT slug which is the small cylindrical piece on the end of the screw. This assembly should be mounted to the aluminum block holding the pointer over the yellow block seen in photo 2885-11. The large block of aluminum with 4 screws in it to the left of the yellow block is the LVDT mount. It will not be possible to determine whether the LVDT itself has been damaged beyond repair until after the rest of the thrust stand has been repaired and reassembled for checkout.

The balls in the background of photo 2885-9 are some of the calibrated masses for the thrust stand calibrator. Some of these rolled out of the chamber when the door was first opened. These balls should be in the hopper of the calibrator which is the object with two vertical posts and an included ramp behind the thrust stand in photo 2885-11. At this time it has not been possible to determine whether all of the required balls have been located or whether any of them have been dented or otherwise damaged in such a way as to make them unusable.

Photos 2885-1 and 2885-13 are close ups looking down into the lower flexure assembly. Photo 2885-2 is looking up into the upper flexure assembly. As may be seen, both flexures have been completely destroyed by the forces resulting from the unrestrained thrust stand beam movements. While there is no major structural damage evident to the thrust stand, the critical alignment of the flexure supports may have been damaged. Assessment of this area will have to await disassembly and cleanup of the thrust stand. Assuming no such misalignment is found, repair will consist of a complete cleanup (including burr and chip removal), flexure acquisition and replacement and reassembly along with the possible need to replace the LVDT and calibrator ball masses.

The other area of major damage is to the thruster itself. Photo 2885-19 shows the condition of the nozzle as it was received. Note that the smaller pieces were placed in a plastic bag at MDAC indicating that it was broken prior to or while being packaged for shipment. RRC and AFRPL personnel had previously examined the PPT nozzle on October 4, 1984. At this time the nozzle was in 2 pieces. One of these pieces was a small flange which could have been easily glued back on the main body of the nozzle. For comparison, photo 2886 (a copy of MDAG photo SSC093352) shows the condition of the nozzle at that time.

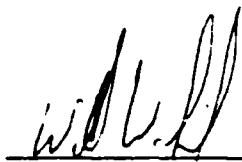
When the thruster was moved it rattled and something could be felt moving inside. Photos 2885-16, -17 and -18 show the inside of the thruster after the cover was removed. The cylindrical object in the center of photo 2885-16 is a coil assembly which should be mounted to the rear of the capacitor bank by the two screws visible in the center foreground of photo 2885-16. Photo 2885-24 shows the thruster with one of the three cryopump absorber assemblies which were in the crate with it along with a box of tools for the cryopump. The thruster was located in the center of the crate by a cardboard ring around it at the bottom. The absorbers and tool box were wrapped in bubblepack and placed in the corners of the crate. These objects could have moved possibly striking the thruster. It is not apparent that the packing method or shipment was definitely responsible for the electrode damage discussed below. However, this possibility does exist.

Photo 2885-23 was ment to show that the lower electrode is slightly bent up (approximately 50), but photographic techniques were insufficient. There are shown, however, several sharp gouges along the edge of the electrode. These gouges appear to have been made by the teeth of a pair of pliers. This would seem to indicate that the electrodes had been damaged prior to or while the thruster was being packaged and an attempt was made to straighten them. It appears that the electrodes cannot be restored to the proper shape and alignment and that they will have to be replaced with new ones.

Photo 2885-20 shows that the cryopump compressor housing has been bent at the bottom. Whether or not this has caused any damage to the compressor itself cannot be determined until the altitude chamber and pump can be reassembled and the pump test run. In addition, the power cord and connector for the pump's cold head motor were not included with the equipment received by RRC. A replacement connector will have to be procured from the pump manufacturer and a cord fabricated before the pump can be operated.

Photo 2885-21 shows a switch on the thruster control console which was broken by being struck by some object. A replacement will have to be procured and installed before the thruster can be operated. Additionally, the digital readout for thermocouples had been removed from the instrumentation console. A replacement unit will have to be procured and installed before the thruster thermocouples can be read out or recorded.

While most of the damage can be quickly and easily repaired, the thrust stand flexures and alignment, the thruster nozzle and electrodes and possibly the LVDT and calibrator mass replacement will significantly impact current schedule and budget profile. A complete estimate of these impacts is the focus of ongoing investigations.



W. W. Smith  
Program Manager



W. A. Arrera  
Supervisor, Electronic Engineering

ER #3

**APPENDIX B - DI CIRCUIT FINAL REPORT**

## DISCHARGE INITIATION CIRCUIT

### MONTHLY REPORT

10/11/85

#### 1.0 INTRODUCTION

The discharge initiation circuit, DI circuit, initiates the plasma discharge in the pulsed plasma thruster, PPT. A benchtop version of the DI circuit has been life-tested at Physics International, PI, to verify that the circuit will operate for the required life of 14 million pulses. In addition, a DI circuit has been fabricated and delivered to Rocket Research for installation in the PPT. The design of the DI circuit delivered to RRC was based on the results of the benchtop test.

#### 2.0 BENCHTOP DI CIRCUIT

The schematic for the DI circuit that was life tested at PI is shown in Figure 1. The 2 kV power supply charges the storage capacitor,  $C_s$ , through the charging resistor,  $R_c$ . Charge current flows through the charging resistor, the storage capacitor, and the primary of the coaxial transformer. Little charge voltage is coupled to the secondary of the transformer because the charge current is low ( $< 1$  mA).

To produce the output pulse which initiates discharge in the PPT, the SCR's are triggered by a command pulse. In the PPT, the command pulse is provided by the PPT electronics; for the bench test, the command pulse was provided by an external trigger source. Voltage sharing by the SCRs in their off-state is insured by the resistive divider,  $R_1$  and  $R_2$ , and the varistor

strings,  $V_1$  and  $V_2$ .  $V_1$  and  $V_2$  consist of 5 series varistors, each rated at 200 V, for a total rating of 1 kV for each varistor string.

Snubber circuits,  $R_{sn}$  and  $C_{sn}$ , are also placed across each SCR to damp any transients applied to the SCRs. The snubber circuits delay rise of voltage across each SCR long enough to allow the other SCR to start current conduction in the event that one SCR fires earlier than the other SCR. Should one SCR not begin conduction after being triggered, the varistors will clamp the voltage across the non-conduction SCR while the storage capacitor discharges slowly through the varistors and the conduction SCR.

### 3.0 BENCHTOP TEST RESULTS

The test plan for life-testing the benchtop circuit is shown in Table 1. The resistive test load was chosen to duplicate the amount of peak current and voltage reversal seen in the DI circuit during operation in the PPT. All configurations in the test plan operate into the coaxial transformer and a .25 ohm load. The DI circuit was operated at 10 Hz into a spark gap and resistive load to confirm the ability of the circuit to operate into a dynamic load. At the rep-rate of 80 Hz, the charging circuit was reconfigured for resonant instead of resistive charging to allow the higher rep-rate. As seen in Table 1, the benchtop test demonstrated the DI circuit lifetime to be greater than 14 million shots.



TABLE 1: Benchtop DI Circuit Test Plan

| Configuration               | Rep-rate | Number of shots |
|-----------------------------|----------|-----------------|
| Resistive Load              | 10 Hz    | 214,800         |
|                             | 20 Hz    | 920,000         |
|                             | 30 Hz    | 750,000         |
| Spark Gap and Resistor Load | 10 Hz    | 170,000         |
|                             | 30 Hz    | 118,000         |
| Resistive Load              | 80 Hz    | 12,901,000      |
| Total                       |          | 15,073,800      |

After minimum life of 14 million shots had been established for the DI circuit, the benchtop circuit was placed in vacuum of  $3 \times 10^{-5}$  Torr to check operation under actual operating conditions. The DI circuit operated for 15 minutes at 8 Hz before an SCR failed. We believe that the failure occurred due to overheating of the SCR during life testing at 80 Hz. At that rep-rate, the SCRs would overheat without forced air cooling. We performed several tests to determine the relationship between SCR leakage current and SCR case temperature. The SCR heating did not affect operation in air. However, the overheating may have caused the hermetic seal on the SCR junction to fail, placing the junction under vacuum, and allowing the SCR to arc internally. Even though one SCR had failed, the circuit continued to function at half voltage, just as designed.

As the temperature of the SCRs increases, the leakage current of the SCRs increases, causing the voltage applied to the storage capacitor to droop. As a result, an estimation of the temperature of the SCRs can be made by looking at the voltage applied to the storage capacitor, provided the relationship between voltage droop and SCR temperature has been determined.

Figure 2 shows the SCR leakage current as a function of SCR case temperature as measured on the DI circuit. Figure 3 shows the voltage droop seen on the storage capacitor as a function of case temperature. The information in Figure 3 applies only to operation at 80 Hz, but we see that the SCR can heat to 55°C without affecting circuit performance.

#### 4.0 TESTING OF PPT DI CIRCUIT

Based on the performance of the benchtop DI circuit, we fabricated a circuit for operation in the PPT at RRC. To improve heat sinking and dissipation in the PPT DI circuit, we used boron nitride as insulating stand-offs for the SCR and varistor assemblies. We also slightly reconfigured the circuit to fit the space limitations in the PPT.

We found that the varistors in the new assembly did not shunt reverse current as effectively as in the benchtop assembly, which caused the SCRs to conduct a substantial amount of reverse current before turning off. To eliminate the conduction of reverse current in the SCRs, we added reverse diodes in parallel with the SCRs, as shown in the circuit diagram of Figure 4.

Output current of the PPT DI circuit is shown in Figure 5. The DI circuit load was .25 ohm with low inductance, so the current waveform of Figure 5 also corresponds to the voltage waveform at 50 V/cm. As final test, the PPT DI circuit was operated in vacuum of less than  $10^{-4}$  Torr for 30 minutes at 8 Hz. Approximately 15,000 shots were accumulated on the DI circuit in vacuum.

## 5.0 SUMMARY

The DI circuit design was demonstrated to have a minimum life of 14 million shots in a bench test at PI. This circuit was then modified for operation in vacuum. The PPT DI circuit was checked at PI for operation in air and vacuum, and has been operated for approximately 15,000 shots in a vacuum of less than  $10^{-4}$  Torr. The PPT DI circuit has been delivered to RRC for installation in the PPT.

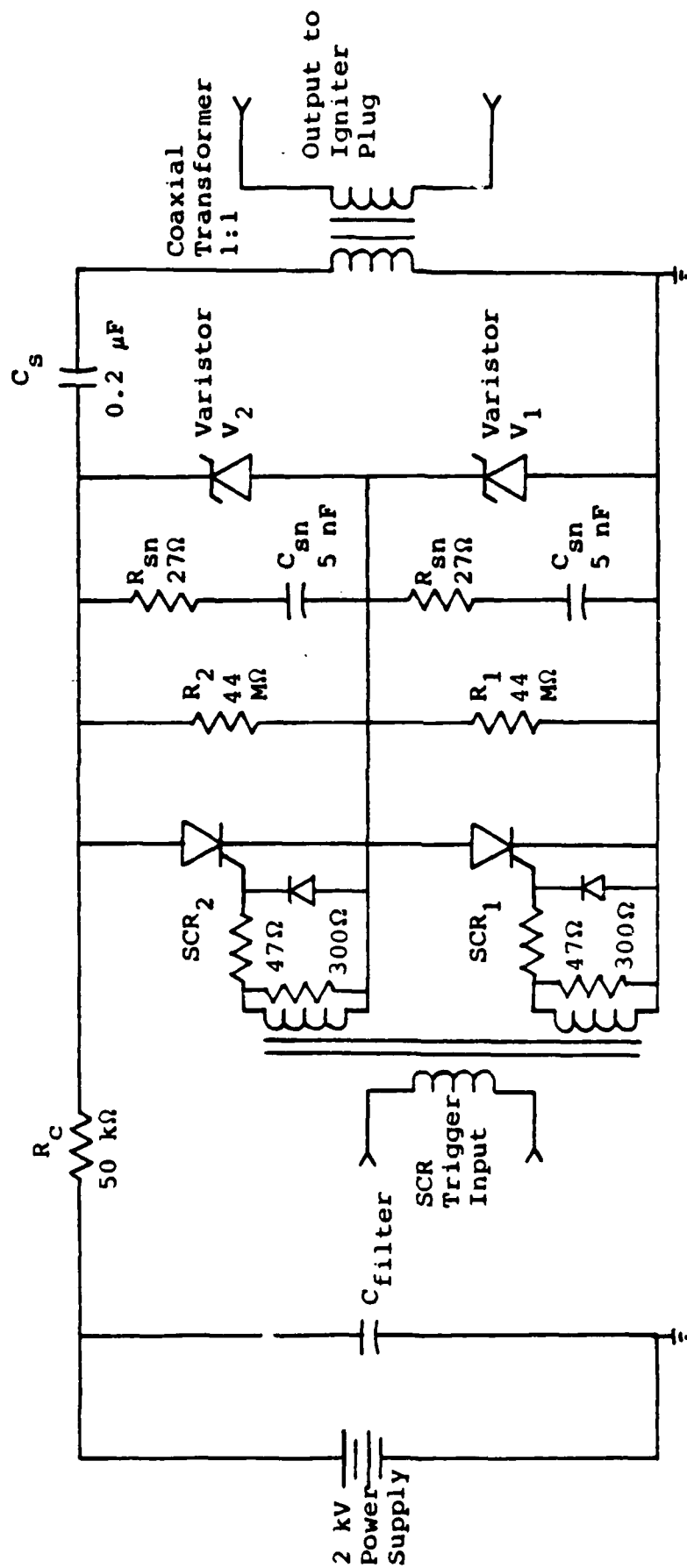


Figure 1: Circuit Schematic of DI Circuit Tested at PI to 14 Million Shots.

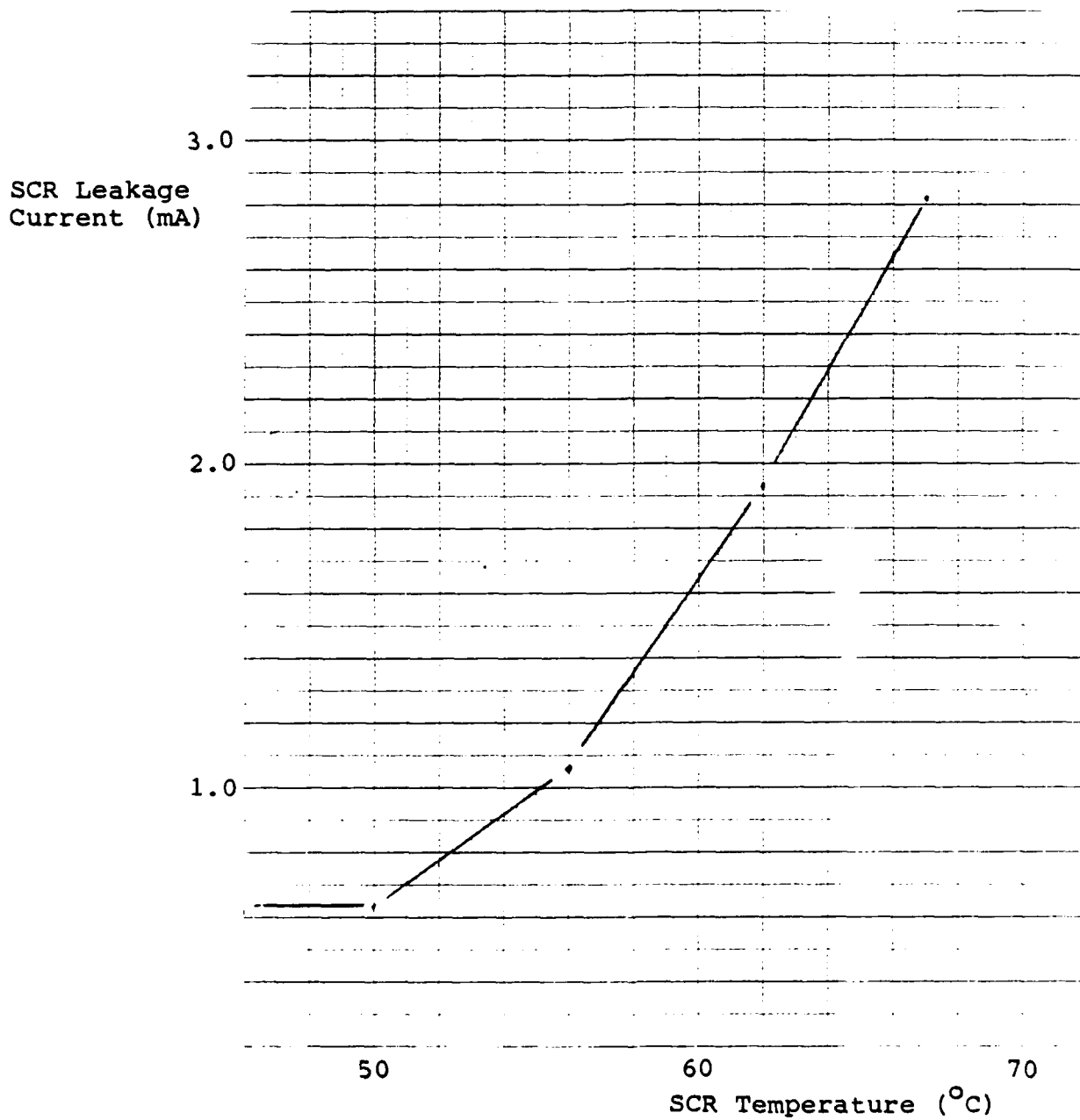


Figure 2: SCR Leakage Current as a Function of SCR Case Temperature, Measured on the Test DI Circuit.

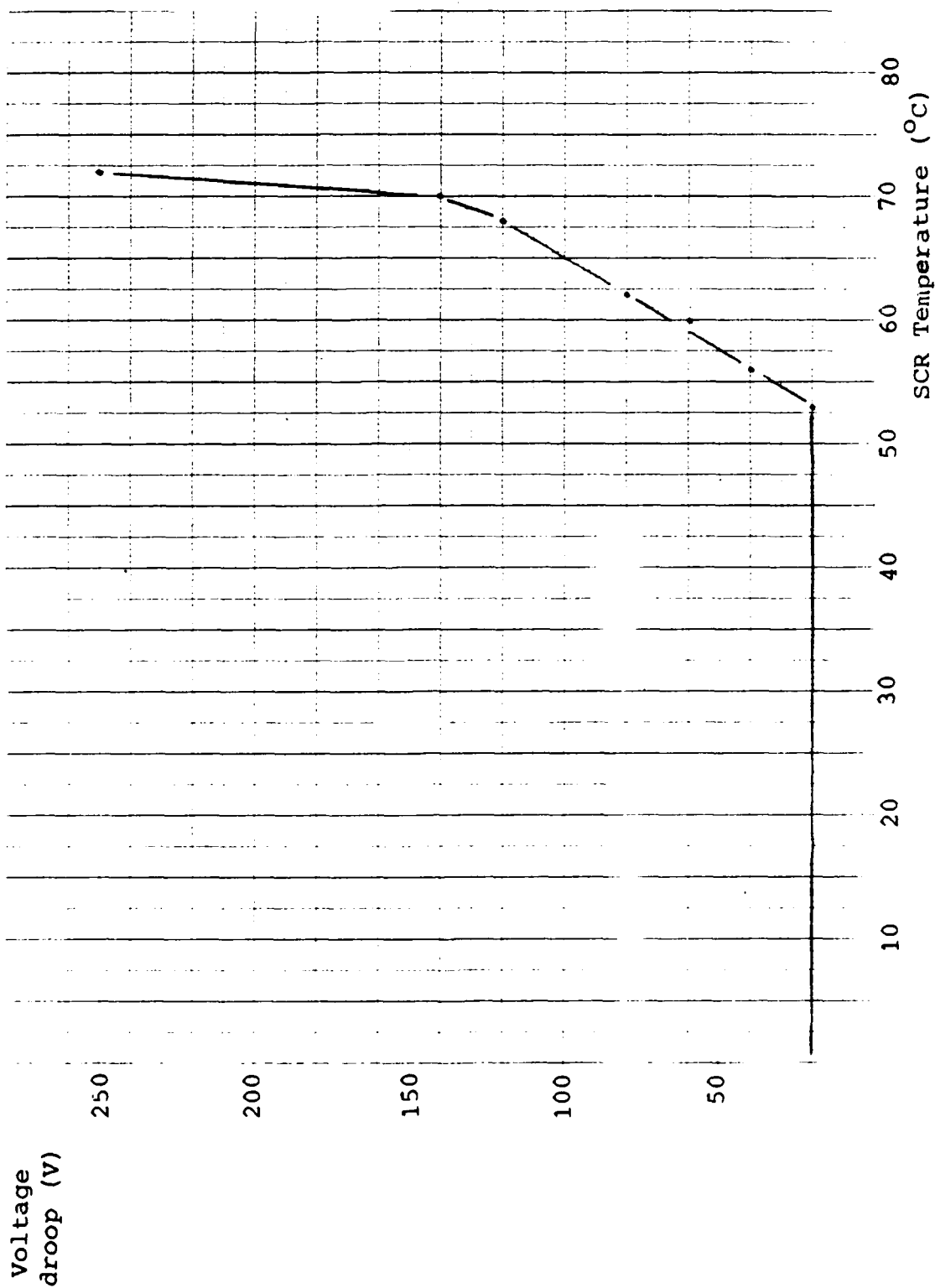


Figure 3: Storage Capacitor Voltage Droop as a Function of SCR Case Temperature for Operation at 80 Hz

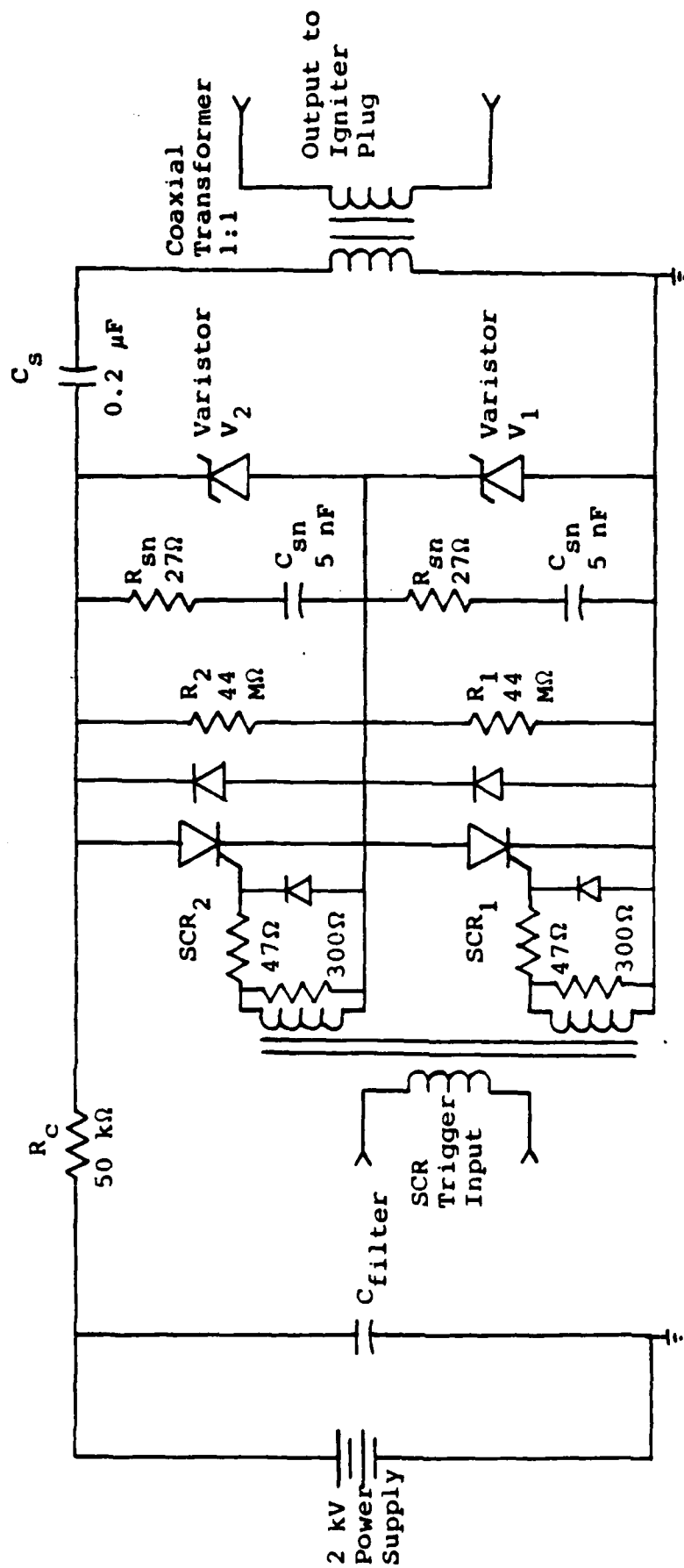


Figure 4: Circuit Schematic of PPT DI Circuit Tested at PI and Delivered to RRC.



2  $\mu$ sec/div  
200 A/div

Figure 5: Output Current Waveform Produced  
by PPT DI Circuit.



**APPENDIX C - CAPACITOR ACCEPTANCE TEST REPORT**

## **PULSED PLASMA THRUSTER CAPACITOR TEST REPORT**

**2/11/86 - 2/14/86**

### **1.0 Introduction**

The propellant for the pulsed plasma thruster, PPT, is generated by creating an arc across a teflon block. The arc is sustained by four capacitors discharging through a low inductance connection to the arc discharge region. Previous testing of the PPT had been halted due to failures of the discharge capacitors in the PPT. Capacitors using state-of-the-art capacitor technology were procured from Sandia to replace the capacitors that had failed. Physics International acceptance tested these capacitors in order to identify any capacitors which might fail early and to characterize any performance anomalies of the capacitors.

### **2.0 Test Procedure Modifications**

The test procedure for acceptance testing the capacitors is shown in Table 1. Each step was taken in the test procedure as outlined with exception to the vacuum high-pot as described in step 5. The second part of step 5 was deleted, which was a high-pot at 2 kV after the high pot at 3 kV. The purpose for the continuation of the vacuum high pot from 3 kV to 2 kV was to ensure that all the freon bubbles in the winding had sufficient time to circulate, and to establish electrostatic pumping of the bubbles in the windings of the capacitor. This function is also performed by pulsing the capacitors for 2 hours. Since the 10 minute high-pot at 2 kV was a small fraction of the 2 hour time required for pulsing, we felt that the 10 minute high-pot at 2 kV was redundant. In addition, we were facing a time constraint in performing the tests and getting the capacitors shipped back to RRC, so we eliminated the 2 kV, 10 minute vacuum high-pot from step 5. In addition to the deletion from step 5, step 4 was

performed before step 3. As before, this change did not affect the validity of the acceptance test.

### 3.0 Test Results

The results of the capacitor acceptance test are shown in Table 2. Capacitance and ESR were recorded when the capacitor arrived, after the vacuum soak and high-pot in air, after the high-pot in vacuum, and after the rep-rate test. The ESR measurement was made for comparison purposes only. The ESR meter was limited to measuring capacitance and D factor at 1 kHz. Since the effective frequency of the capacitors seen during discharge is 17 kHz, the actual ESR of the capacitors during discharge will be different than the value measured by the ESR meter.

Time for the initial vacuum soak of the capacitors was counted from the point at which a vacuum of  $10^{-4}$  torr was achieved. During the four hour vacuum soak, the vacuum dropped to as low as  $2 \times 10^{-5}$  torr. The initial vacuum soak was performed to verify that the capacitors would operate in vacuum without developing leaks. After the vacuum soak, each capacitor was inspected for leaks or defects, and a picture was taken of the capacitor and placed in the log books. Each capacitor survived the vacuum soak with no defects noted.

The next step was to apply 3 kV to the capacitors in air for five minutes, then discharge the capacitors and measure the capacitance and ESR. Little change was noted in the ESR or capacitance for any of the capacitors except number 014. The capacitance of 014 dropped slightly, while the ESR dropped by almost 50% (see Table 2). In addition, all of the other capacitors had a capacitance and ESR which were roughly equivalent. Capacitor number 014 had an initial ESR which was 3

times the value of the other capacitors. The results of the rest of the tests will indicate if we have a problem with capacitor number 014.

After the high-pot in air, we applied 3 kV to the capacitors for 10 minutes with the capacitors in a vacuum of about  $10^{-4}$  torr. The actual operating vacuum ranged from  $2 \times 10^{-5}$  to  $2 \times 10^{-4}$  torr from capacitor to capacitor. After the vacuum high-pot, the ESR and capacitance of the capacitors was remeasured. As before, no change was noted in any of the capacitors except number 014. In this instance, the ESR increased slightly, and the capacitance decreased slightly.

The final phase of the acceptance test was a rep-rate test under PPT operating conditions for 2 hours. As shown in the test circuit schematic of Figure 1, the capacitor under test, CUT, was placed in the vacuum chamber while all other equipment was placed outside the vacuum chamber. The CUT was charged by the power supply through an isolation resistor of 5 k $\Omega$ , the load resistor of 0.15  $\Omega$ , and 40 feet of RG/213 coaxial cable. The cable penetrated the vacuum chamber through a plexiglass vacuum interface diaphragm. The CUT was discharged into the 0.15  $\Omega$  load by triggering the NL-7703 ignitron. The PPT discharge initiation circuit was used to trigger the ignitron.

Typical output current waveforms for each capacitor under pulsed conditions are shown in Figure 2 for each capacitor. The capacitors were charged to 2.5 kV and discharged at a rep-rate of .2 Hz, corresponding to the actual operating voltage and rep-rate seen by the capacitors in the PPT. In addition, the load resistance was chosen to provide the same reversal and approximately the same pulse width as the PPT discharge.

During the rep-rate test of capacitor 015, the coaxial cable feeding the capacitor shorted, discharging the capacitor through a low inductance short. After the cable failure, the

Table 1: CAPACITOR TEST PROCEDURE

1. Log each capacitor as it comes in.  
Each capacitor should be logged by serial number and arrival date.  
A separate log book should be kept on each capacitor.  
Take a picture of each capacitor and place in log book.
2. Capacitance and ESR for each capacitor should be measured and logged.
3. Capacitor should be high-potted to rated voltage + 20% for five minutes.  
Remeasure and record capacitance and ESR.  
Inspect capacitors for visual defects.
4. Put capacitors in vacuum of  $10^{-4}$  tor for 4 hours.  
Remove capacitors and inspect for visual defects.  
Take picture of each capacitor and place in log book.
5. Put capacitors in vacumm and high-pot at rated voltage + 20% (3 Kv) for 10 minutes. Drop down to 2kv and let sit for 10 minutes.  
Remove capacitors and inspect for visual defects.  
Measure capacitance and ESR. Record.  
Take a picture of each capacitor and place in log book, if any visual defects are found.

Table 1: CAPACITOR TEST PROCEDURE (cont.)

6. Replace capacitors in vacuum and pulse at .2 Hz into sufficient resistance to provide 20% reversal. Operate in this mode for 2 hours.

Measure case, end and terminal temperature.

Record temperature as a function of time. Measure every 15 minutes.

Record capacitor voltage and current.

7. Remove capacitors and measure capacitance and ESR. Inspect for visual defects. Take a picture of each capacitor and place in log book.

Basis for rejection of capacitors:

1. Change in capacitance ( $\pm 5\%$ ).
2. Change in ESR ( $\pm 5\%$ ).
3. Evidence of physical change, such as can bulging, leaking impregnant, etc.
4. Excessive rise in temperature during .2 Hz testing.

Table 2: RESULTS OF CAPACITOR ACCEPTANCE TEST

|                     | CAP #004 |      | CAP #010 |      | CAP #014 |       | CAP #015 |      | CAP #016 |      |
|---------------------|----------|------|----------|------|----------|-------|----------|------|----------|------|
|                     | C        | ESR  | C        | ESR  | C        | ESR   | C        | ESR  | C        | ESR  |
| As Received         |          |      |          |      |          |       |          |      |          |      |
| 2/11/86             | 57.3     | 0.15 | 58       | 0.11 | 58.7     | 0.302 | 57.8     | 0.11 | 57.5     | 0.11 |
| After Vacuum Soak   |          |      |          |      |          |       |          |      |          |      |
| and High Pot in Air | 57.5     | 0.15 | 58.1     | 0.10 | 58.4     | 0.18  | 57.4     | 0.10 | 57.1     | 0.10 |
| After High-Pot      |          |      |          |      |          |       |          |      |          |      |
| in Vacuum           | 57.6     | 0.15 | 58.1     | 0.10 | 58.1     | 0.23  | 58.1     | 0.10 | 57.7     | 0.11 |
| After Rep-Rate      | 57.6     | 0.11 | 58.2     | 0.10 | 58.7     | 0.10  | -        | -    | 57.8     | 0.11 |

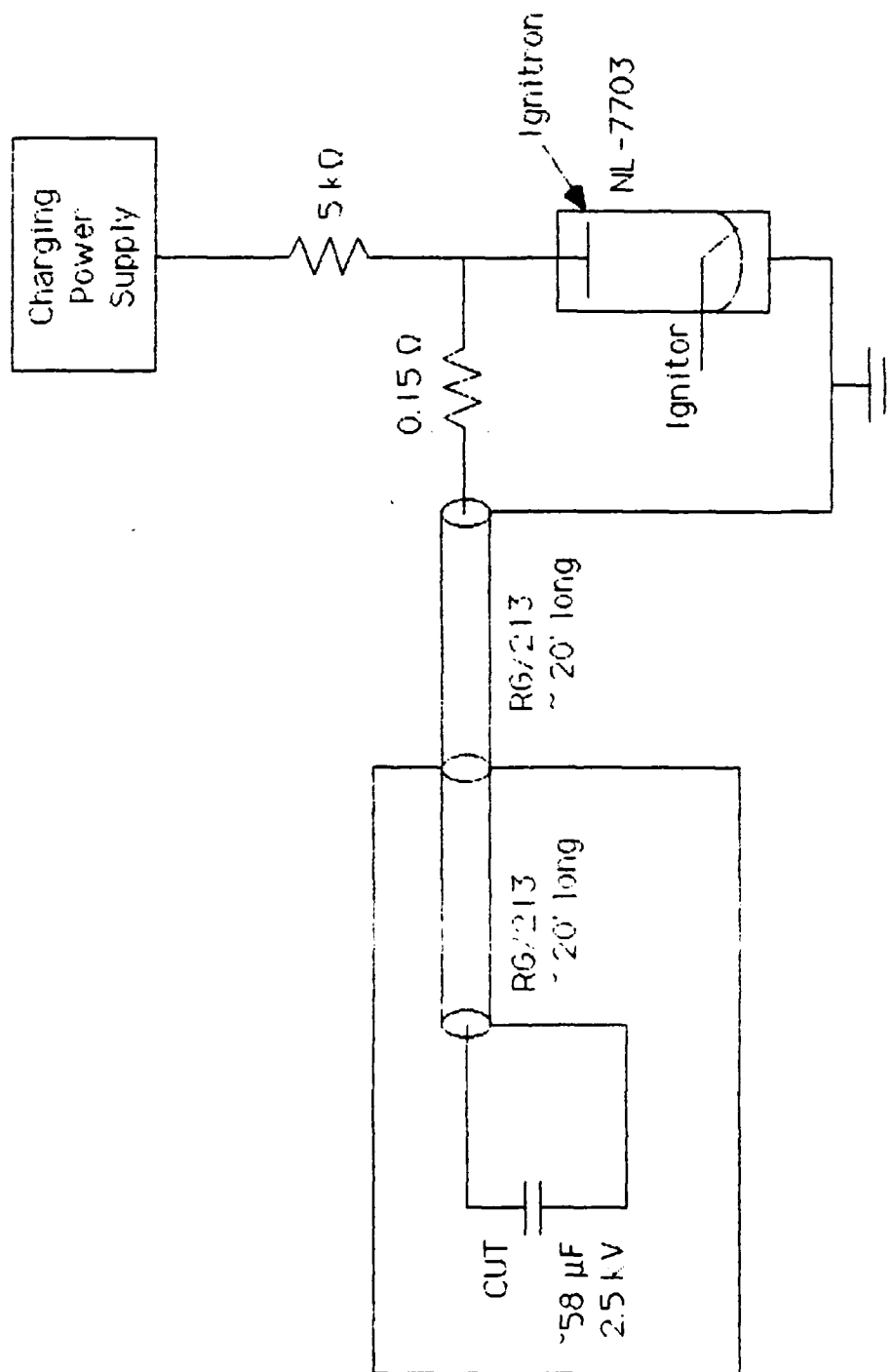
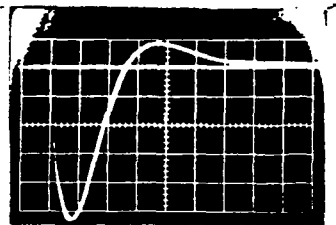
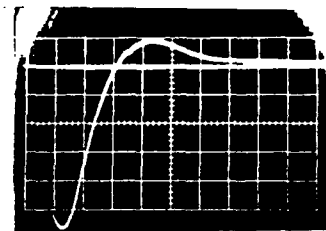


Figure 1 Schematic of test circuit for testing capacitor under rep-rate conditions in vacuum.

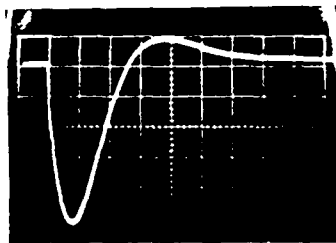




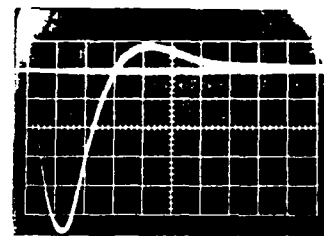
Capacitor #004  
1 kA/div 20  $\mu$ sec/div



Capacitor #010  
1 kA/div 20  $\mu$ sec/div



Capacitor #014  
1 kA/div 20  $\mu$ sec/div



Capacitor #016  
1 kA/div 20  $\mu$ sec/div

Figure 2. Output current waveforms for each capacitor tested except #015, the capacitor that failed. Each capacitor was charged to 2.5 kV then discharged through a total series resistance of  $0.25\Omega$  and a total series inductance of  $3.5\mu\text{H}$ .

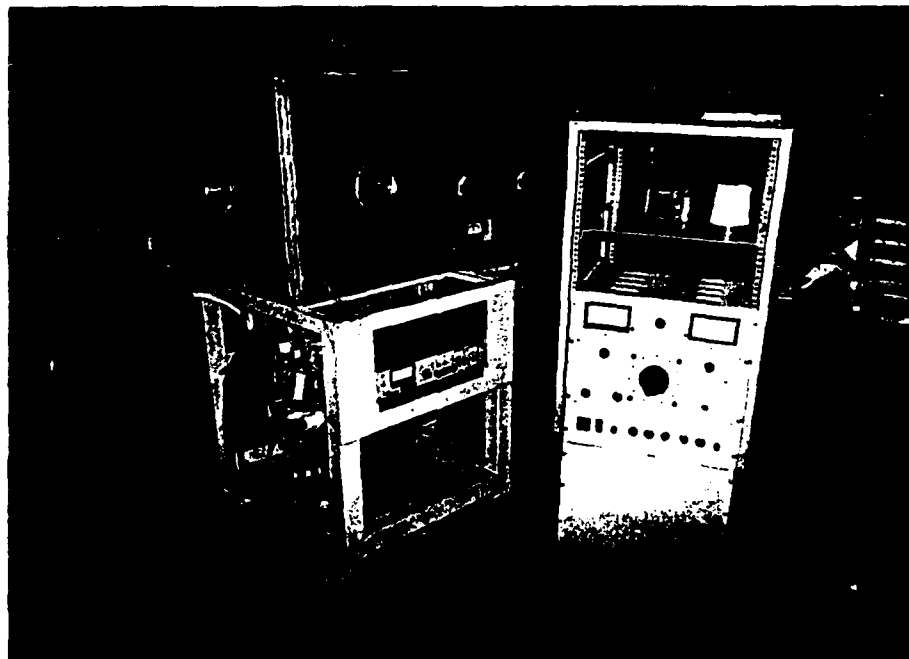
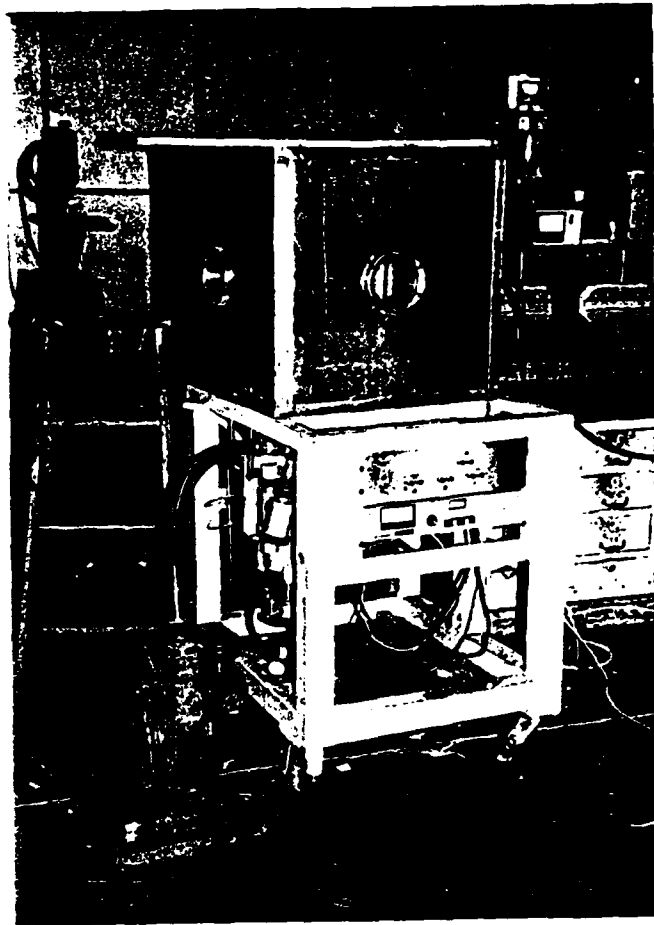
capacitor was removed from the vacuum chamber and checked; the capacitor had failed shorted, internally. Two other capacitors, numbers 010 and 104, were accidentally arced when the vacuum chamber was brought to air while voltage was still applied to the capacitor. These arcs did not seem to affect the capacitor performance.

No other failures were encountered during the rep-rate test. Capacitance and ESR were remeasured for each capacitor after the rep-rate test. All capacitors except 014 had capacitance and ESR similar to previous readings. Capacitor 014 had an ESR which was three times less than its initial value, but more in line with the values measured on the other capacitors.

Temperature of the capacitor can was measured during the rep-rate test. With the capacitor sitting on the floor of the metal vacuum tank, the initial temperature was 75°C and the temperature after 2 hours of testing was 75°C. We then put the capacitor on a piece of plexiglas to thermally insulate the capacitor from the metal vacuum tank. Initial case temperature was 79°C, and remained at that point for the next 8 minutes of testing.

#### 4.0 Summary

Based on the results of capacitor test, capacitors 004, 010, and 016 are acceptable, and will perform as required in the PPT. Capacitor 014 may fail during operation in the PPT. The basis for this determination is the wide variation in ESR noted during the capacitor acceptance test. The people involved in the Sandia capacitor development program might be able to give an explanation for why the ESR of capacitor 014 matched that of the other capacitors after rep-rate testing. Capacitor 015 completely failed during testing, and has been sent back to Sandia for autopsy.



Test setup at PI for testing PPT capacitors.  
Vacuum tank is in top photo, and power supply  
is in the right rack, bottom photo.

## **APPENDIX D - PPT ENDURANCE TEST PLAN**

**PULSED PLASMA MISSION ENDURANCE TEST PROGRAM**

**TEST PLAN**


Prepared for:

**Air Force Rocket Propulsion Laboratory**  
AFRPL/LKCJ, Stop 24  
Edwards AFB, California 93523

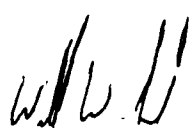
Submitted by:

**Rocket Research Company**  
A Division of ROCKCOR  
P.O. Box 97009  
Redmond, Washington 98073-9709

Prepared by:

  
R. J. Cassady  
Sr. Development Engineer

Approved by:

  
W. W. Smith  
Manager,  
Electric Propulsion

April 4, 1986

D-1

tah#3

## **PPT MISSION ENDURANCE TEST**

### **1.0 TEST PLAN**

#### **1.1 Test Scope**

The PPT Mission Endurance Test will place the millipound Pulsed Plasma Thruster (PPT) under life test, with the goal of demonstrating 14 million pulses. The life test will stress several critical components within the PPT, including the discharge initiation circuit, the propellant feed mechanisms, and most notably, the high energy discharge capacitors. As a result, some failures are anticipated and must be diagnosed promptly to enable preventive action to be taken or repairs to be made before a catastrophic system failure occurs. Early diagnosis requires careful monitoring of the thruster discharge parameters; however, the length of the test and its continuous nature precludes constant operator monitoring. Therefore, the test will be automated, with trend data periodically evaluated to diagnose potential failures. As a further safety precaution, the automated test console contains interlocks to disable the test in the event of any parameters straying out of a pre-determined range. Further details of the individual phases of the test and a detailed test procedure are given in the following sections.

#### **1.2 Test Objectives**

The overall objective of the test is to demonstrate 14 million pulses lifetime for the solid teflon PPT. As subtasks, performance and other parameters will be monitored during the test. These are described in each of the next three paragraphs.

##### **1.2.1 Monitored Testing**

Upon completing check-out of the PPT/ground test console/test chamber integrated system a period of monitored testing will begin. The monitored testing will take place with a Test Operator in attendance. It is intended to serve as a shake-down phase prior to automated testing. The monitored test will begin by following the test start-up procedures outlined in Appendix A: Test Procedures. The Test Operator will bring the system up and initiate the .2 Hz duty cycle pulsing of the thruster. Data to be monitored is shown in Table 1 and will include thrust per pulse, discharge voltage, ignitor plug resistance and capacitor temperatures. In addition the discharge waveform will be

| PARAMETER                                 | RANGE  | RECORDING DEVICE   | FREQUENCY    |
|---|--|--------------------|--------------|
| $E_{CB}$ CAPACITOR BANK VOLTAGE           | 0-3000 Volts                                 | OSCILLOSCOPE       | CONTINUOUS   |
| $I_D$ DISCHARGE INITIATION CURRENT        | 0-500 AMPS                                   | OSCILLOSCOPE       | CONTINUOUS   |
| F THRUST                                  | 0-2 MLBF                                     | STRIP CHART        | CONTINUOUS   |
| $T_1$ - $T_8$ CAPACITOR TEMPERATURES      | 0-100°C                                      | VISUAL             | 4 TIMES/HOUR |
| TBD WARMEST CAP. TEMP                     | 0-100°C                                      | STRIP CHART        | CONTINUOUS   |
| $T_9$ THERMAL SHUNT TEMP.                 | 0-100°C                                      | VISUAL             | 4 TIMES/HOUR |
| $T_{10}$ , $T_{11}$ POWER CONVERTER TEMP. | 0-100°C                                      | VISUAL             | 4 TIMES/HOUR |
| $T_{12}$ THRUSTER BOTTOM PLATE TEMP.      | 0-100°C                                      | VISUAL             | 4 TIMES/HOUR |
| $T_{13}$ THRUSTER TOP PLATE TEMP.         | 0-100°C                                      | VISUAL             | 4 TIMES/HOUR |
| $T_{14}$ ANODE HEAT SINK TEMP.            | 0-100°C                                      | VISUAL             | 4 TIMES/HOUR |
| $T_{15}$ CATHODE HEAT SINK TEMP.          | 0-100°C                                      | VISUAL             | 4 TIMES/HOUR |
| $P_o$ VACUUM LEVEL                        | $1 \times 10^{-5}$ - $1 \times 10^{-3}$ TORR | VISUAL             | 4 TIMES/HOUR |
| $E_s$ SUPPLY VOLTAGE                      | 0-30 VDC                                     | VISUAL             | 4 TIMES/HOUR |
| $I_s$ SUPPLY CURRENT                      | 0-15 ADC                                     | VISUAL             | 4 TIMES/HOUR |
| N PULSE NUMBER                            | $0-1 \times 10^5$                            | VISUAL             | 4 TIMES/HOUR |
| $R_p$ IGNITOR PLUG RESISTANCE             | $0-1 \times 10^6$ OHMS                       | DIGITAL MULTIMETER | 1 TIME/HOUR  |

TABLE 1 DATA TO BE RECORDED - MONITORED TESTING

monitored. Should any anomalies be detected, the Test Operator will immediately shut down the test and summon the Development Engineer and the Electrical Engineer. The data will be reviewed and a decision will be made on how to proceed. If after a period of one week all monitored testing appears to be going well, the system will be converted to full automated testing. Thereafter, only a short period (approximately 30 minutes) each day will be dedicated to monitored operation.

### **1.2.2 Automated Testing**

The automated test portion of the PPT Mission Endurance Test will conduct the 24-hour-a-day testing for the 810 days required to achieve 14 million pulses. Automated testing was deemed necessary because of the extreme duration of the life test. During the automated test phase, operation of the PPT will be monitored via the test console. Interlocks will shut down the test if any parameters vary from their present ranges. Examples of parameters to be automatically monitored include the capacitor temperatures, vacuum level and capacitor bank voltage. The parameters are listed in Table 2. Daily spot-checks of the thruster parameters will be made and logged by the Test Operator for review by the Development Engineer on a regular weekly basis. If any parameter shows a large deviation, though not enough to trip the interlocks, the Test Operator will report the data immediately to the Development Engineer. Periodic shut-downs will be required to clean the cryo-pump. Also, at approximately 8 to 8.5 million pulses, a shutdown will be required to add the Teflon required to complete the life test. These shut-downs will be performed under manual supervision and during start-up a period of monitored testing will be maintained for two hours to ensure correct operation before switching to automated control.

### **1.2.3 Performance Evaluation**

Throughout the monitored and automated testing, performance of the PPT will be recorded and evaluated. Performance data to be gathered includes the discharge voltage, the discharge impulse-bit, the DI circuit current, and the discharge voltage pulse shape. Real time data analysis will give immediate thruster performance such as instantaneous thrust per pulse and peak power. Trends will be monitored over the course of the life test, especially for impulse-bit, igniter plug resistance, and pulse shape. Any trends will be documented by the Development Engineer and included in the final report. During the test, the need for thrust stand re-calibration is anticipated. For this reason, the rolling ball calibrator will be used periodically (during shut-downs for pump maintenance, for example) to check the thrust stand calibration. The Test Operator will record the results



| PARAMETER                                 | RANGE  | RECORDING DEVICE   | FREQUENCY  |
|---|--|--------------------|------------|
| $E_{CB}$ CAPACITOR BANK VOLTAGE           | 0-3000 VOLTS                                 | STRIP CHART        | CONTINUOUS |
| $I_D$ DISCHARGE INITIATION CURRENT        | 0-500 AMPS                                   | STRIP CHART        | CONTINUOUS |
| F THRUST                                  | 0-2 MLBF                                     | STRIP CHART        | CONTINUOUS |
| $T_1$ - $T_8$ CAPACITOR TEMPERATURES      | 0-100°C                                      | VISUAL             | ONCE/DAY   |
| TBD WARMEST CAP. TEMP.                    | 0-100°C                                      | STRIP CHART        | CONTINUOUS |
| $T_9$ THERMAL SHUNT TEMP.                 | 0-100°C                                      | VISUAL             | ONCE/DAY   |
| $T_{10}$ , $T_{11}$ POWER CONVERTER TEMP. | 0-100°C                                      | VISUAL             | ONCE/DAY   |
| $T_{12}$ THRUSTER BOTTOM PLATE TEMP.      | 0-100°C                                      | VISUAL             | ONCE/DAY   |
| $T_{13}$ THRUSTER TOP PLATE TEMP.         | 0-100°C                                      | VISUAL             | ONCE/DAY   |
| $T_{14}$ ANODE HEAT SINK TEMP.            | 0-100°C                                      | VISUAL             | ONCE/DAY   |
| $T_{15}$ CATHODE HEAT SINK TEMP.          | 0-100°C                                      | VISUAL             | ONCE/DAY   |
| $P_o$ VACUUM LEVEL                        | $1 \times 10^{-5}$ - $1 \times 10^{-3}$ TORR | VISUAL             | ONCE/DAY   |
| $E_s$ SUPPLY VOLTAGE                      | 0-30 VDC                                     | VISUAL             | ONCE/DAY   |
| $I_s$ SUPPLY CURRENT                      | 0-15 ADC                                     | VISUAL             | ONCE/DAY   |
| N PULSE NUMBER                            | $0-2 \times 10^7$                            | VISUAL             | ONCE/DAY   |
| $R_p$ IGNITOR PLUG RESISTANCE             | $0-1 \times 10^6$ OHMS                       | DIGITAL MULTIMETER | ONCE/WEEK  |

TABLE 2 DATA TO BE RECORDED - AUTOMATED TESTING

of the periodic re-calibrations for inclusion with the other performance data. Additionally, inspection of the thruster components will be performed upon completion of the life test. Photo documentation of the condition of all thruster components will be made as part of the final disassembly and inspection.

### **1.3 Safety Considerations and Hazards**

Pursuant to the RRC company policy (RRC Policy 18) all steps to ensure the safety and health of the employees will be taken. As a first step in this procedure, hazards associated with the PPT Mission Endurance Test have been identified on a component level and rated by severity. The following definitions were used in the hazard analysis ratings:

|                |   |
|----------------|---|
| Catastrophic - | May cause death or loss of system.  |
| Critical -     | May cause severe injury, severe occupational illness, or major system damage. |
| Marginal -     | May cause minor injury, minor occupational illness, or minor system damage.   |
| Negligible -   | Will not result in injury, occupational illness, or system damage.            |

The results of the hazard analysis are given in Appendix B: Preliminary Hazard Analysis. Safeguards have been incorporated into the system including interlocks, automatic shut-down in the event of power failure or vacuum loss, capacitor over-temperature sensors and automatic dump circuit, and manual shorting wands. Employee training will stress that under no circumstances should this system of safeguards be disabled or bypassed.

### **1.4 Data Acquisition and Reduction**

The PPT Mission Endurance Test poses a unique data acquisition problem due to the extremely short nature of the thruster discharge and the extremely long period of the life test. The conflicting requirements lead to the selection of strip chart recorders to monitor trend data expected to slowly vary throughout the life test and a fast digital oscilloscope to record the traces of the individual thruster pulses. A complete instrumentation list is given in Table 3.

As previously mentioned, the automated portion of the life test will rely on sensor

| <u>NOMENCLATURE</u>    | <u>MFG.</u>     | <u>MODEL NUMBER</u> | <u>CALIBRATION INTERVAL</u> |
|------------------------|-----------------|---------------------|-----------------------------|
| Ground Test console    | Fairchild       | 197A0001C           | 6 Months                    |
| Oscilloscope Mainframe | Tektronix       | 5223                | 6 Months                    |
| Oscilloscope Amplifier | Tektronix       | 5A21N               | 6 Months                    |
| Oscilloscope Time Base | Tektronix       | 5B25N               | 6 Months                    |
| Oscilloscope Camera    | Tektronix       | C50                 | Maintain as Req'd.          |
| Strip Chart            | Hewlett-Packard | 7100B               | 3 Months                    |
| Digital Multimeter     | Hewlett-Packard | 3478A               | 6 Months                    |
| Vacuum Gauge           | Veeco           | RG83                | 12 Months                   |
| Thrust Stand           | Fairchild       |                     | 1 Month                     |

TABLE 3 INSTRUMENTATION LIST

circuitry that will shut down the test if critical parameters vary outside pre-set limits. A complete list of these parameters and the limits determined for shut-down are shown in Table 4.

The data acquisition equipment used for the program will be periodically re-calibrated to maintain NBS traceable measurement accuracy throughout the more than two years of the test. Each piece of equipment or instrumentation is listed with its calibration requirements in Table 3.

Data reduction will be accomplished on a periodic basis throughout the life test. It will consist mostly of reducing strip chart data to numerical records, converting oscilloscope trace data to numerical records and applying the thrust stand calibration to the impulse-bit data to reduce it to a numerical record. All data records will be entered in a laboratory notebook together with the date and time of the entry. Performance calculations will be made on a weekly basis and included in the notebook.

#### **1.5 Retest and Rework Criteria**

The PPT Mission Endurance Test is perceived as a "hands-off" life test. Therefore, only indications that a component failure is imminent will cause the test to be stopped and the component replaced or repaired. Changes in characteristics of a component alone will not be sufficient to warrant its replacement or refurbishment. If such action is required, it will be noted in the laboratory notebook, together with the number of pulse fired cumulative prior to the repair action. Only in the event of an "infant mortality" failure (within the first 10,000 pulses) will a complete restart of the life test be considered. After that any failure or repair resulting in the halting of the life test will be recorded at the point in the test where it occurred and the test will resume from that point.

**TABLE 4**  
**AUTOMATED TEST SHUTDOWNS**

| CAUSE                                  | RESULT  | LIMIT                              |
|--|---|------------------------------------|
| Loss of 110 volt input                 | GTC shuts down, pulsing stops                           | N/A                                |
| Opening rear cover of GTC              | Microswitch shuts down GTC, pulsing stops               | N/A                                |
| Loss of 28Vdc input to Power converter | GTC shuts down, pulsing stops                           | N/A                                |
| Loss of telemetry from thruster        | GTC shuts down, pulsing stops                           | N/A                                |
| Thruster pre-fire or mis-fire          | GTC shuts down, pulsing stops                           | Less than 5.5 sec. between fire    |
| Excessive capacitor charging time      | GTC shuts down, pulsing stops                           | Greater than 5.5 sec. between fire |
| Loss of vacuum                         | Pressure switch shuts down GTC, pulsing stops           | Greater than 5 Torr                |
| Capacitor overtemp                     | Temperature sensor cutout shuts down GTC, pulsing stops | Greater than 60°C                  |

## APPENDIX A: TEST PROCEDURE

The following is an item-by-item procedure to be followed in the conduct of testing for the PPT Mission Endurance Test, deviations from this procedure must be approved by the Development Engineer and the Project Manager.

### TEST STARTUP

- 010 Visually verify that all electrical connections to the thruster and thrust stand are properly made.
- 020 Turn on cooling plate water flow and verify that there are no leaks.
- 030 Verify that fixed and adjustable stops are both backed away from the thrust stand arm.
- 040 Close and clamp chamber door. Open isolation valve and turn on the roughing pump. When vacuum level reaches  $4 \times 10^{-5}$  torr close isolation valve and shut down the roughing pump. Start up the cryopump per its operating manual.
- 050 Verify all switches on the Ground Test Console (GTC) are off (down). Turn on AC Power breaker and press the AC Power button. Verify that AC Power On lamp is lit. Turn on Utility and DC breakers. Turn on Instrument Power and verify that DPMs are on. Scan through all thermocouples and verify that each indicates ambient temperature properly. Set TM mode to TM Analog and TM Channel Selector to Main Bank. Set damping oil heater controller to 80°F and turn on heater power. Turn on switch on Schaevitz CAS LVDT amplifier.

### MONITORED TESTING

- 060 Route D.I. Current signal to channel 1 of oscilloscope set to 10 V/Div. (100 amps/div.), set zero position to 1 div. above center. Route Analog Out (Main Bank voltage) to channel 2 of oscilloscope set to 1 V/div. (512.82 volts/div.), set zero position to bottom of screen. Trigger on channel 1. Route LVDT output to channel 1 of strip chart set to 1 volt range. Note that LVDT signal is negative going. Route temperature DPM output to channel 2 of strip chart set to 100 mV range (10°C per inch). Set limit switch on channel 2 of strip chart to open at 6 inches (60°C). Set zero position of strip chart channel 1 to left margin and of channel 2 to 7 inches. Route Plug Resistance signal to Digital Multimeter (DMM) set to autoranging resistance mode.
- 070 Operate thrust stand leveling motor as required to bring zero position of LVDT signal within the 7 to 8 inch range. Roll calibration balls one at a time (separate each ball by at least 30 seconds) and verify that the resulting output pulse does not over-range the chart. Roll balls continuously until the trace position has stabilized, adjust the zero of the strip chart if required to keep the trace on the chart. Stamp and label data on strip chart record.

- 080      Verify that vacuum level is at least  $1 \times 10^{-4}$  torr.
- 090      Turn on Plug Resistance Enable switch and note resistance reading shown on the DMM. Turn off the Plug Resistance Enable switch.
- 100      Set Thruster Firing Mode to Single Shot. Momentarily operate the Converter Latch switch to apply power to the thruster electronics. Turn on the Standby Enable and TM Enable switches and verify that their indicator lamps light. Turn on the Thruster Enable switch and verify that its indicator is lit. Set up oscilloscope to record data and operate the strip chart at 0.1 inches/second. Zero the pulse counter.  
NOTE: Except at the direction of the Development Engineer, do not zero the pulse counter again at any later time throughout the entire test. The counter is battery operated and will retain the count even when GTC power is removed.
- 110      Record all data on Data Sheet including plug resistance noted in operation 090.
- 120      Press the Single Pulse button once to fire the thruster. Verify (from LVDT output) that thruster fires. If required, fire additional pulses and adjust oscilloscope and strip chart to properly record data.
- 130      Test and Development Engineers verify that the entire system is operating correctly.
- 140      Set Thruster Firing Mode to Full to initiate continual firing.
- 150      Every 15 minutes record all data on Data Sheet except plug resistance. Once per hour include a photograph of the oscilloscope traces and make a plug resistance reading per operation 160. Leave the thermocouple selector set to whichever capacitor temperature (T1-T8) is the warmest and note which channel this is on the strip chart record and in the Remarks section of the Data Sheet.
- 160      To measure plug resistance: Turn off Thruster Enable switch. Raise the red cover and turn on the Capacitor Dump switch. Turn on the Plug Resistance Enable switch and record the resistance reading from the DMM. Turn off the Plug Resistance Enable switch. Close the red cover on the Capacitor Dump switch. Turn on the Thruster Enable switch to resume the test.
- 170      Repeat operations 150 and 160. At the end of each day: Turn off the Thruster Enable, TM Enable and Standby Enable switches; momentarily operate the Converter Unlatch switch; raise the red cover and turn on the Capacitor Dump switch and turn off the strip chart drive; leave all other equipment turned on. At the start of each day: Close the red cover on the Capacitor Dump switch, momentarily operate the Converter Latch switch, turn on the Standby Enable and TM Enable switches and verify that their indicator lamps light and turn on the Thruster Enable switch to start the thruster firing. Repeat operations beginning at operation 150.

#### **AUTOMATED TESTING**

- 180      Test and Development Engineers verify that the entire system is operating correctly and is ready to be placed in the Automated Operation mode.

- 190 Remove oscilloscope from the setup. Route the D.I. Current signal to channel 1 of a second strip chart set to the 50 volt range (50 amps per inch). Set the zero position of this channel at 7 inches. Route the Analog Out (Main Bank Voltage) signal to channel 2 of the second strip chart set to the 5 volt range (256.41 volts per inch). Set the zero position of this channel at the left margin. Operate both strip charts at 1 inch/minute. Stamp and label data on both strip chart records.
- 200 Close red cover on Capacitor Dump switch. Momentarily operate the Converter Latch switch. Turn on Standby Enable and TM Enable switches and verify that their indicator lamps are lit. Turn on strip chart drives. Set Thruster Firing Mode to Full. Turn on Thruster Enable switch to begin thruster firing.
- 210 At the beginning of each weekday record all data on Data Sheet except plug resistance and replace strip chart paper. Stamp and label data on new strip chart records. Each Monday also record plug resistance per operation 160. The first Monday of each month also record at least 20 individual calibration ball rollings (separate each ball by at least 30 seconds). At this time also reconnect the oscilloscope per operation 060 and record and photograph pulse shapes. Attach the photograph to the Data Sheet. The oscilloscope may then be removed.
- 220 After the first month of automated operation the strip charts may be slowed to conserve paper at the option of the Development Engineer.
- 230 If at any time the Thruster Malfunction lamp is lit, the GTC power is off (can be caused by a power failure, strip chart limit switch or actuation of the vacuum pressure switch) or any anomaly is noted in the data or operation of the system turn off the Thruster Enable switch, raise the red cover and turn on the Capacitor Dump switch, record all data on Data Sheet including plug resistance and describe the condition in the Remarks section of the Data Sheet. Contact the Test and Development Engineers for resolution of the problem.

### **TEST SHUTDOWN**

- 240 If the vacuum chamber must be opened for any reason such as test completion, cryopump maintenance or anomaly investigation/correction perform the following operations. Turn off Thruster Enable switch. Raise the red cover and turn on the Capacitor Dump switch. Record all data on the Data Sheet including plug resistance and describe the situation in the Remarks section of the Data Sheet. Verify from telemetry DPM that Main Bank Voltage has been reduced to zero. Turn off strip charts. Turn off RM Enable and Standby Enable switches. Momentarily operate the Converter Unlatch switch. Turn off DC, Utility and AC Power breakers. Turn off cooling plate water flow. Shut down the cryopump per its operating manual. After the cryopump has warmed to ambient temperature open the chamber backfill valve and completely backfill the chamber. Close the chamber backfill valve. Open the isolation valve and turn on the roughing pump. When vacuum level reaches  $4 \times 10^{-3}$  torr close the isolation valve and shut down the roughing pump. Open the chamber backfill valve.

### **CAUTION**

The main capacitor bank in the thruster can store a LETHAL charge.



- 250 As soon as the chamber door is opened CAREFULLY measure the voltage on the red and black leads to the Capacitor Dump box on top of the thruster to verify that no charge remains in the Main Bank capacitors. DO NOT PROCEED until this voltage is ZERO. Connect a shorting jumper across the red and black leads. Position the fixed and adjustable stops against the thrust stand arm to lock it into position. Proceed with further work at the direction of the Test and Development Engineers. Record all work in the Remarks section of a Data Sheet.

#### **TEST RESTART**

- 260 Perform operations 010 to 030. Remove the shorting jumper from the red and black leads on the capacitor dump box. Perform operation 040 and 050. Verify that vacuum level is at least  $1 \times 10^{-4}$  torr. If the test is to resume with a period of monitored testing continue operations in sequence beginning at operation 060. If the test is to resume automated testing continue operations in sequence beginning at operation 200.

**APPENDIX B:**  
**PRELIMINARY HAZARD ANALYSIS**

# PULSED PLASMA MISSION ENDURANCE TEST

## PRELIMINARY HAZARD ANALYSIS

| HAZARD<br>DESCRIPTION                             | HAZARD<br>EFFECTS  | HAZARD<br>SEVERITY | PLANNED OR RECOMMENDED<br>SAFETY ACTION  |
|---|--|--------------------|--|
| Electrical power applied<br>in low vacuum ambient | Test experience has demonstrated that<br>electrical arc and internal short circuit<br>occurs.  | Critical           | Pressure switch provides<br>automatic shutdown if vacuum<br>level rises above 5 Torr.  |
| Loss of input power during<br>test                | Automatic test cycling of thruster will<br>stop.   | Critical           | Procedure specifies capacitor<br>dump to be activated, voltage<br>on dump circuit to be measured<br>and shorting jumper to be<br>connected across dump circuit.                                      |
| Electrical short or open<br>circuit               | Failure to recharge the discharge<br>initiation capacitors and/or the energy<br>storage capacitors. Thruster will<br>fail to operate.          | Critical           | Procedure specifies capacitor<br>dump to be activated, voltage<br>on dump circuit to be measured<br>and shorting jumper to be<br>connected across dump circuit.                                      |
| Capacitor housing rupture                         | Loss of capacitor and probable damage<br>to neighboring PPT parts and contam-<br>ination of vacuum chamber and test<br>instrumentation.        | Critical           | Follow capacitor temperature<br>trends closely. If thermal<br>runaway becomes evident shut<br>down test and replace capacitor.<br>Automated shutdown for<br>capacitor overtemp greater than<br>60°C. |
| Capacitor housing leakage                         | Loss of capacitor and possible damage<br>to neighboring PPT parts and probable<br>contamination of vacuum chamber and<br>test instrumentation. | Critical           | Follow capacitor temperature<br>trends closely. If thermal<br>runaway becomes evident shut<br>down test and replace capacitor.<br>Automated shutdown for<br>capacitor overtemp greater than<br>60°C. |

# PULSED PLASMA MISSION ENDURANCE TEST

## PRELIMINARY HAZARD ANALYSIS

Continued

| <u>HAZARD<br/>DESCRIPTION</u>                           | <u>HAZARD<br/>EFFECTS</u>  | <u>HAZARD<br/>SEVERITY</u> | <u>PLANNED OR RECOMMENDED<br/>SAFETY ACTION</u>  |
|---|--|----------------------------|--|
| High temperature exposure                               | High temperature exposure can result in capacitor rupture or leakage, or degradation and damage of power converter components. | Critical                   | Follow capacitor temperature trends closely. If thermal runaway becomes evident shut down test and replace capacitor. Automated shutdown for capacitor overtemp greater than 60°C. |
| Personnel contact with high voltage charge on capacitor | Severe electrical shock and perhaps death.   | Catastrophic               | Safety briefing to all personnel prior to test initiation. Stress that procedures must be followed.  |

## **APPENDIX E - 7PT THRUST STAND CALIBRATION PROCEDURE**

THRUST STAND  
OPERATIONS MANUAL

November 1976

Prepared for  
AIR FORCE ROCKET PROPULSION LABORATORY  
Edwards Air Force Base  
California

**FAIRCHILD**  
REPUBLIC COMPANY  
Farmingdale, L.I. New York 11735

## CONTENTS

| <u>Section</u>  | <u>Page</u> |
|---|-------------|
| 1.0 INTRODUCTION  |             |
| 1.1 General Description of Thrust Measurement System        | 1           |
| 1.2 Thrust Stand  | 1           |
| 1.3 Readout Equipment                                       | 1           |
| 1.4 Ball Calibrator   | 2           |
| 2.0 THRUST STAND NOMENCLATURE<br>AND ASSEMBLY INSTRUCTIONS  | 2           |
| 2.1 Fixed Base Assembly                                     | 5           |
| 2.2 Adjustable Base Plate, Vertical Support and Balance Arm | 5           |
| 3.0 INSTALLATION OF THRUST STAND                            | 12          |
| 3.1 Mechanical Aspects                                      | 12          |
| 3.1.1 Thrust Stand Alignment                                | 12          |
| 3.1.2 Ball Calibrator Installation                          | 14          |
| 3.2 Electrical Hook-up                                      | 14          |
| 4.0 FINAL ADJUSTMENT  | 21          |
| 4.1 LVDT Center Adjustment                                  | 21          |
| 4.2 LVDT Linearity Verification                             | 24          |
| 5.0 CALIBRATION OF BALL CALIBRATOR                          | 26          |
| 5.1 Fundamental Concept                                     | 26          |
| 5.2 Calibration Procedure                                   | 28          |
| 5.3 Initial Trajectory                                      | 31          |
| 5.4 Rebound Trajectory                                      | 33          |
| 6.0 THRUSTER INSTALLATION ON THRUST BALANCE                 | 36          |

## CONTENTS (cont'd)

| <u>Section</u>         | <u>Page</u> |
|------------------------|-------------|
| 7.0 THRUST MEASUREMENT | 38          |
| 7.1 Data Generation    | 38          |
| 7.2 Data Reduction     | 39          |
| 8.0 TROUBLESHOOTING    | 40          |
| 9.0 REPAIRS            | 42          |
| APPENDIX               | 43          |



## ILLUSTRATIONS

| <u>Figure</u>  | <u>Page</u> |
|--|-------------|
| 1. Assembled Thrust Stand                                  | 3           |
| 2. Leveling Motor Detail                                   | 4           |
| 3. Base Plate, Vertical Support and Balance Arm            | 6           |
| 4. Assembly Isometric                                      | 8           |
| 5. Assembly Isometric                                      | 9           |
| 6. Assembly Isometric                                      | 10          |
| 7. Assembly Isometric                                      | 11          |
| 8. Ball Calibrator Assembly                                | 15          |
| 9. Wiring Schematic - Thrust Measurement System            | 16          |
| 10. Control Panel  | 18          |
| 11. Control Panel Wiring Diagram                           | 20          |
| 12. Recorder Pen Displacement vs. Balance Arm Displacement | 25          |
| 13. Ball Calibrator with CAD in Position                   | 29          |
| 14. Coordinate System - Initial Trajectory                 | 32          |
| 15. Coordinate System - Rebound Trajectory                 | 34          |

## TABLES

|  | <u>Page</u> |
|--|-------------|
| Table I. y-Coordinates   | 32          |
| Table II. Distance of CAD from Position<br>3 Lower to Any Other Position | 34          |

## 1.0 INTRODUCTION

### 1.1 General Description of Thrust Measurement System

The thrust measurement system consists of three major components. These are the thrust stand, the ball calibrator, and the displacement readout equipment. This system is capable of accurately measuring the thrust produced by propulsion systems delivering from 50 micropounds to 6 millipounds of thrust. The accuracy of the system is  $\pm 3\%$  over this range.

### 1.2 Thrust Stand

The thrust stand utilizes the well-known seismic or "swinging gate" pendulum principles. It is capable of measuring either a steady state thrust or impulse bit. The thruster is supported from an arm having a fixed vertical pivot axis. The vertical axis is given a slight tilt ( $1.5^\circ$ ), yielding a low point in the arm's circle of movement around the pivot such that the arm will always return to this low point if displaced. The thrust produced by a thruster is linearly related to the displacement of the arm from this point, within the limits of linearity of the system.

### 1.3 Readout Equipment

The amount of thrust (or magnitude of impulse) produced by a thruster is linearly related to the displacement of the movable arm from its zero position within the range of linearity of the system. This movement is sensed by a linear variable differential transformer (LVDT) which has its coil mounted to the stationary stand base plate and its passive slug attached to the moving arm. A Schaevitz model 050HR AC LVDT is supplied with the stand. This LVDT is used in conjunction with a Hewlett-Packard

model 7402A two-channel oscillographic recorder and model 17403A AC carrier preamplifier plug-in, which are also supplied.

#### 1.4 Ball Calibrator

The measurement of thrust produced by a given propulsion system is accomplished by relating the amplitude of the signal recorded by the oscillographic recorder when the thruster is fired to the amplitude recorded when a known amount of thrust is applied to the movable arm. The device used to produce this known amount of thrust is called the ball calibrator, which consists of a closed loop of ball bearings which are rolled down an inclined plane either at a constant rate of one per second, or individually. The balls collide with a hardened tool steel block which is fastened to the movable arm, thereby imparting an impulse to the arm. Because each ball produces the same impulse, running the balls at a rate of one per second results in an equivalent steady-state thrust equal to the magnitude of the impulse bit times one Hertz. Thus, steady state thrusters producing thrust in the specified range can be measured by rolling the balls continuously and impulse type thrusters can be measured by rolling the balls individually. The quantity which must be accurately known is the magnitude of the impulse bit produced by the balls. The technique used to measure this quantity is described in a subsequent section of this manual.

#### 2.0 THRUST STAND NOMENCLATURE AND ASSEMBLY INSTRUCTIONS

A photograph of the completely assembled thrust stand is shown in Fig.

1. The major components of this assembly are the fixed base assembly, adjustable base plate, vertical support, hinge modules, and movable balance

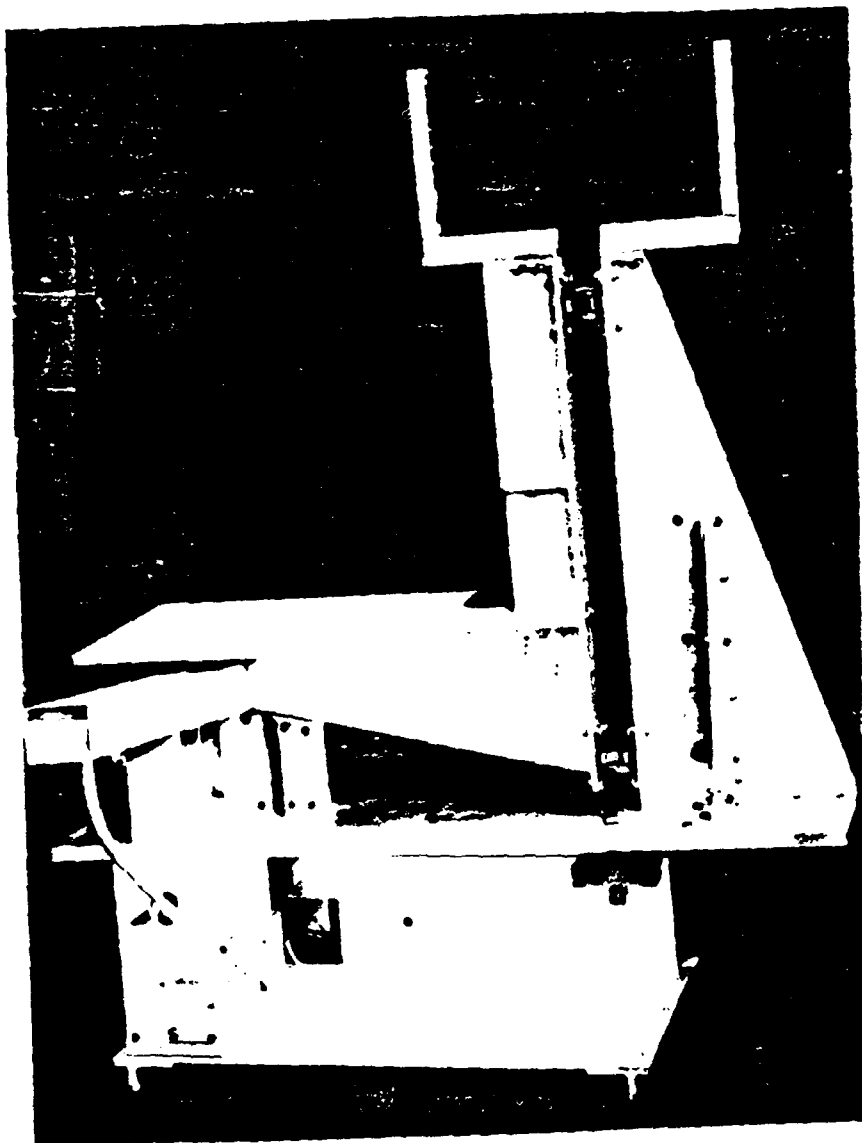


Figure 1. Assembled Thrust Stand

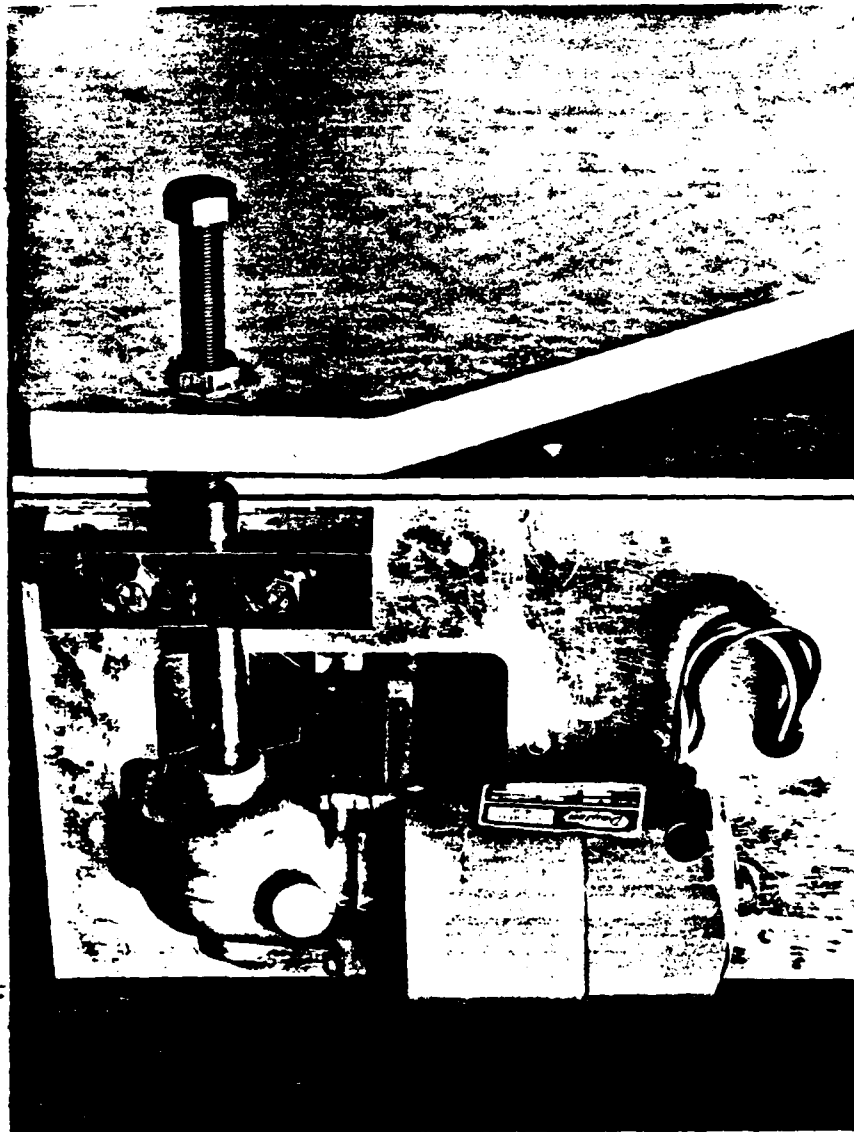


Figure 2. Leveling Motor Detail

arm assembly. In addition to these major components, there are several minor assemblies which are fastened to the adjustable base plate and balance arm. Their purpose and nomenclature are described in subsequent paragraphs.

## 2.1 Fixed Base Assembly

The fixed base assembly is a welded box structure to which various appendages are bolted. The top plate, calibrator support plate, leveling motor and reduction gear unit, and three support point assemblies are bolted to the welded box. No maintenance or repair work should ever require disassembly of any of these components with the exception of the leveling motor and gear reduction unit shown in Fig. 2. Removal of these components is straightforward, should the need to do so ever arise, but one must be careful to replace the support point assembly in precisely the same orientation on reassembly as it is in prior to disassembly. Failure to do this will result in misalignment. The leveling motor and gear reduction unit are available from Dayton Electric. The motor is model 2M172, 1/15 HP, 5000 RPM and the mating 1787:1 gear reduction unit is model 2Z797. This motor is operated from a DC power supply capable of 24 VDC at 600MA. The motor is wired to the jacks at the side of the base assembly. Electrical hookup to this motor is covered in a subsequent section of this manual.

## 2.2 Adjustable Base Plate, Vertical Support and Balance Arm

These three components are shown in Fig. 3. The assembly isometric presented in Fig. 4 shows how the vertical support, balance arm immobilizer, linear range stop assembly, and fluidic damping oil container are mounted

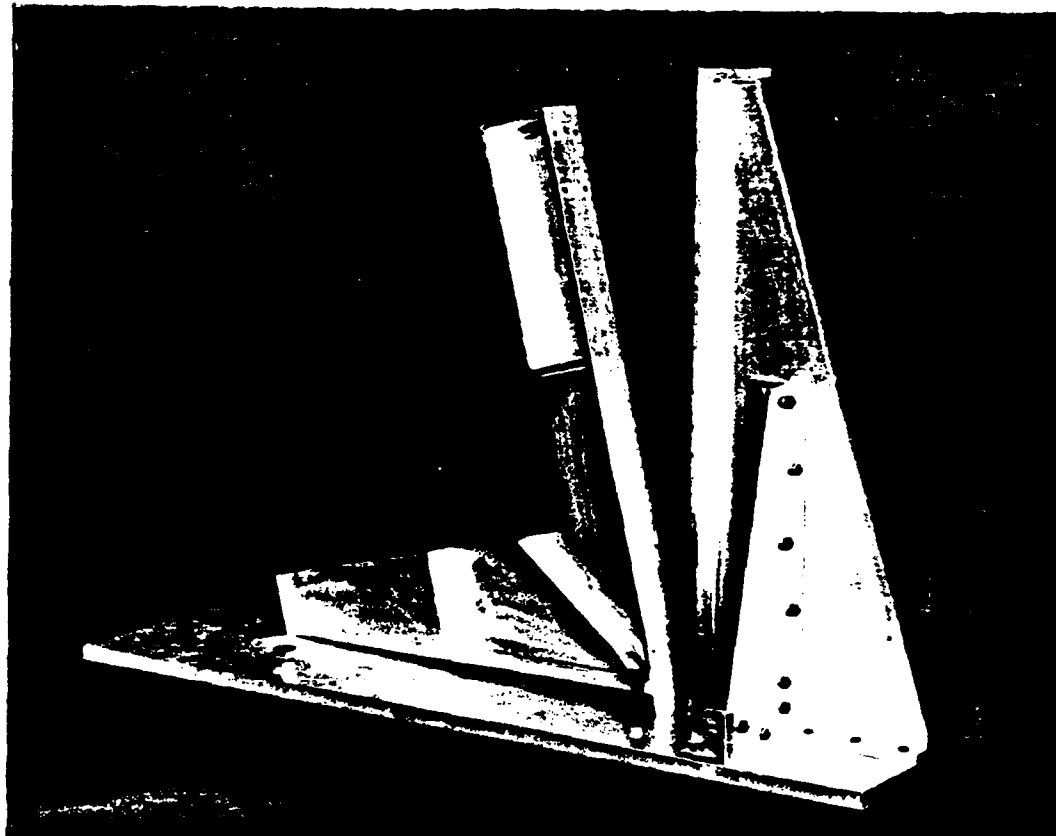


Figure 3. Base Plate, Vertical Support and Balance Arm

to the adjustable base plate. This figure also shows that the female half of the hinges is fastened to the vertical support. All interfaces shown in Fig. 4 are bolted. Figure 5 shows these components in position and also shows the balance arm and male hinge halves. Bendix Flexural Pivots join the balance arm and vertical support. Set screws in the two legs of the female hinge and in the male hinge retain the balance arm. The flexural pivots are Bendix cat. no. 6028-800. Two spares are provided with the thrust balance in the event these pivots must be replaced. Particular attention is drawn to the detail sketches in Fig. 5 indicating the proper orientation for the flexural pivots in the lower and upper hinges. Failure to insert these hinges properly will result in breakage once the balance arm is carrying a load. During installation of the balance arm the balance arm immobilizer should be moved to its position as close to the vertical support as possible. The balance arm may then be rested on the immobilizer for insertion of the flexural pivots. Figure 6 shows the balance arm in position. The immobilizer should remain in position with the arm resting on it until the LVDT slug holder assembly and fluidic damper paddle are attached to the end of the balance arm as shown in Fig. 7. The LVDT transformer holder may also be mounted to the base plate at this time, after which the transformer is placed in the holder with the slug as close to center in the transformer as is visually possible. A refinement to the center position will be made later. The stand may now be placed on the fixed base assembly being sure to locate the three machined  $\frac{1}{2}$ -20 bolts over the support point assemblies.



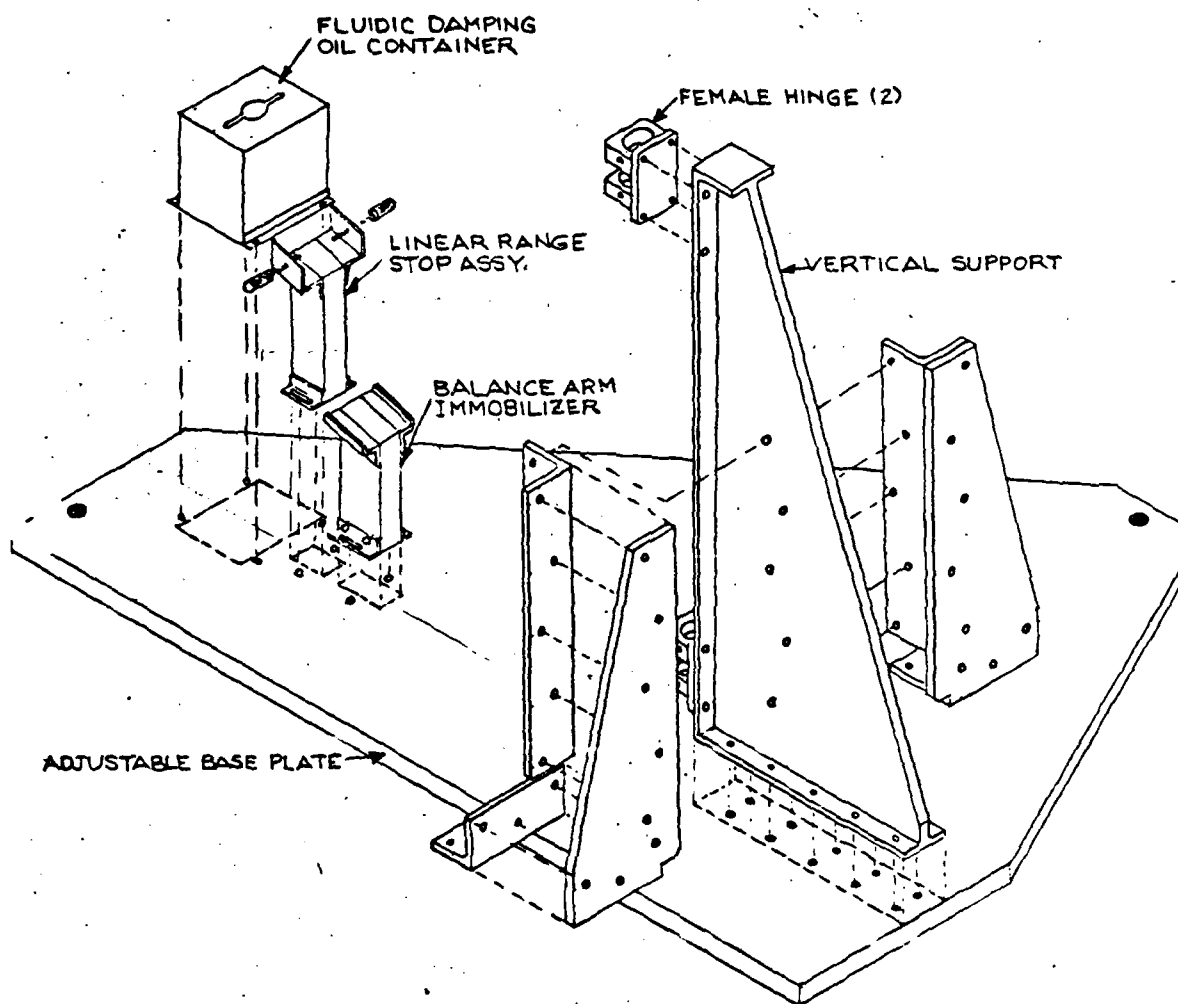


Figure 4. Assembly Isometric

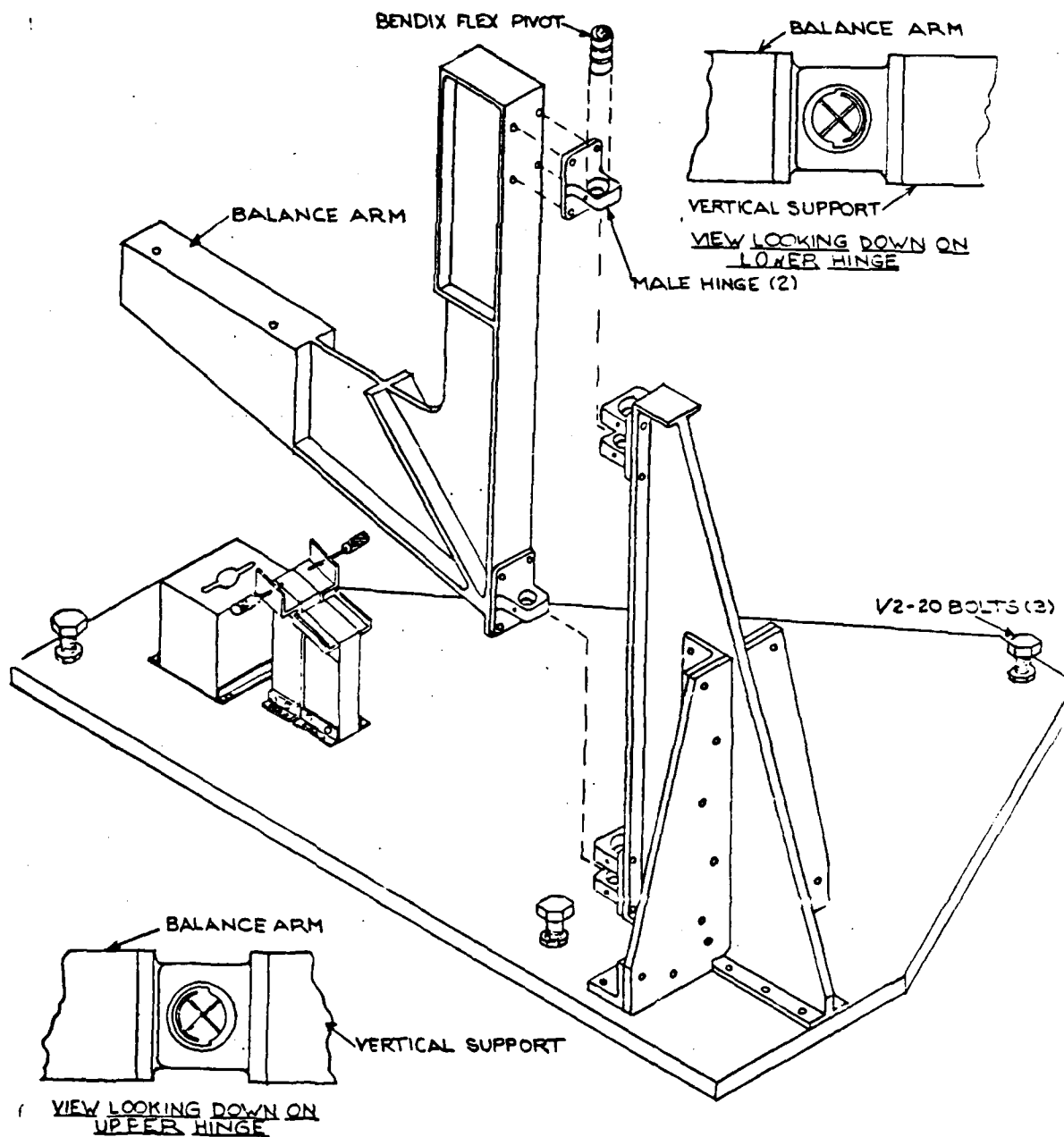


Figure 5. Assembly Isometric

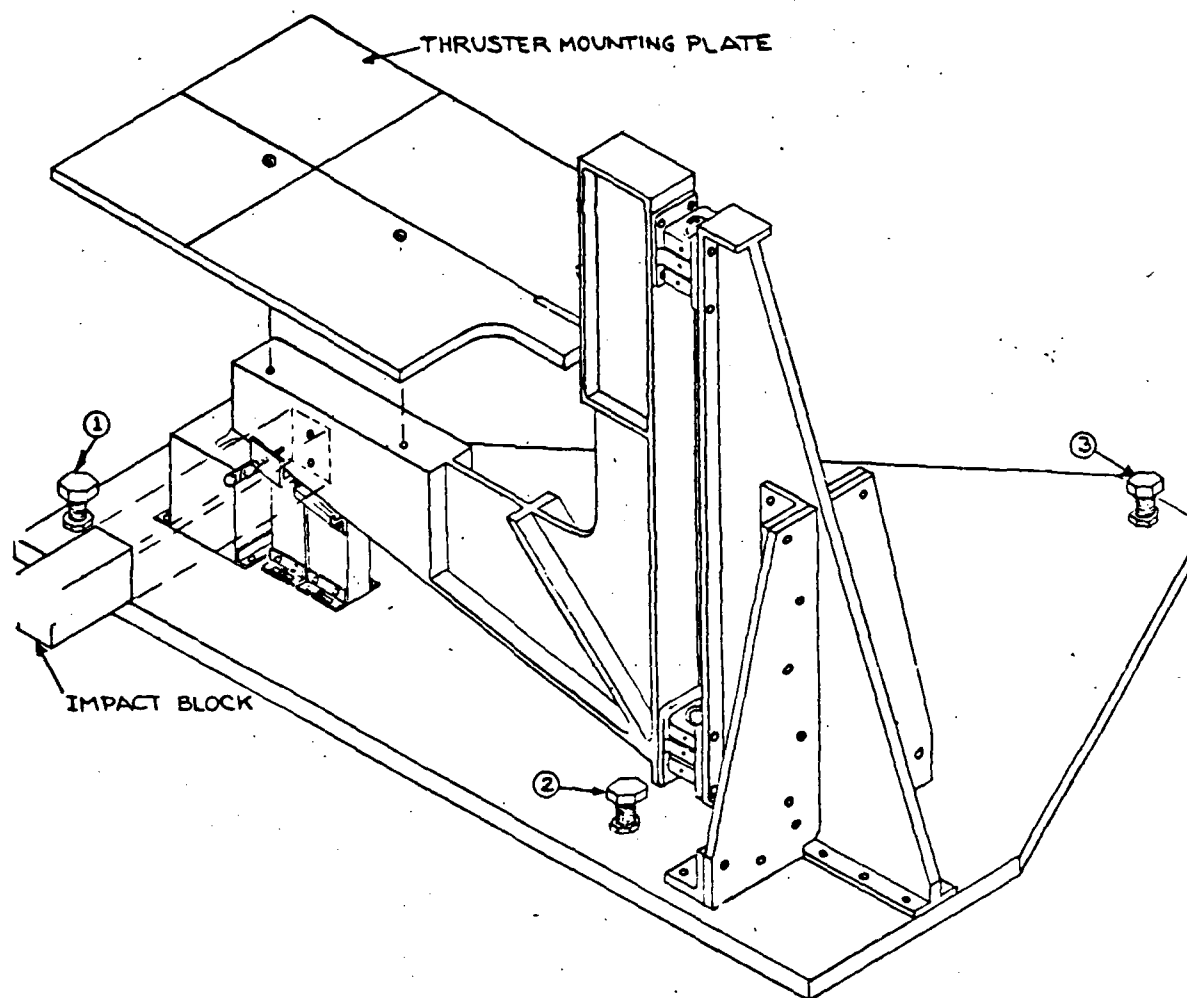


Figure 6. Assembly Isometric

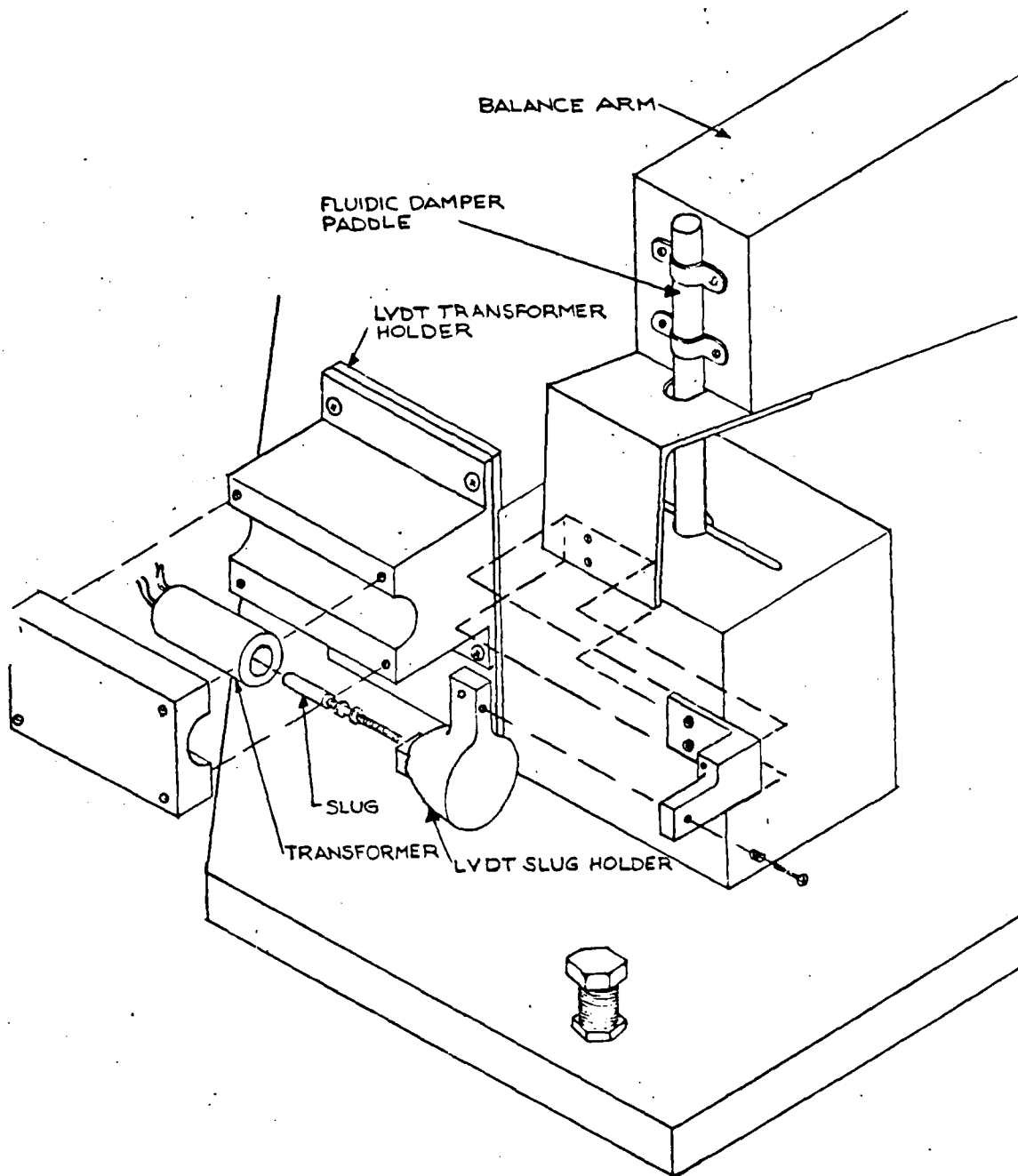


Figure 7. Assembly Isometric

The thruster mounting platform, impact block, and electrical wire cross-over standoffs are the final items to be fastened, completing the assembly.

### 3.0 INSTALLATION OF THRUST STAND

#### 3.1 Mechanical Aspects

##### 3.1.1 Thrust Stand Alignment

The first item to be installed within the vacuum facility is the base assembly. It is important that this assembly be rigidly fastened to the chamber so that if inadvertently bumped it will not move. It is also important that the base assembly be as level as possible. This should be checked along both the length and width using an inclinometer.

After satisfactory installation of the base assembly the assembled thrust stand may be placed on it making sure that the three  $\frac{1}{2}$ -20 bolts are resting in their corresponding support point assemblies on the base assembly.

At this point the damping fluid can be mixed and the damping container filled. The oil used for damping is a mixture of two halocarbon oils which are available from Halocarbon Products Corp. The two oils used are series 14-25 and series 10-25. One quart of each is supplied with the thrust stand. These particular oils are used because of their very low vapor pressure, making them ideally suited for vacuum work. Using a 50-50 mixture by volume of these oils produces the desired viscosity of around 2500 centistokes. The container need only be filled approximately 60% and a mixture of 230 ml of each fluid is all that is necessary. The depth to which the paddle is submersed in the fluid and the angle which

the paddle makes with the direction of motion of the stand are adjustable parameters. A larger dampening is produced by either submerging more paddle in the fluid or increasing the angle of the paddle with respect to the direction of motion, up to  $90^{\circ}$ . It is preferable to keep the paddle at as small an angle as is practical and make minor adjustments of the paddle depth to achieve the best balance between balance arm sensitivity and output signal amplitude (i.e., maximum signal to noise ratio). The paddle depth will be a function of the particular thruster mounted on the balance arm and hence final adjustment should not be made until the thruster to be tested is installed.

The next step in the installation of the thrust stand is to orient the adjustable base plate properly. This is done using the  $\frac{1}{2}$ -20 bolt. First, an inclinometer is oriented along the thrust direction on line with the number 2 and 3 bolts (see Fig. 6). Adjustments to the bolts are then made to level the base plate in this direction. Next, the inclinometer is oriented transverse to this thrust direction and on line with number 1 and 2 bolts. Number 1 bolt is then adjusted so as to cause the base plate to tilt  $1.5^{\circ}$  counterclockwise when viewed from the impact block side of the stand. After alignment the three  $\frac{1}{2}$ -20 bolts are locked by tightening the lock nuts. The final mechanical procedure in the installation of the thrust stand is to lock the balance arm immobilizer assembly in its extreme position away from the vertical support, thereby freeing the balance arm and placing the two centering shims one on either side of the linear range stop assembly between the screw stops and balance arm.

### 3.1.2 Ball Calibrator Installation

A photograph of the ball calibrator assembly is shown in Fig. 8. A continuous closed loop system of approximately 70 ball bearings having a  $0.375 \pm .0001$  inch diameter are fed through the aluminum tube onto the inclined plane by a Hurst model GA synchronous AC motor at a rate of one per second. Although this motor is reversible it is used in only one direction of rotation. The ball bearings can be any metal but must have very close tolerance on the diameter and sphericity. Those supplied with the thrust stand are Tungsten Carbide balls manufactured by Carbaloy; stock number GB-12.

Installation of the ball calibrator is straightforward but requires accurate positioning. The two screws on the centerline of the calibrator base are used to hold the calibrator in position once properly aligned. The other two screws, normal to the centerline on either side at the fore end are for alignment. When properly aligned the base must be level in the direction normal to the centerline and the inclined ramp must be at an angle of  $7^{\circ}$  with respect to the horizontal. The adjustments should be made using an inclinometer to insure accuracy. While making these adjustments the hold down screws are inserted but not tightened and the other set of screws is used to adjust the position. Once properly aligned the hold down screws are tightened and alignment rechecked. The calibrator motor is then plugged into the mating receptacle in the base assembly.

### 3.2 Electrical Hook Up

The ball calibrator motor and leveling motor are already wired into the banana jack receptacles on the side of the base assembly. The LVDT is wired into the banana jack receptacles fastened to the base plate.

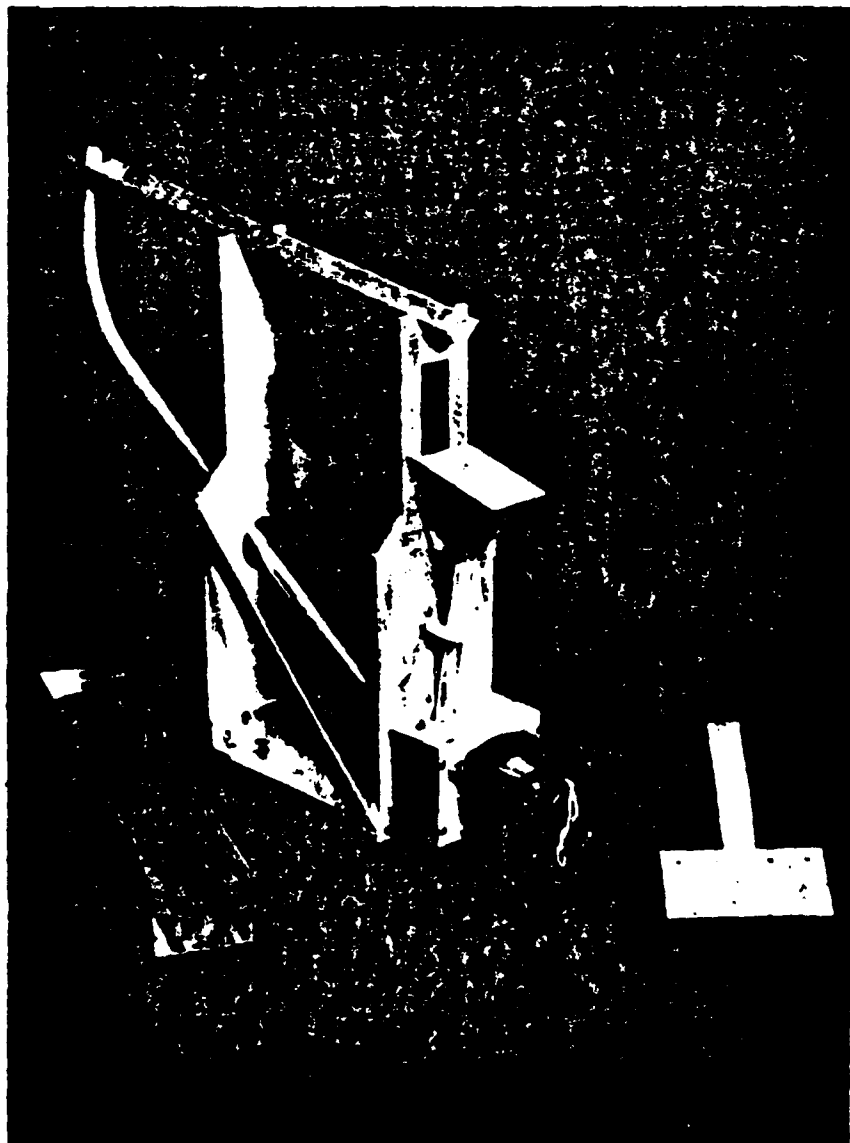


Figure 8. Ball Calibrator Assembly



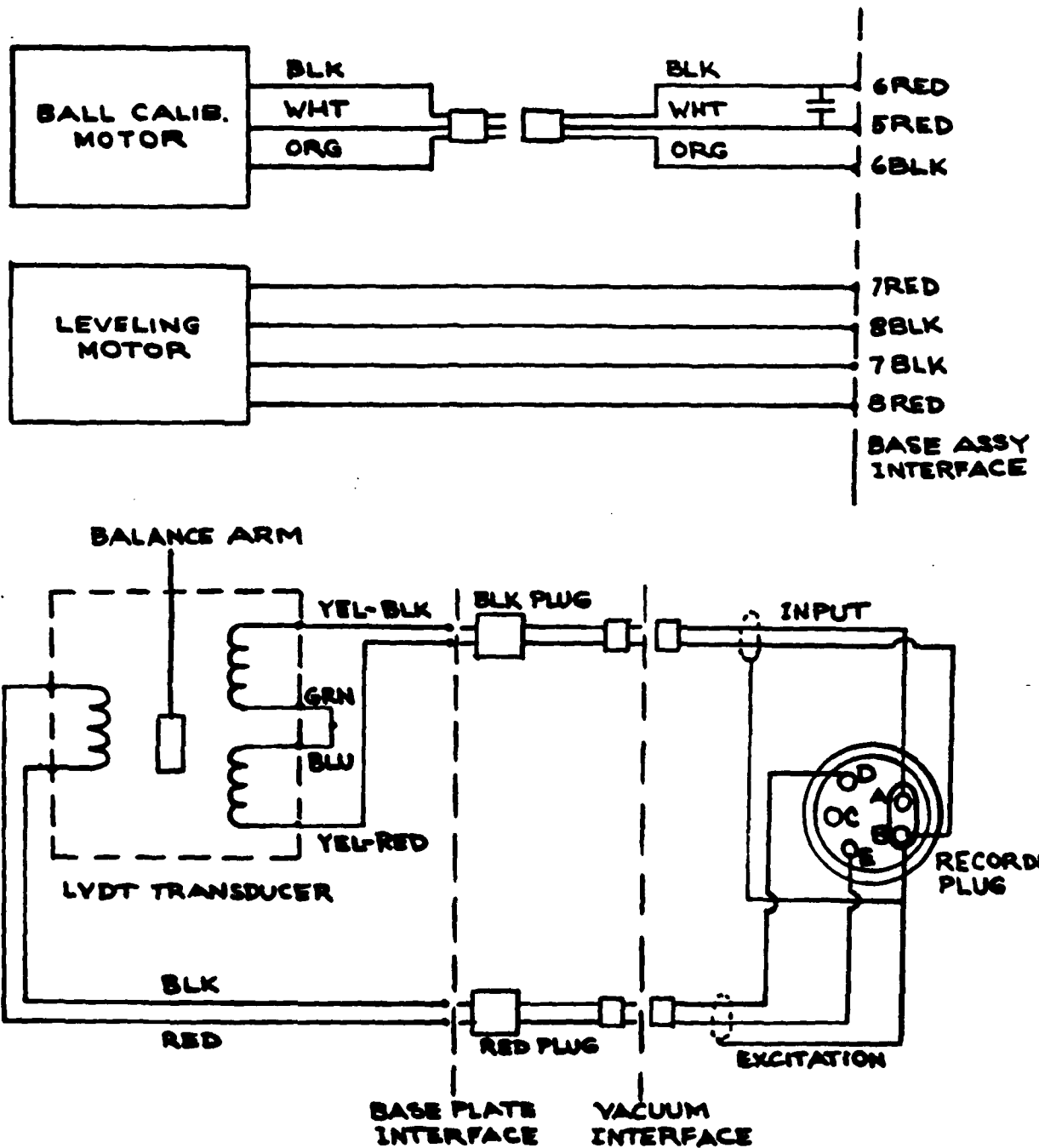


Figure 9. Wiring Schematic - Thrust Measurement System

Two sets of leads are supplied for connecting and interfacing the LVDT with the oscillographic recorder. One of these sets is connected between the receptacles on the thrust stand and the vacuum feed through bulkheads. The other set is connected from the vacuum feed through to the recorder. These are the only connections necessary for operation of the LVDT. In making these hook-ups, care must be exercised to insure that the cables marked input and output are mated properly. A schematic of these connections is shown in Fig. 9.

For remote operation of the ball calibrator and leveling motors, a switch panel is supplied with the thrust balance. A photograph of this panel is provided for reference in Fig. 10. Two sources of power are required. These are normal 115VAC and 24VDC power supply capable of delivering 600MA. The AC power is supplied by plugging in the power cord. The DC power supply is connected to the panel using the banana jack receptacles in the center with the + lead plugged into the red receptacle.

The output terminals are located on the back of the panel. These are numbered one through eight. Terminals one and two go directly to the ball calibrator motor, input receptacles 6 red and 6 black on the base assembly. In order to operate the ball calibrator the toggle switch on the right hand side must be switched to the ON position. When this is done the red indicator light will go on and power is received at the remote hand held box containing a single normally open/momentary closed push-button. Depressing the push-button will immediately cause the ball calibrator to operate. To roll a single ball this button should be depressed for approximately one second. If this button is depressed and held, balls will continuously roll at a rate of one per second until the button is released.

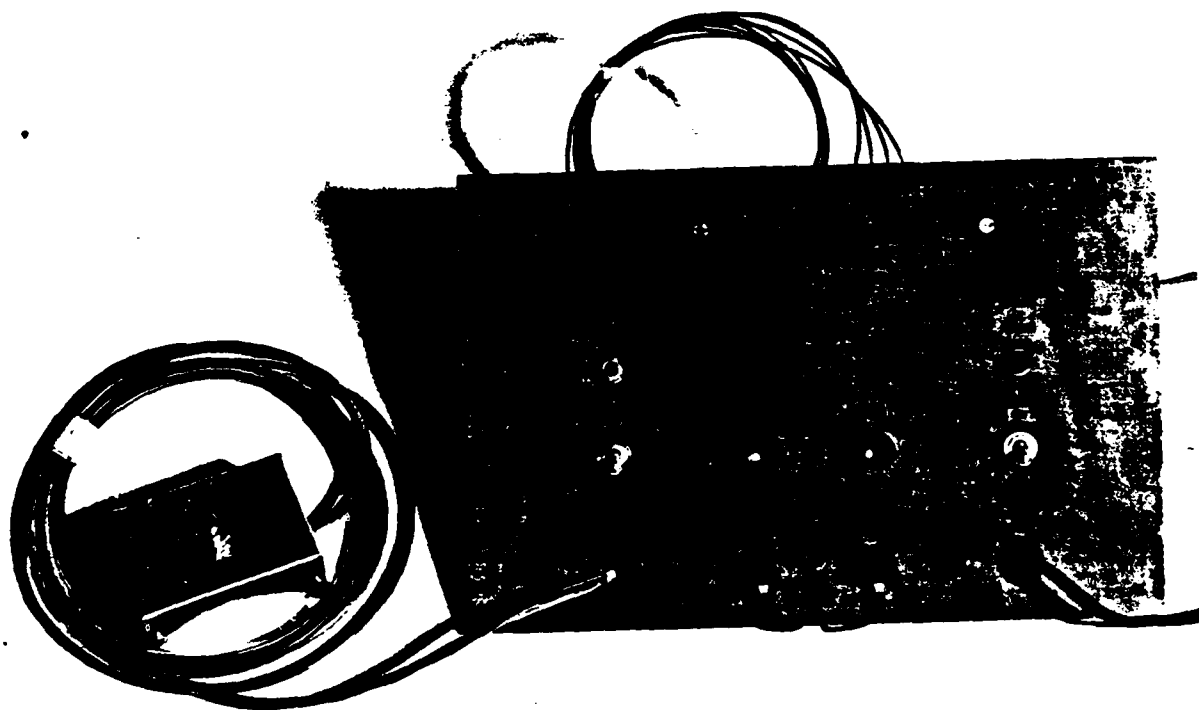


Figure 10. Control Panel

The leveling motor is operated via the two normally open/momentary closed push buttons in the center of the panel. The button on the left (red) will cause the motor to rotate clockwise and the button on the right (black) will cause the motor to rotate counterclockwise when connections are made as described in the following text. Output terminals number 3, 4, 5 and 6 on the back of the panel control the leveling motor. Terminal number 3 is connected to receptacle number 7 red on the base assembly; terminal number 4 to number 8 black on the base assembly; terminal number 5 to number 7 black on the base assembly; and terminal number 6 to number 8 red on the base assembly. The two push buttons are labeled left and right, corresponding to motion of the recorder pen to the left or right, whichever is required to center the balance arm prior to making the thrust measurement.

The toggle switch on the left side of the panel has been provided for use in conjunction with a thruster safety dump circuit. Such a circuit would contain a high voltage solenoid relay in series with a large (5000 ohms) power resistor. The relay would be activated by 115VAC at terminals 7 and 8 on the panel when this toggle switch is in the ON position, lighting the white indicator lamp adjacent to it.

A schematic of the connections described above is presented in Fig. 11. After all connections have been made, the thrust stand is ready for final adjustments described in the next section of this manual.

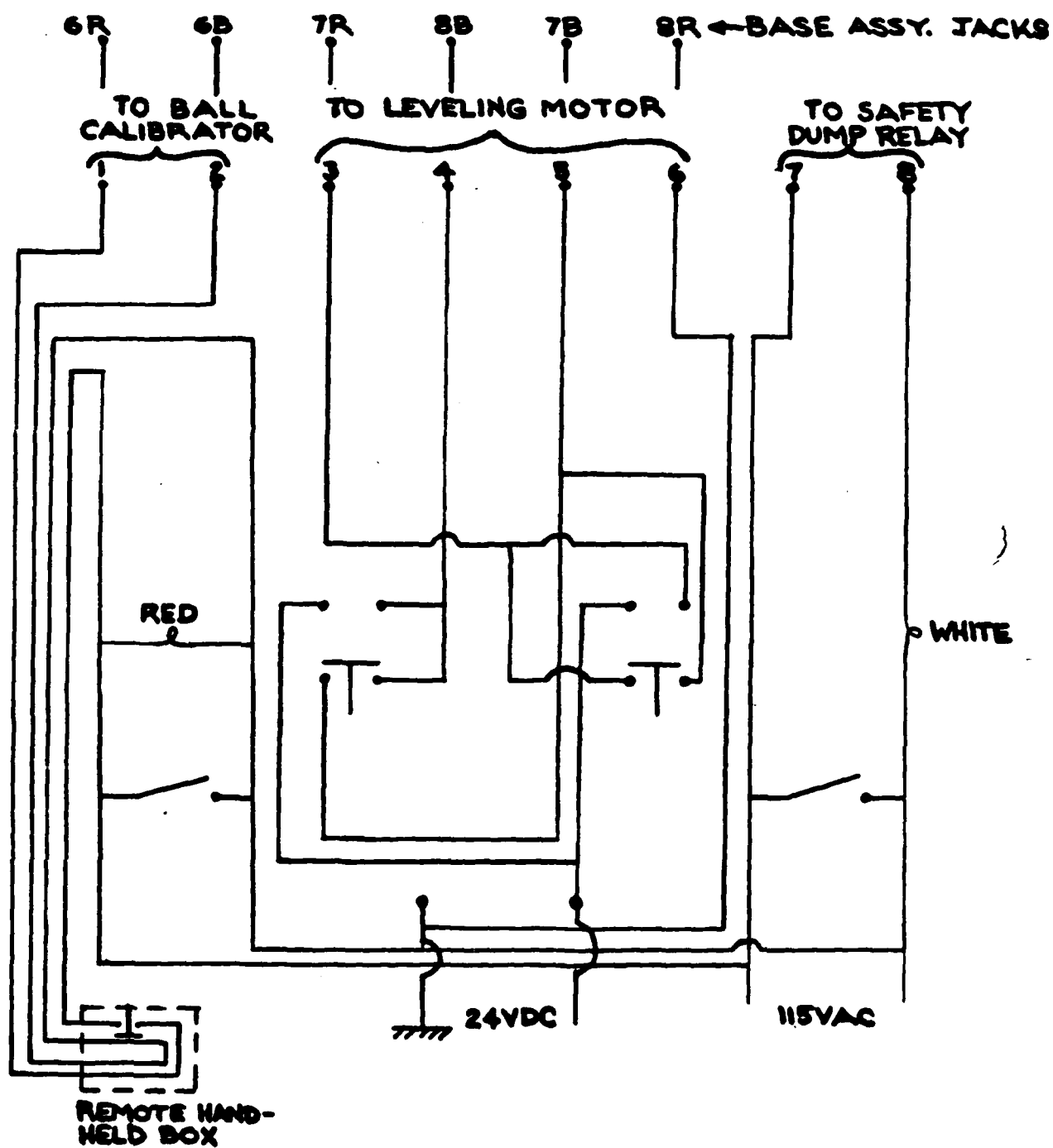


Figure 11. Control Panel Wiring Diagram

#### 4.0 FINAL ADJUSTMENT

##### 4.1 LVDT Center Adjustment

The LVDT passive slug must be centered on the transformer windings in order to insure linear operation within the range of motion of the balance arm. The Schaevitz 050HR LVDT supplied with the thrust stand is linear in the range  $\pm .050$  in. about the center position. The percent linearity is a function of the amount of displacement in this range, being .05% linear up to one half of the total linear range and .1% linear for the remainder of this range. Centering shims, which are fabricated from .040 in. Aluminum, placed on either side of the balance arm between the balance arm and adjustment screws in the linear range stop assembly, insure that the balance arm motion is restricted to  $\pm .040$  about the centered position. The process of finding the precise location of this center position is described in this section.

Prior to actually centering the slug, it is necessary to position the balance arm such that its centerline and the "null" hinge centerline (i.e., position of zero torque produced by the flexural pivots) are coincident. A line corresponding to the null hinge centerline has been scribed into the base plate. There is also a line scribed into the thruster mounting plate which is the center of the balance arm. These two lines must be coincident. The procedure for insuring this is described below.

- a) Clamp an 18 inch accurate straight edge to the mounting platform such that the edge is coincident with the scribed centerline and overhangs the mounting plate by approximately 3".
- b) Position a 12" long accurate square on the base plate with the edge of the square on the hinge centerline scribe mark.
- c) By simultaneously screwing and unscrewing the linear range stop screws with the shims in place, adjust the position of the balance arm until the two straight edges just touch.
- d) Tighten the lock nuts on the linear range stop screws to insure no further motion of the balance arm.

Having insured proper positioning of the balance arm, the LVDT center position may now be located. In order to make this adjustment properly, an oscilloscope capable of sweeping at a rate of 0.2 ms/cm with plug in amplifier capable of .001 v/cm attenuation is required. A test lead consisting of a length of BNC cable with a BNC connector on one end and banana jack plug on the other is supplied with the thrust stand for purposes of centering the LVDT. This lead is connected to the scope on the BNC end and to the INPUT set of banana jack receptacles (i.e., black) affixed to the base plate on the other end. The EXCITATION cable from the oscillograph recorder is plugged into the other set of receptacles (red) on the base plate, insuring that the ground pin on the banana jack plug is to the left. Scope settings at this point should be .2 ms/cm and 1V/cm.

Before proceeding to center the LVDT slug in the axial direction, it must be visually centered on the I.D. of the transformer windings. This is done by viewing the windings and slug from the back end and adjusting the ball joint connection and spring loaded screws on the slug holder until the slug is centered on the windings (equal spacing

between the slug and winding I.D. all around). Visual location is sufficient for this operation.

Loosen the four retaining screws in the transformer holder slide assembly until the slide assembly is free to move forward and back. Make sure that the ATTENUATOR switch on the carrier preamp is in position 1 and that the BRIDGE switch is in the FULL position (see HP operators manual on the 17403A preamp). Turn the oscillograph recorder on. At this time a sine wave will appear on the oscilloscope. Move the transformer slide assembly in the direction which decreases the amplitude of this sine wave. When the amplitude appears to be zero switch to the next smaller attenuation of the scope. Continue this process to finer and finer scope attenuation settings. At some point it will be observed that moving the slide assembly will first tend to decrease and then to increase the amplitude of the sine wave. It is this minimum amplitude position which is desired. When finally an attenuation of .001 v/cm is attained on the scope the minimum amplitude will be approximately 2cm. At this time the slug will be in the proper location and the retaining screws are to be tightened very carefully observing the oscillogram as this is done to insure that the center position is not changed in doing so. Tighten the retaining screws only up to a point where the slide will not move easily. Do not overtighten these screws or damage to the transformer winding may result. This completes the centering operation.



It is now only necessary to balance the oscillograph recorder. Disconnect the test lead and replace it with the INPUT lead from the oscillograph recorder (black plug into black receptacles, groundpin to the left). Follow the instructions in paragraph 3-17 on page 3-6 in the preamp operators manual to balance the oscillograph.

#### 4.2 LVDT Linearity Verification

This procedure need not be performed unless it is suspected that the LVDT is not functioning properly. The linearity has been verified at FRC prior to delivery of the thrust stand and was found to be satisfactory. The details of precisely how this is done are presented in the following text.

- a) Center the balance arm on the hinge centerline (see 4.1).
- b) Wrap a rubberband around the LVDT slug holder assembly and the LVDT transformer holding assembly so that the balance arm is being pulled against the back shim.
- c) Remove the fore shim after the slug center position has been verified (see 4.1).
- d) Position a depth gage or calipers graduated to .001 in. in such a way as to measure the displacement of the balance arm with respect to some fixed reference position.
- e) Set the ATTENUATOR switch to position 100 and the BRIDGE switch to FULL on the preamp. Balance the recorder.
- f) Set the SENSITIVITY control to 2 and unscrew the VERNIER control all the way.
- g) Move the balance arm several thousandths of an inch and read the dimension from the fixed reference point to the nearest thousandth. Record this value on the chart at the new pen position.
- h) Continue performing step (g) until the entire width of the chart has been spanned, stopping at a minimum of ten positions to record the dimension. This should correspond to a total balance arm motion of .070 to .080 in. (i.e. .035 - .040 in. to either side of center).

46 1513

10 X 10 1/2 THE CENTIMETER 18 X 25 CM  
KEUFFEL & ESSER CO. MADE IN U.S.A.

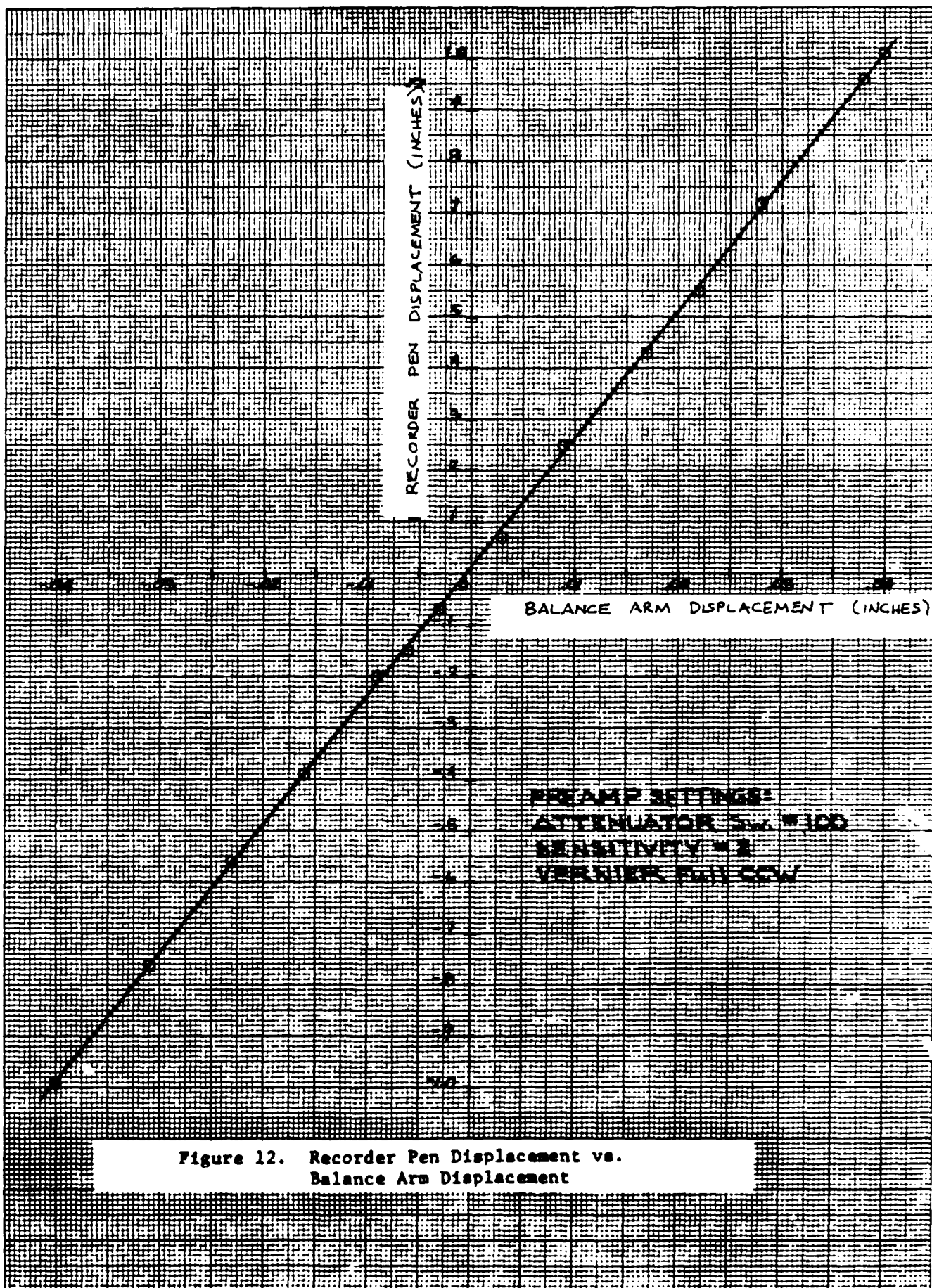


Figure 12. Recorder Pen Displacement vs.  
Balance Arm Displacement

- i) Return the balance arm to the center position before replacing the fore shim and relocking the linear stop screws. Remove the rubberband.
- j) Plot the measured pen deflection. This should result in a straight line, within the tolerance limits on linearity of the LVDT (see 4.1).

The above procedures, when performed at FRC, led to the graph presented in Fig. 12. This plot demonstrates the linearity of the LVDT in the range of interest.

## 5.0 CALIBRATION OF BALL CALIBRATOR

### 5.1 Fundamental Concept

Determination of the amount of impulse delivered to the thrust stand balance arm upon collision of a ball with the impact block is done by measuring the trajectory of the ball before and after impact. A knowledge of the equations of motion for a free falling body indicates that the trajectory should be parabolic, having the equation

$$y = y_0 + \tan \theta_0 (x - x_0) + \frac{g}{2v_{0x}^2} (x - x_0)^2$$

where  $y_0$  and  $x_0$  are the initial vertical and horizontal position of the body; respectively,  $\theta_0$  is the initial angle of the trajectory with respect to the horizontal,  $v_{0x}$  is the initial velocity in the horizontal direction,  $g$  is the acceleration due to gravity ( $32.2 \text{ ft/s}^2$ ) and  $y$  and  $x$  are the coordinates of the center of mass of the body with  $y$  measured in the direction of  $g$  and  $x$  orthogonal to  $y$ . The above equation assumes of course that aerodynamic drag on the ball is negligible, which is an excellent approximation for the normal ball size and speed associated with the ball calibrator.

Measurement of the trajectory before and after impact will yield a set of coordinates  $(x_i, y_i)$ ,  $i = 1, N$  in each case. These  $N$  data points are then fitted to a parabola using the method of least squares. The coefficient of  $x^2$  is the one of interest since it is  $v_{ox}$  that is desired, but all coefficients should be solved for so that the error of the curve fit can be estimated point for point by comparing calculated values of  $y$  at each  $x_i$  and the corresponding measured value  $y_i$ .

The least squares procedure results in the following set of equations for the coefficients of the equation  $y = ax^2 + bx + c$ :

$$b = (F_1 F_3 - F_4 F_2) / (F_3 F_3 - F_2^2)$$

$$a = (F_1 - b F_3) / F_2$$

$$c = (Y_0 - a X_2 - b X_1) / N$$

where

$$F_1 = Y_1 - X_1 Y_0 / N$$

$$F_2 = X_2 - X_1 X_1 / N$$

$$F_3 = X_2 - X_1^2 / N$$

$$F_4 = Y_2 - X_2 Y_0 / N$$

$$F_5 = X_4 - X_2^2 / N$$

$$Y_n = \sum_{i=1}^N y_i x_i^n ; \quad n = 0, 1, 2$$

$$X_n = \sum_{i=1}^N x_i^n ; \quad n = 1, 2, 3, 4$$

The sensitivity of these calculations is normally severe enough to require that all operations be carried out to a minimum of six significant digits. The point-for-point error of the fit is given by

$$\%e = 100 |y - y_i| / y_i$$

the velocity  $v_{0x}$  is then given by

$$v_{0x} = (g/2a)^{\frac{1}{2}}$$

Denoting the velocity after impact as  $v_{0x}^1$  (in the opposite direction)

the impulse produced by the balls is

$$I_b = m_b(v_{0x} + v_{0x}^1)$$

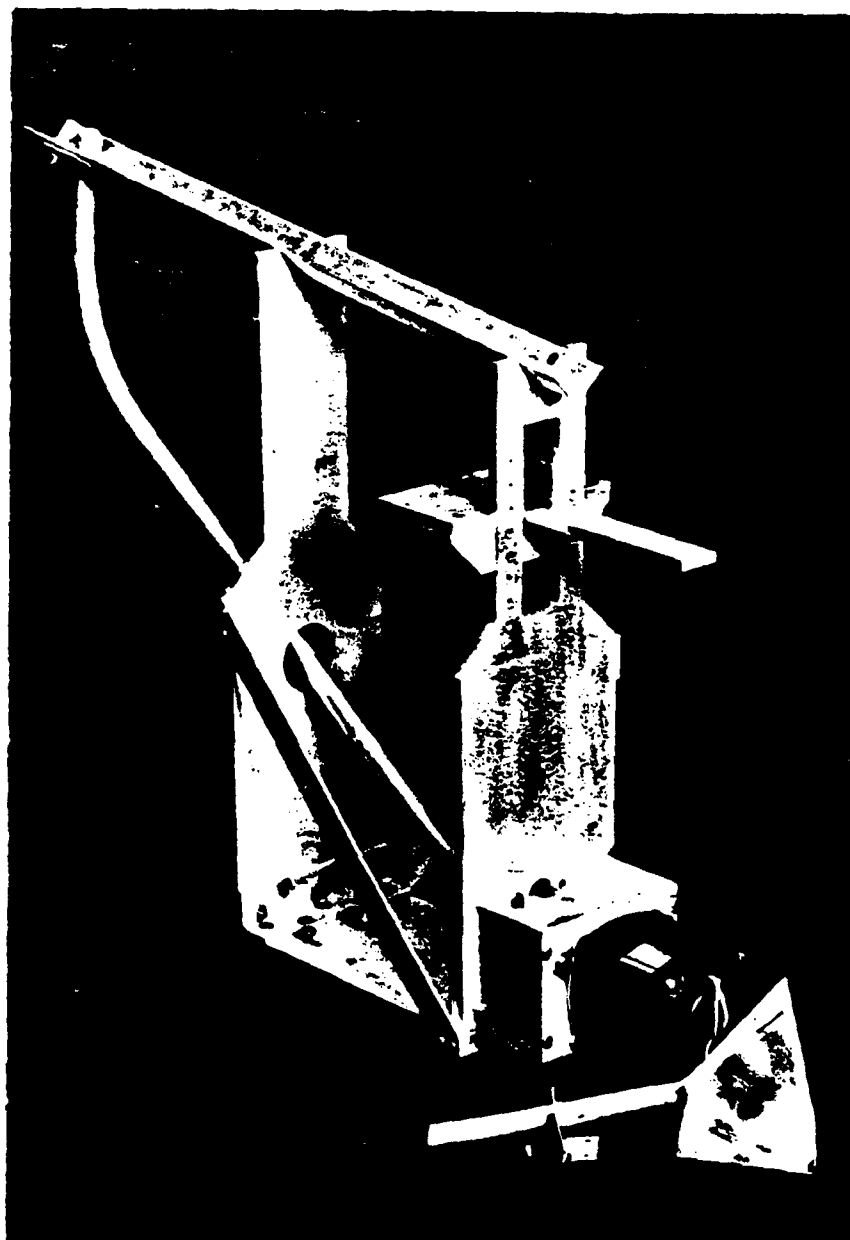
where  $m_b$  is the mass of the ball obtained by weighing a random sample of ten balls and dividing this weight by ten. The weight should have accuracy  $\pm .2$  mg.

## 5.2 Calibration Procedure

Calibration of the ball calibrator is based on obtaining a sample set of coordinates  $(x_i, y_i)$  for both the initial and rebound trajectories. A minimum of six coordinate pairs should be obtained for each trajectory, but as large a number of data points as one desires can be generated and the technique explained in the previous section will remain valid. The methodology of generating the coordinate pairs is explained in this section.

The ball calibrator does not have to be removed from the thrust stand in order to generate coordinates of either the initial or rebound trajectory. It is necessary, however, to remove the fiberglass cover and the capture chute prior to beginning calibration. To calibrate the initial trajectory it will also be necessary to remove the impact block from the balance arm. After these items have been removed, one is ready to begin generating data for the initial trajectory.

To facilitate generating the coordinates of either trajectory a calibration assist device (CAD) is supplied with the ball calibrator. The tongue of this device is just wide enough to fit in the slot cut out of the forward support on the ball calibrator. A photograph of the ball calibrator with the CAD fastened at one of the possible locations on the ball calibrator is presented in Fig. 13. There are a total of nine sets of threaded holes in the ball calibrator forward support to which the CAD can be mated. These holes are spaced very close to one half inch apart in the vertical direction. Either of the two sets of holes in the flange of the CAD will mate with any of the nine sets of threaded holes in the calibrator. The two sets of holes in the CAD are spaced very close to one quarter of an inch apart. There are, therefore, 18 possible configurations for the CAD on the ball calibrator. The generation of data consists of positioning the CAD a known vertical distance from the initial position of the center of gravity of the balls and measuring the horizontal distance traveled by the balls at that known vertical position. The horizontal distance is obtained by taping a 3/4 inch wide strip of plain white paper onto the CAD. A strip of carbon paper is laid on top of this and the impact of the ball with the CAD is thereby recorded as a dot on the white paper beneath the carbon paper. A total of fifteen balls are rolled down the inclined plane to generate each coordinate pair, leaving a total of fifteen black dots on the white data sheet. Generation of the horizontal and vertical reference points for each of the trajectories is described in the following text.



### 5.3 Initial Trajectory

Positioning the CAD with the upper set of holes mated to the first set of threaded holes in the calibrator places the CG of the .375 inch diameter ball a distance of .811 inches above the surface of the CAD when the CG of the ball is directly above the edge of the inclined ramp (see Fig. 14). It is only necessary to locate the edge of the ramp on the data sheet prior to beginning the calibration run. This may be done using an accurate square and sharp edge against the lip of the inclined ramp, scribe a mark at the projected vertical location of this lip onto the white paper, using carbon paper to imprint this location. Now run 15 balls down the ramp by feeding two at a time into the helical feed gear housing with the motor running. Remove the carbon paper and circle the resulting group of dots. Note the position of the CAD (i.e.; #4 upper, #3 lower, etc.) alongside the circled grouping. Move the CAD to a position at least one inch away from the preceding position and run 15 more balls, recording the impact as before and noting the CAD position. It is recommended that only three different positions be recorded on any one sheet of white paper, after which a new sheet should be taped to the CAD and the edge of the ramp located each time a new sheet is used.

After all desired data has been taken (a minimum of six different positions) the data is ready to be reduced to coordinate pairs. The coordinate system shown in Fig. 14 is convenient. The x-coordinate of the CG of the balls is the measured distance from the lip of the inclined ramp to the center of the cluster of dots and the corresponding y-coordinate is the dimension shown in Table I.



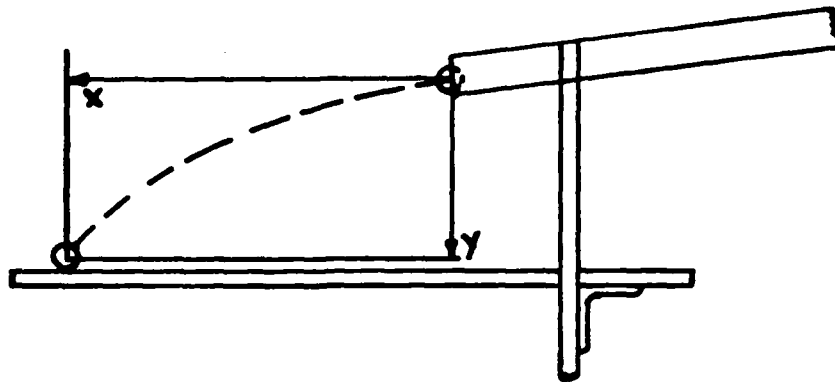


Figure 14. Coordinate System - Initial Trajectory

Table I. y - coordinates

| Position of CAD | y-Coord (inches) |
|-----------------|------------------|
| 1 Lower         | -                |
| 1 Upper         | 0.811            |
| 2 Lower         | 1.056            |
| 2 Upper         | 1.311            |
| 3 Lower         | 1.564            |
| 3 Upper         | 1.807            |
| 4 Lower         | 2.048            |
| 4 Upper         | 2.303            |
| 5 Lower         | 2.549            |
| 5 Upper         | 2.800            |
| 6 Lower         | 3.044            |

The x-dimension should be measured using a scale which is graduated in hundredths of an inch to the nearest .005 inches.

#### 5.4 Rebound Trajectory

The procedure for generating coordinate pairs corresponding to the rebound trajectory is the same as that used for the initial trajectory. There are, however, certain differences which result from the fact that the height of the impact block with respect to the lip of the inclined ramp can be different from one setup to the next. The closest position to the impact block in which the CAD can be set is number 3 lower and calibration will begin there. The first dimensions required are those from some fixed horizontal reference plane to the point at which the balls hit the impact block and from the same reference to the surface of the CAD when located in number 3 lower position. To generate these dimensions a height gage or similar instrument graduated in thousandths of an inch should be used. The procedure is as follows:

- a) With the impact block fastened tightly to the balance arm and the calibrator fixed rigidly to the thrust stand at the proper  $7^\circ$  angle, place the shims on either side of the balance arm and tighten the linear stop screws to insure no motion of the balance arm.
- b) Take a piece of carbon paper to the impact block across its face and run 15 balls two at a time.
- c) Remove the carbon paper. The points of impact will be clearly visible on the steel face of the block. Measure the distance from the reference plane to the center of this cluster of dots and to the top of the CAD surface. Subtract the height of the CAD from the height of the impact point and subtract the radius of the ball ( $r = .188$  inches) from the result. Record this dimension.

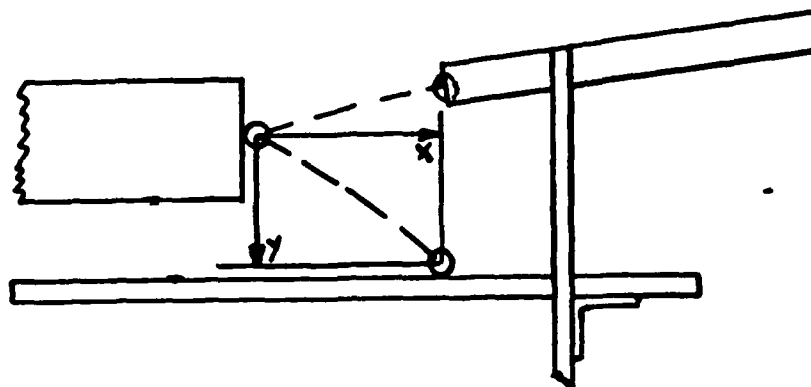


Figure 15. Coordinate System - Rebound Trajectory

Table II. Distance of CAD from Position 3 Lower to any other Position

| Position of CAD | Distance to Position 3 Lower |
|-----------------|------------------------------|
| 3 Lower         | 0 -                          |
| 3 Upper         | 0.243 , 0                    |
| 4 Lower         | 0.484 , 24                   |
| 4 Upper         | 0.739 , 5 E6                 |
| 5 Lower         | 0.985                        |
| 5 Upper         | 1.236                        |
| 6 Lower         | 1.480                        |
| 6 Upper         | 1.731                        |
| 7 Lower         | 1.960                        |
| 7 Upper         | 2.221                        |
| 8 Lower         | 2.472                        |
| 8 Upper         | 2.726                        |
| 9 Lower         | 2.965                        |

• 2 4 3

0

2 4 5

5 2 8

Locate the vertical projection of the face of the impact block on the paper taped to the CAD using an accurate square as was done to locate the lip of the inclined ramp. This must be done each time a new piece of paper is taped to the CAD.

After running as many positions as desired the data is ready for conversion to coordinate pairs. A convenient coordinate system is shown in Fig. 15. Referring to this figure, the x-coordinate is obtained by measuring the distance from the projected impact face location to the center of the cluster of dots at each CAD position and subtracting the radius of the balls from this dimension. The y-coordinates are obtained by adding the dimension from the point of impact to the CAD in position 3 lower to the dimension between position 3 lower and the position in question (these dimensions are tabulated in Table II).

It is noted that a considerably greater degree of scatter during any given run of 15 balls will be evident for the rebound trajectory than for the initial trajectory as one gets farther from the impact block. This is due mainly to the difference in spin between one ball and another and partly due to the microscopic differences in surface condition between various points on the surface of each ball, both of which effect the coefficient of spinning restitution at impact. It is not surprising, however, that even though these differences are present, each ball produces very nearly (within  $\pm 2\%$ ) the same impulse on impact. This is so because the parameter which is effected by these differences is the y-component of velocity after

impact and not the x-component. In making the calibration, therefore, one should not be too concerned over the degree of scatter and if it is not possible to accurately estimate the center of any given grouping it is recommended that the points be measured individually and an arithmetic mean be used to get the x-coordinate.

A typical complete calibration run and calculation of impulse is presented for reference in the Appendix of this manual.

#### 6.0 THRUSTER INSTALLATION ON THRUST BALANCE

There are several important considerations when mounting a thruster on the thrust stand for testing.

1. The thruster center of gravity location transverse to the thrusting direction must be positioned precisely on the balance arm centerline scribed into the mounting plate. This is very important since balancing the stand in the null position will be very difficult if not impossible should misalignment exist.
2. The center of thrust (i.e., thruster nozzle) must be positioned at an accurately known distance from the center of rotation of the flexural pivots since the ratio of this distance to the distance at which the balls strike the impact block will determine the appropriate calibration factor to be used in reducing thrust data.
3. The thruster must be electrically isolated from the thrust stand. A sheet of 10 mil thick mylar between the thruster and mounting plate is sufficient to insure this.

4. In passing over the flexural pivots between the two cross-over standoffs, all wires and tubing must be draped approximately one inch before clamping them in place. Wires and/or tubes must not be in contact with one another.
5. Thrusters weighing more than 100 pounds must not be mounted on the thrust balance at a distance greater than 17.5 inches from the center of rotation of the flexural pivots. To do so would result in unstable operation or structural failure of the pivots.
6. After installing the thruster the LVDT slug should be re-centered both axially and radially because mechanical deflection of the balance arm under the load of the thruster will generally cause the slug position to change.
7. The depth and angle of the fluidic damper paddle are the final adjustments to be made and should be made by first adjusting the height with the paddle at zero angle with respect to the thrust direction. If further damping is required after the paddle is as deeply submerged as possible the angle of the paddle should gradually be increased in small increments to achieve the best ratio of signal to noise.

A routine check of all systems should be made with the door to the vacuum facility closed prior to pumping down. These checks should include, as a minimum, verification that the thrust stand balance arm is moving freely, can be balanced in the null position, and respond properly to impact by the ball calibrator.

Any electrical tests to insure that the thruster will operate properly once pump down is completed should also be made. Electrical isolation of the thruster should be checked using a megohmmeter. A minimum of one megohm of isolation should exist.

## 7.0 THRUST MEASUREMENT

### 7.1 Data Generation

The following procedure should be followed each time thrust is measured.

- 1) Shut down thruster.
- 2) Center the balance arm using leveling motor to bring the recorder pen to the center of the chart paper with the pen position control knob centered.
- 3) Move the pen to the right using the pen position control knob until it is roughly 1cm off the right hand margin.
- 4) Run the chart at a speed of one mm per second.
- 5) Fire the thruster. If a steady state thruster is being tested a firing of 40 to 50 seconds is sufficiently long. If an impulse type thruster is being tested fire the thruster only once.
- 6) Allow the thrust stand to return to the null position and record for a minimum of 20 seconds before proceeding to the next step. Note that a slight drift of the null position may exist. This is due to the thruster cooling down and a possible consequent shift in the thruster center of gravity as a result.

- 7) Run the ball calibrator for a minimum of 40 - 50 seconds if a steady state thruster is being tested. A single ball should be allowed to impact in the case of an impulse type thruster.
- 8) Repeat steps (5) through (7) at least 5 times before resuming continuous thruster operation. Should the pen move to its rightmost position at any time during data taking use the pen position control to bring it back and then continue.

## 7.2 Data Reduction

The data obtained via the procedure outlined in Section 7.1 will consist of a minimum of 5 records, each containing the representative recorded deflection output of the thruster and ball calibrator. Using a straight edge and sharp No. 2 pencil draw straight lines between the recorded nulls before and after each thruster firing and ball calibration. For steady state thrusters also draw straight lines through the maximum deflection of both thruster and balls. Measure the deflections from the null line and record these. The ratio of average thruster and average ball deflections is determined next. The thrust produced by steady state thruster is then given by

$$F_T = \frac{r_B \delta_T}{r_T \delta_B} I_B$$

where  $r_B$  and  $r_T$  are the distances from the pivot axis to the point of impact of the balls and to the center of thrust, respectively.  $\delta_T$  is the average deflection produced by the thruster,  $\delta_B$  is the average deflection produced by the balls, and  $I_B$  is the impulse produced by the balls. For impulse type thrusters the same equation holds with  $F_T$  replaced by  $L_T$ , the impulse produced by the thruster.



The impulse produced by impulse type thrusters can also be measured by firing the thruster at a sustained pulse rate  $f$  if  $1/f$  is greater than 5 seconds. In this case the above equation will yield the equivalent steady-state thrust produced at that firing frequency and the impulse bit is given as  $I = F_T/f$ .

#### 8.0 TROUBLESHOOTING

The basic electromechanical simplicity of the thrust stand allows for only a few things which can go wrong. The problems which can arise are:

- 1) Balance arm does not center upon activating leveling motor.
- 2) Response to impulse bits produced by ball calibrator appears not to be proper.
- 3) Ball calibrator does not work.

Regarding item (1) the following checks should be made:

- a) Make sure 28VDC is getting to the leveling motor.
- b) Insure that the balance arm is moving freely with nothing touching it. Check wires across the pivots to insure free motion. Check center of gravity location of thruster to insure it is centered properly on the balance arm. Check the angle on the damper paddle.

Regarding item (2) the following checks should be made:

- a) Insure that the balance arm is moving freely with nothing touching it. Check wires across the pivots to insure free motion. Check the angle on the damper paddle.

- b) Check to insure that balls are hitting impact block with no interference during the initial trajectory.
- c) Insure that impact block is fastened rigidly to the balance arm.

Regarding item (3) the following checks should be made:

- a) Insure that 115VAC is getting to the ball calibrator motor when the push-button is depressed.
- b) Check motor.
- c) If motor is working check the universal coupling connecting the motor to the helical feed gear to insure free motion of the shaft and corresponding rotation of the feed gear.
- d) Disassemble feed gear housing to check for jammed balls.

## 9.0 REPAIRS

The inherent ruggedness of this thrust measurement system precludes breakage of the majority of component parts under normal handling. Those components which can fail or begin functioning improperly must normally be completely replaced rather than repaired. These include both electrical motors, the LVDT, and the flexural pivots. Spare flexural pivots are supplied with the thrust balance in the event that those on the assembly are overstressed and fail. A listing of these components and their availability is presented below in case replacement is necessary.

|                       |   |   |
|-----------------------|---|---|
| Ball Calibrator Motor | Hurst Mfg. Co.<br>1551 E. Broadway<br>Princeton, Ind. 47670         | Model GA Synchronous<br>AC Motor, 600RPM,<br>600 inch-ounce |
| Leveling Motor        | W. W. Granger<br>137 Express St.<br>Plainview, N.Y.                 | Model 2M172 AC/DC<br>Electric Motor,<br>1/15HP, 5000RPM     |
| Gear Reduction Unit   | " "   | Model 22797, 1787:1   |
|                       | Schaevitz Engineering<br>US Rt. 30 & Union Ave.<br>Pennsauken, N.J. | Model 050HR   |
| Flexural Pivots       | Bendix Corp.<br>211 Seward Ave.<br>Utica, N.Y.                      | Flexural Pivot Module<br>Stock No. 6028-800.                |

In addition to the above, the oscillograph recorder will eventually require paper and ink supplies. One extra roll of paper and one extra ink cartridge have been supplied with this unit. Additional ink and paper can be ordered through local HP distribution houses.